Formation and deformation of hyperextended rift systems: insights from rift domain mapping in the Bay of Biscay-Pyrenees

J. Tugend[1*], G. Manatschal[1], N. J. Kusznir[2], E. Masini[1], G. Mohn[3] and I. Thinon[4]

[1]Institut de Physique du Globe de Strasbourg, CNRS-UMR 7516, EOST, Université de Strasbourg, 1 rue Blessig, F-67084 Strasbourg Cedex, France

[2]Department of Earth and Ocean Sciences, University of Liverpool, Liverpool L69 3BX, UK

[3] GEC, Université de Cergy-Pontoise, F-95 000 Cergy, France

[4] BRGM, 3 avenue Claude Guillemin, BP6009, 45060 Orléans cedex 2, France

*Corresponding author: J. Tugend, Institut de Physique du Globe de Strasbourg, CNRS-UMR 7516, EOST, Université de Strasbourg, 1 rue Blessig, F-67084 Strasbourg Cedex, France tugend@unistra.fr, (33) 03.68.85.04.47

Key points:

- 3D rift architecture depends on the pre-rift structuration of the lithosphere
- The rift systems presented are strongly segmented both offshore and onshore
- The formation of the Pyrenean orogen is controlled by rift domain inheritance

Abstract

The Bay of Biscay and the Pyrenees correspond to a Lower Cretaceous rift system including both oceanic and hyperextended rift domains. The transition from preserved oceanic and rift domains in the West to their complete inversion in the East enables us to study the progressive reactivation of a hyperextended rift system. We use seismic interpretation, gravity inversion and field mapping to identify and map former rift domains and their subsequent reactivation. We propose a new map and sections across the system illustrating the progressive integration of the rift domains into the orogen. This study aims to provide insights on the formation of hyperextended rift systems and discuss their role during reactivation. Two spatially and temporally distinct rift systems can be distinguished: the Bay of Biscay–Parentis and the Pyrenean–Basque–Cantabrian rifts. While the offshore Bay of Biscay represent a former mature oceanic domain, the fossil remnants of hyperextended domains preserved onshore in the Pyrenean–Cantabrian orogen record distributed extensional deformation partitioned between strongly segmented rift basins. Reactivation initiated in the exhumed mantle domain before it affected the hyperthinned domain. Both domains accommodated most of the shortening. The final architecture of the orogen is acquired once the conjugate necking domains became involved in collisional processes. The complex 3D architecture of the initial rift system may partly explain the heterogeneous reactivation of the overall system. These results have important implications for the formation and reactivation of hyperextended rift systems and for the restoration of the Bay of Biscay and Pyrenean domains.

Keywords:

Continental rifted margin, inheritance, reactivation, collisional orogen formation, Pyrenees, Bay of Biscay

1. Introduction

The description of repeated opening and closing of oceanic basins also referred to as the "Wilson Cycle" [*Wilson*, 1966] represents one of the main achievements of the plate tectonic theory. Plate tectonic cycle evolution suggests that mountain belts build on the former site of conjugate rifted margins and intervening oceanic domains. Therefore, the understanding of the formation and deformation of rift systems is critical to further understand plate tectonics. Over the past decades, the development of high-resolution long-offset seismic reflection data improved the imaging of the crustal architecture of rifted continental margins. These geophysical data combined with drill hole observations show that many rifted continental margins are formed by hyperextended domains consisting in extremely thinned continental crust and/or exhumed sub-continental mantle (e.g. Iberian margin: [*Boillot et al.,* 1987; *Péron-Pinvidic and Manatschal,* 2009]; Exmouth plateau: [*Driscoll and Karner,* 1998]; West-African margin: [*Contrucci et al.,* 2004; *Aslanian et al.,* 2009; *Unternehr et al.* 2010]; mid-Norwegian margin: [*Osmundsen and Ebbing,* 2008]; Australian and Antarctica margins: [*Espurt et al. 2012*]).

In the meantime, on land studies in mountain belts showed that remnants of hyperextended domains could also be identified in internal parts of collisional orogens (e.g. Alps: [*Lemoine et al.* 1987; *Manatschal*, 2004; *Mohn et al.,* 2010; *Masini et al.,* 2012; Beltrando *et al.*, 2014]; Pyrenees: [*Lagabrielle and Bodinier*, 2008; *Jammes et al.,* 2009; *Lagabrielle et al.,* 2010; *Clerc et al.,* 2012, 2013; *Masini et al.,* 2014]; Caledonides: [*Andersen et al.*, 2012]). In spite of these discoveries, most studies on the formation of collisional orogens have not yet integrated the complexity of the pre-collisional rift architecture. The implications of the former rift-related thinning and the role of rift inheritance are progressively being further investigated [e.g. Roca *et al*., 2011; Jammes *et al*., 2014; Mohn *et al.*, 2014].

In this study, we focus on the Bay of Biscay and the Pyrenees, one of the rare examples where both the formation and progressive reactivation of rifted margins can be investigated in one and the same system. This area corresponds to a polyphased Triassic to Early Cretaceous rift system leading to the formation of hyperextended basins and ultimately oceanic crust in the western Bay of Biscay [e.g. *Vergés and García-Senz,* 2001 and reference therein]. The late Cretaceous to Cenozoic convergence between the European and Iberian plates led to the heterogeneous deformation of the rift system, illustrated by changes in compressional architecture along strike [e.g. *Muñoz,* 2002]. Reactivation was relatively moderate along the southern Cantabrian margin [e.g. *Pulgar et al.,* 1996; *Gallastegui et al.,* 2002; *Roca et al.,* 2011]. In contrast the former hyperextended rift basins from the Pyrenean–Cantabrian domain (e.g. the Mauléon and Basque–Cantabrian basins [*Pedreira et al.,* 2007; *Jammes et al.,* 2009; *Lagabrielle et al.,* 2010; *Roca et al.,* 2011]) are completely inverted and integrated into the orogenic system. At present the compressional units characterizing the Pyrenean orogen are well-known [e.g. *Mattauer*, 1968; *Choukroune and Séguret*, 1973; *Mattauer and Henry*, 1974; *Choukroune*, 1992]. In contrast, the rift-related paleogeographic domains remain poorly or only locally defined and their architecture is mainly described on 2D sections [e.g. *Jammes et al.,* 2009; *Lagabrielle et al.,* 2010; *Masini et al.,* 2014]. A well-defined and uniform definition of pre-compressional rift domains across the overall system is still missing. This results in controversial interpretations of the continuity of some pre-compressional structures and of their role during the rifting episode (e.g. the North Pyrenean fault; [*Mattauer and Seguret,* 1971; *Canérot et al.,* 2001; *Canérot*, 2008]).

The aim of this work is twofold (1) to illustrate the complex 3D evolution of strain partitioning and architecture within hyperextended rift systems and (2) to investigate the progressive role of rift inheritance from the initiation of reactivation to continental collision. We apply for the first time a new multidisciplinary approach designed by *Tugend et al.,*

93 [accepted] to characterize and identify diagnostic elements defining similar rift domains in
94 offshore and onshore settings. We combine gravity inversion results and seismic
95 interpretations with field observations to propose a new map of rift domains from the offshore
96 Bay of Biscay to their onshore fossil equivalents preserved in the Pyrenean orogen.
97 The mapping approach used in our study may be used in other orogenic systems and may
98 bring new insights on the interpretation of the architecture of collisional orogens as well as on
99 the restoration of the spatial and temporal evolution of fossil rift systems.

100 **2. Geological framework**

101 The Bay of Biscay corresponds to a V–shaped oceanic basin opened westwards towards the
102 Atlantic Ocean. Located between the European and Iberian plates, it is bordered to the North
103 by the Western Approach and Armorican margins and to the South by the North Iberian
104 margin (fig 1). The eastern termination is characterized by several Mesozoic rift basins
105 recording geophysical and/or geological evidence for extreme crustal thinning both offshore
106 (e.g. the Parentis basin: [*Pinet et al.,* 1987; *Bois and Gariel*, 1994; *Tomassino and Marillier*,
107 1997; *Jammes et al.,* 2010a, 2010c]) and onshore (e.g. the Aulus basin: [*Lagabrielle and*
108 *Bodinier* 2008; *Lagabrielle et al.,* 2010; *Clerc et al.,* 2012]; the Arzacq–Mauléon basin:
109 [*Daignières et al.,* 1994; *Jammes et al.,* 2009; *Lagabrielle et al.,* 2010; *Debroas et al.,* 2010;
110 *Masini et al.,* 2014] and the Basque–Cantabrian basin: [*Pedreira et al.,* 2007, *Roca et al.,*
111 2011]).

112 ***2.1. Tectonic and sedimentary evolution of the Bay of Biscay and Pyrenean domains***

113 The Bay of Biscay and Pyrenean domains represent a strongly structured region that is the
114 result of consecutive extensive and compressive tectonic cycles that initiated in the early
115 Palaeozoic. The formation of the Variscan orogen during the Carboniferous resulted from the
116 collision of the Laurussia and Gondwana continental margins with intervening oceanic

117 domains and micro-continents such as Armorica [for a review see *Matte*, 1991, 2001]. The
118 post-Variscan evolution is related to the emplacement of strike-slip or transform faults
119 throughout the Late Carboniferous to the Early Permian (e.g. Toulouse fault, Cévennes fault,
120 Ventaniella fault, North Pyrenean fault) that strongly structured the lithosphere. Two main
121 scenarios have been proposed for this post-Variscan evolution: one that includes a
122 compressional episode independent of Variscan tectonics [*Arthaud and Matte*, 1975, 1997]
123 and a second that proposes an extensional to transtensional phase related to the post-orogenic
124 collapse of the chain [*Burg et al.,* 1994a, 1994b].

125 The following Triassic to Jurassic rift events resulted in the formation of intra-continental
126 basins bounded by NE–SW trending normal faults that may partly reactivate Palaeozoic
127 structures (e.g. Aquitaine basin: [*Curnelle et al.,* 1982]). They are filled by thick sequences of
128 Triassic siliciclastics, carbonates and evaporites (Germanic Facies: [*Curnelle*, 1983;
129 *Fréchengues*, 1993]). Deposits belonging to the Keuper formation are associated with
130 tholeitic magmatism [e.g. *Montadert and Winnock*, 1971; *Winnock*, 1971; *Rossi et al.,* 2003].
131 The latest Triassic and Jurassic marine transgression led to the formation of a carbonate
132 platform whose lateral extent is poorly constrained.

133 A major change occurred in the Late Jurassic to Early Cretaceous, related to the northward
134 propagation of the Atlantic rift. The deposition of marine sediments in the Western Bay of
135 Biscay is contemporaneous with the E–W reorganisation of the depocenters in the present-day
136 Arzacq, Tarbes and Parentis basins [*BRGM*, 1974; *Biteau et al.,* 2006]. Extreme crustal
137 thinning in the Bay of Biscay resulted in continental break-up and seafloor spreading
138 initiation during latest Aptian to early Albian time [e.g. *Montadert et al.,* 1979b; *Boillot*,
139 1984]. At this stage, crustal and mantle exhumation in onshore rift basins (e.g. Basque–
140 Cantabrian and Arzacq–Mauléon basins: [*Jammes et al.,* 2009; *Lagabrielle et al.,* 2010; *Roca*
141 *et al.,* 2011]) is related to an acceleration of subsidence. This event is recorded by the

deposition of deep marine sediments [*Ducasse and Velasque*, 1988]. It is accompanied by alkaline magmatism (including intrusions and volcanic products) from Late Aptian to Early Santonian time (~113 to 85 Ma; [*Lamolda et al.,* 1983; *Montigny et al.,* 1986]).

Onset of compressional deformation is recorded in Santonian sediments by a regional unconformity [*Garrido-Megías and Rios,* 1972; *McClay et al.,* 2004] and a weak reactivation in the Northern Bay of Biscay [*Thinon et al.,* 2001]. The major collision phase was reached during the Eocene and continued until the end of the Oligocene [*Muñoz*, 2002; *Vergés et al.,* 2002] with the generalized uplift of the chain and formation of foreland basins.

Because this paper is mainly focused on the formation and reactivation of hyperextended basins, we will sub-divide the sedimentary deposits into pre-, syn-, and post-hyperextension and syn- to post-compressional sequences.

2.2. A controversial Late Jurassic to Early Cretaceous plate kinematic context

At present, there is no consensus on the Late Jurassic to Early Cretaceous kinematic evolution leading to the formation of the Bay of Biscay. Opening in a back-arc setting is proposed by *Sibuet et al.* [2004] and *Vissers and Meijers* [2012]. Other hypotheses suggest that left-lateral strike-slip to transtensional deformation was accommodated along the North Pyrenean fault or within pull-apart basins [e.g. *Le Pichon et al.,* 1971; *Mattauer and Séguret*, 1971; *Choukroune and Mattauer*, 1978].

Most of the plate kinematic models proposed previously rely on the identification and restoration of magnetic anomalies of the M-series in the North Atlantic between Iberia and Newfoundland [e.g. *Olivet*, 1996; *Srivastava et al.,* 2000; *Sibuet et al.,* 2004]. These restorations assume minor pre-breakup movements. This hypothesis is questioned by the discovery of hyperextended domains that can be mapped over hundreds of kilometres continentward of the first unambiguous magnetic anomaly related to breakup [*Tucholke et al.,* 2007 or *Péron-Pinvidic and Manatschal*, 2009]. Controversies also arise from the

interpretation of the age and nature of magnetic anomalies in the Bay of Biscay and the southern North Atlantic in general., The M-series (M3-M0, 126 to 118.5 Ma) identified in the Iberia–Newfoundland and Bay of Biscay margins [e.g. *Sibuet et al.,* 2004] have been reinterpreted as either related to mantle exhumation [*Sibuet et al.,* 2007] or magmatic underplating [*Bronner et al.,* 2011 and references therein]. Therefore, these anomalies do not necessarily represent isochrons. This justifies a revision of existing plate kinematic models depending on the restoration of the M-series magnetic anomalies [see *Bronner et al.,* 2011, 2012 and *Tucholke and Sibuet*, 2012].

Based on these new discoveries combined with field observations, new plate kinematic scenarios were proposed. Some authors suggested that the left lateral displacement of the Iberian plate was already initiated in the Late Jurassic, resulting in a transtensional setting along the European and Iberian plates [e.g. *Wortmann et al.,* 2001; *Schettino and Scotese*, 2002; *Canérot*, 2008, *Jammes et al.,* 2009, 2010a]. Indirect evidence for this pre-Aptian movement comes from the thick Late Jurassic to Early Cretaceous sedimentary sequences in the Parentis and Cameros basins [e.g. *Salas and Casas*, 1993; *Mas et al.,* 1993; *Jammes et al.,* 2010a]. A major break occurred in Aptian time [*Olivet*, 1996] as a result of the counter-clockwise rotation of Iberia [*Gong et al.,* 2008; *Jammes et al.,* 2009, 2010a]. As a consequence of this rotation, a NNE–SSW to NE–SW extension is initiated in rift basins preserved onshore [*Jammes et al.,* 2009; *Lagabrielle et al.,* 2010; *Roca et al.*, 2011; *Tavani*, 2012] as emphasized by the NE–SW segmentation observed (e.g. Pamplona, Toulouse, Cevennes faults). These NE–SW transfer faults cross the Iberian-European plate boundary and are locally sealed by Albian sediments (Pamplona fault, between the Basque–Cantabrian and Arzacq–Mauléon basins; [*Razin,* 1989; *Claude,* 1990]). In this paper, we will show that the complex polyphased history strongly influenced the 3D architecture of the Bay of Biscay-Parentis and Pyrenean-Basque-Cantabrian rift systems.

2.3. Pyrenean reactivation and shortening estimations

The palaeogeographic evolution of the Bay of Biscay and Iberia–Newfoundland rifted margins is relatively well-constrained after the quiet magnetic period of the Cretaceous and the identification of the magnetic anomaly 34 (83 Ma, Santonian) [e.g. *Roest and Srivastava*, 1991; *Rosenbaum et al.,* 2002]. The northward movement of the African plate during the Late Cretaceous resulted in the initiation of compression in the Bay of Biscay and the Pyrenees. Although the shortening direction is reasonably coherent between different kinematic models (N–S to NE–SW; respectively [*Roest and Srivastava*, 1991; *Rosenbaum et al.,* 2002]), the total amount of Late Cretaceous relative to Cenozoic shortening is still a matter of debate. At the scale of the Bay of Biscay and Pyrenean–Cantabrian orogen, the transition from embryonic subduction in the North Iberian margin to continental collision in the Pyrenees is interpreted to have resulted from an increase in convergence from west to east. Based on the restoration of magnetic anomalies, *Rosenbaum et al.* [2002] estimated about 144 km of shortening in the Western Pyrenees as compared to 206 km in the Eastern Pyrenees. Classical palinspastic restorations of sections across the Pyrenees have usually been based on restorations of the thick-skin deformation observed in the Axial zone [e.g. *Teixell*, 1998; *Muñoz*, 2002]. This approach underestimates the shortening related to the reactivation of hyperextended domains. It is therefore unable to decipher the overall amount of convergence accommodated in the Pyrenean domain.

3. Mapping hyperextended domains: combining onshore and offshore observations

3.1. Hyperextended rift domains: terminology and identification

In spite of variable magmatic, structural and sedimentary evolution, that in turn depend on the amount and rates of extension, thermal history and inheritance, most magma-poor rifted margins share comparable large-scale architectures [*Reston*, 2009; *Péron-Pinvidic et al.,* 2013]. Using first-order geological and/or geophysical observations, distinctive structural rift

217 domains can be identified. From continent to ocean the following domains can be
218 distinguished: the proximal, necking, hyperthinned, exhumed mantle and oceanic domains
219 (fig 2, see also fig 1 in *Tugend et al.* accepted for comparison with alternative classifications).
220 Extensional deformation related to the formation of these domains is polyphased,
221 progressively localizing towards the location of final break-up [e.g. *Péron-Pinvidic and*
222 *Manatschal*, 2009; *Sutra et al.,* 2013]. Therefore, these domains reflect successive steps in the
223 formation of magma-poor rifted margins, suggesting that they may also correspond to genetic
224 domains.

225 We use the approach developed by *Tugend et al.* [accepted] to enable the characterization
226 and identification of comparable rift domains in present-day magma-poor rifted margins and
227 their fossil analogues preserved in collisional orogens (fig 2). This approach and its related
228 results are summarized hereafter. Offshore, quantitative techniques provide estimations of
229 accommodation space, crustal thickness and lithosphere thinning while seismic interpretation
230 enables the recognition of extensional settings (low- and high-β settings; [*Wilson et al.,*
231 2001]). Onshore, the identification relies on the description of key outcrops preserving the
232 nature of sediments, basement rocks and of their interface. This geological/geophysical
233 approach can be further used as an interface between onshore and offshore observations and
234 to suggest analogies. Offshore seismic interpretations can take advantage of onshore
235 observations regarding the nature of sediment, basement and of their interface. The large scale
236 geometry and stratigraphic architecture imaged offshore can be used to restore onshore fossil
237 remnants back into a rifted margin context (fig 2).

238 This combined approach is applied for the first time to map the overall rift system from the
239 offshore Bay of Biscay to its onshore fossil analogues preserved in the Pyrenees (including
240 the Basque–Cantabrian basin). Interpretations of structural domains along offshore seismic
241 reflection profiles are combined with mapping of crustal thickness, lithosphere thinning and

242 Moho depth using gravity inversion. Onshore mapping relies on the identification of remnants
243 of the rift system preserved within well-defined compressive tectonic units.

244 ***3.2. Onshore: Mapping remnants of the rift system***

245 The mapping of rift domains in onshore deformed analogues depends on the ability to
246 decipher the deformation and sedimentary history. The definition of compressive units is
247 based on the identification of first order compressive structures corresponding to the first
248 generation of thrusts. These coherent tectonic units are usually bounded by major thrust
249 contacts, but are often only weakly deformed internally. The methodology used to map rift
250 domains onshore is here exemplified by the example of the Arzacq–Mauléon basin. A
251 summary of main observations is given below and summarized in fig 3 [detailed descriptions
252 of field observations in *Jammes et al.,* 2009; *Tugend et al.,* accepted].

253 *3.2.1. Defining coherent tectonic units: history of compressional deformation*

254 In the Arzacq–Mauléon basin different phases of deformation can be identified resulting in
255 two opposite directions of thrusting. The shortening related to the initiation of Pyrenean
256 compression is accommodated by Late Cretaceous, south-directed thrust systems (e.g.
257 Sarrance, Mail Arrouy or Lakoura thrust systems; [*Casteras et al.,* 1970a; 1970b; 1970c;
258 *Teixell*, 1998]; figs 2 and 3). This initial sampling of the distal parts of the former rift system
259 is locally overprinted by a second phase of deformation resulting in north-directed thrusts
260 (e.g. the Saint Palais, Sainte Suzanne and Ossau thrusts; [*Canérot et al.,* 2001]) and south-
261 directed back-thrusting in the Axial zone (e.g. Gavarnie, Guarga thrust systems; [*Teixell*,
262 1998]). As a result of this structural analysis several tectonic units can be defined within the
263 Arzacq–Mauléon basin (fig 2). Within each unit, key outcrops preserving primary contacts
264 between basement and the pre-, syn-, and post-hyperextensional sediments can be found [e.g.
265 *Canérot*, 2008; *Jammes et al.,* 2009, *Lagabrielle et al.,* 2010; *Debroas et al.,* 2010; Masini et
266 al. 2014].

267 *3.2.2. Outcrops preserving remnants of the former rift system*

268 Remnants of rift domains can be defined in the Arzacq-Mauléon basin from South to North
269 (fig 2 and 3, see also [*Tugend et al.,* accepted]).

270 *In the axial zone (southernmost external Pyrenean unit) – former proximal rift domain,*
271 upper crustal rocks from the basement are eroded and directly onlapped by shallow marine
272 post-hyperextensional sediments (fig 3) suggesting no or only a weak rift-related thinning.

273 *In the Bedous–Mendibelza unit – former necking domain,* the exhumed basement of the
274 Mendibelza and Igounze massifs [*Johnson and Hall*, 1989a, 1989b; *Miranda-Avilez et al.,*
275 2005; *Masini et al.,* 2014] is onlapped by syn-hyperextension sequences progressively
276 thickening and deepening northwards. This domain marks a progressive transition from
277 shallow to deep-water sediments (conglomerates from the Mendibelza formation, passing
278 laterally to turbidites and marls) as a consequence of the initiation of crustal thinning.

279 *In the Layens–Labourd unit – former hyperthinned domain,* granulites derived from the
280 pre-hyperextension middle crust [*Vielzeuf*, 1984] are exhumed in the Labourd massif [*Jammes*
281 *et al.,* 2009]. They are onlapped by late syn-to post-hyperextension sediments containing
282 reworked pieces of exhumed granulite (Bonloc breccias; [*Claude*, 1990]). Observations from
283 this domain indicate that at least locally, the whole upper crust had been removed and
284 consequently the crust had to be thinned.

285 *In the Sarrance – Mail Arrouy unit (internal orogenic unit) – former exhumed mantle*
286 *domain,* syn-hyperextension sediments are more than 4 km thick near the city of Mauléon
287 [*Roux*, 1983; *Fixari*, 1984; *Souquet et al.,* 1985]. Numerous outcrops of mantle rocks are
288 observed associated to thin slices of continental crust [*Duée et al.,* 1984; *Fortané et al.,* 1986;
289 *Lagabrielle et al.,* 2010; *Debroas et al.,* 2010]. Mantle rocks are also reworked in
290 Cenomanian breccias indicating that at least locally, mantle rocks had to be exhumed at the

291 seafloor (fig 3; e.g. Urdach breccias: [*Jammes et al.,* 2009; *Lagabrielle et al.,* 2010; *Debroas*
292 *et al.,* 2010; *Masini et al.*, 2014]).

293 *In the Grand Rieu high unit – former hyperthinned domain,* a thick post-hyperextension
294 sequence may directly onlap onto basement as indicated by the Cardesse 2 drill-hole (location
295 fig 3; [*BRGM*, 1974; *Serrano et al.,* 2006]). This local observation may reflect a large
296 sedimentary aggradation consecutive to post-hyperextension thermal subsidence in a former
297 hyperthinned domain (fig 2).

298 *In the Arzacq basin – former proximal to necking domain*: the progressive thinning of the
299 continental crust (from about 25 km to the north to about 20 km below the Grand Rieu high;
300 [*Daignières et al.,* 1982, 1994]) is concomitant with a southward thickening of syn-
301 hyperextension sequences [*Biteau et al.,* 2006]. This progressive creation of accommodation
302 space may indicate the progressive transition from a proximal to a necking domain (from
303 north to south).

304 The mapping of former rift domains onshore relies on the exposed surface observations
305 (here locally supported by drill-hole data) and reflects the integration of the former rift into
306 the orogenic system.

307 ***3.3. Offshore: seismic interpretations and gravity inversion mapping***

308 Gravity inversion results have already been used to characterize and identify structural
309 domains on 2D sections at rifted continental margins (fig 2; [*Tugend et al.,* accepted]). In this
310 paper, the aim is to associate this technique with local seismic interpretations to map and
311 unravel the spatial evolution of structural/genetic rift domains from the offshore Bay of
312 Biscay to the onshore Mesozoic Arzacq basin buried under post-hyperextension sediments
313 and the thick syn-compressional sequences of the Tertiary Aquitaine basin.

314 *3.2.1. Gravity inversion: scheme and datasets*

315 Gravity inversion was based on public domain data (fig 4): free air gravity [*Sandwell and*
316 *Smith,* 2009], bathymetry [*Smith and Sandwell*, 1997] and oceanic isochrons [*Müller et al.,*
317 1997]. Information on sedimentary thickness comes from a compilation of offshore seismic
318 interpretations combined with the depth to basement map of the Aquitaine basin from Serrano
319 *et al.* [2006] (fig 4). Seismic reflection data were derived from different surveys: the Norgasis
320 survey [*Avedik et al.,* 1993, 1996; *Thinon* 1999], the ECORS Bay of Biscay section [*Pinet et*
321 *al.,* 1987; *Bois and Gariel*, 1994], the IAM 12 and the ESCIN 4 seismic lines [e.g. *Banda et*
322 *al.,* 1995; *Gallastegui et al.,* 2002; *Gallart et al.,* 2004].
323 Moho depth, crustal thickness, continental lithosphere thinning factor and residual
324 continental crust maps (fig 5) were produced by gravity inversion. This technique includes a
325 thermal gravity anomaly correction and a parameterization of decompression melting to
326 predict volcanic additions (detailed scheme described by [*Greenhalgh and Kusznir*, 2007;
327 *Chappell and Kusznir*, 2008a; *Alvey et al.,* 2008; *Cowie and Kusznir*, 2013]; parameters for
328 this study are presented in table 1). A compaction controlled density-depth relationship is
329 applied to sedimentary sequences [*Chappell and Kusznir*, 2008b].

330 *3.2.2. 3D mapping derived from gravity inversion and seismic interpretations*

331 The maps resulting from gravity inversion presented in fig 5 were computed assuming a
332 "normal" volcanic addition (corresponding to a standard oceanic crust thickness of about 7
333 km; [*White et al.,* 1992]). This solution assumes the occurrence of decompression melting
334 during rifting once the lithosphere is thinned below a critical value (γ = 0.7; table 1),
335 producing magmatic additions to the extended continental crust. In the case of a magma-poor
336 rifted margin as proposed for the Bay of Biscay [e.g. *De Charpal et al.,* 1978; *Montadert et*
337 *al.,* 1979b; *Avedik et al.,* 1982; *Le Pichon and Barbier*, 1987; *Thinon et al.,* 2003] the
338 transition zone between unequivocal oceanic and continental crusts may be interpreted as
339 exhumed mantle (fig 2). The characterisation of structural domains on 2D sections (fig 2)

partly relies on diagnostic elements determined from gravity inversion results [*Tugend et al.,* accepted]. The combined analysis of Moho depth, crustal thickness and lithosphere thinning maps (fig 4) can be further used to delimit offshore structural domains and identify their evolution in 3D.

The proximal domain presents relatively constant and limited values of crustal and lithosphere thinning (fig 5d) and a smooth Moho topography (fig 5a). The rapid increase in lithospheric thinning values coincides with a Moho rise delimiting the proximal from the necking domain (fig 5a/d). The transition from the necking to hyperthinned domain can be identified on seismic sections (fig 2; e.g. [*Sutra et al.,* 2013]) and corresponds in this example to thinning values between 0.5 to 0.6 and crustal thicknesses of about 10 to 15 km (fig 5b/c). The beginning of the exhumed mantle domain can be interpreted at a first order at the termination of the continental crust (fig 5c). Moho topography derived from gravity inversion [*Greenhalgh and Kusznir*, 2007; *Chappell and Kusznir*, 2008a; *Alvey et al.,* 2008] is slightly curved through this domain enabling the shallowest Moho depth to be reached (fig 5a). Gravity inversion provides indirect observations compatible with the existence of an exhumed mantle domain in the Bay of Biscay. This hypothesis is further supported by reflection and refraction seismic interpretations [e.g. *Fernández-Viejo et al.,* 1998; *Thinon et al.,* 2003; *Ruiz*, 2007] and by analogy with the existence of such a domain onshore (Arzacq–Mauléon; fig 3). The oceanic domain is marked by a deepening of the Moho (fig 5a) and a thickening of the crust at the oceanward edge of the exhumed mantle domain (fig 5b). Residual patches of thicker crust are observed within the oceanic domain (fig 5 c/d) and can be interpreted as a locally overthickened oceanic crust (in comparison with the 7 km thick volcanic addition used for gravity inversion; table 1).

The resulting maps show the present day distribution of oceanic and continental crust as well as a possible extent of exhumed mantle in the Bay of Biscay. In areas that underwent

365 reactivation and crustal thickening during compression (e.g. the North Iberian margin), these
366 maps need to be interpreted carefully and are further constrained by seismic interpretations.
367 Onshore, in the Western Pyrenees, the former rift-related thinning of the northern Arzacq
368 basin can still be deduced from lithosphere thinning and crustal thickness maps (fig 5).

369 **4. Map of the Bay of Biscay–Pyrenean rift system (fig 6)**

370 Offshore and onshore observations are combined to recognize, describe and map
371 structural/genetic rift domains and their compressional overprint from the Bay of Biscay to
372 the Pyrenean-Cantabrian orogen (fig 6). We apply the terminology and
373 geological/geophysical approach described in the previous section and synthetized in fig 2
374 (see also *Tugend et al*., accepted).

375 ***4.1. Definition of rift domains***

376 *4.1.1. Proximal domain*

377 Proximal domains are characterized by only weak to no rift-related lithosphere and crustal
378 thinning (fig 5). Creation of accommodation space is restricted to graben and half-graben
379 basins characterizing low-β extensional systems (fig 2). The sedimentary record of this
380 domain may include sub-aerial exposure, continental to shallow water sedimentary systems,
381 and no or minor aggradation of post-rift sequences (figs 2 and 3).

382 Offshore, this domain corresponds to the continental shelves (e.g. the Armorican platform,
383 the western part of the North Iberian shelf, near Ortegal Spur, Landes high; fig 6). Onshore, it
384 can be mapped in external parts of the orogen and may be partly buried below Tertiary
385 foreland basins such as the Duero basin (south of the Basque–Cantabrian orogen), the Jaca
386 and Ebro basins south of the Pyrenees or in the northern part of the Aquitaine basin (fig 6).

387 *4.1.2. Necking domain*

Lithosphere and crustal thinning are initiated in the necking domain (fig 5). The oceanward increasing accommodation space and deepening of the top basement coincides with the ascending Moho topography defining a taper geometry [*Osmundsen and Redfield*, 2011]. The necking domain is limited by the oceanward embrittlement of the continental crust in the hyperthinned domain [*Pérez-Gussinyé and Reston*, 2001] that controls mode of deformation of the continental crust [*Sutra et al*., 2013]. Deformation is decoupled at mid-crustal ductile levels in the necking domain [*Sutra et al.,* 2013]. In the hyperthinned domain, deformation is coupled at the scale of the crust, i.e. faults may cut through the remaining continental crust and penetrate into mantle [*Pérez-Gussinyé and Reston*, 2001]. The transition from decoupled to coupled deformation at a crustal scale is interpreted to occur at the coupling point [*Sutra et al.,* 2013]. It is accompanied by a tectonic migration of the deformation indicated by a change in the age of the syn-tectonic sediments that are getting younger oceanwards (as observed for the Iberian margin [Péron-Pinvidic *et al.,* 2007] or in the Alps [Mohn *et al.* 2010, Masini *et al.* 2013]). Tilted block geometries and/or exhumation surfaces related to top basement detachment faulting can be observed (fig 2). The sedimentary architecture can often be defined by offlapping packages and by onlaps backwards onto the basement of the necking domain (outcrop scale observations; fig 2). The progressive creation of accommodation space can be recorded by deltaic sedimentary systems or slope facies including gravitational systems. A transition from shallow to deeper marine environments can also be observed in underfilled basins (fig 2).

In the Bay of Biscay, the necking domain corresponds to the continental slope of the Western Approach (over the Meriadsek Terrace), Armorican and North Iberian margins (including the "Le Danois basin" in the eastern part; fig 6). The southern part of the Basque–Cantabrian basin, the Organya and Pedraforca basins (as suggested by the restorations of [*Muñoz*, 1992; *Vergés and Garcia-Senz*, 2001; *Lagabrielle et al.,* 2010]) and most of the

413 Arzacq basin may represent fossil analogues of this domain (fig 6). Narrow remnants of this
414 domain can also be mapped in basins from the eastern and western Pyrenees, respectively
415 south of the North Pyrenean Frontal thrust and north of the Lakoura thrust (fig 6; e.g. in the
416 Mendibelza massif [*Masini et al.,* 2014]).

417 *4.1.3. Hyperthinned domain*

418 Continental crust is typically less than 15 to 10 km thick and associated with a large
419 accommodation space (figs 2 and 5). Both low and high-β extensional settings may be
420 observed (fig 2) and are characterized by half-graben and hyperextended sag basin
421 architectures (fig 2 in [*Tugend et al.,* accepted]). Top basement detachment faults commonly
422 lead to local exhumation of mid to lower crustal levels as observed in onshore fossil remnants
423 (e.g. [*Manatschal*, 2004]; fig 2). The infilling history of this domain mainly depends on
424 sedimentary supply and sedimentary sources but is usually associated to thick aggradational
425 sequences and/or deep marine sedimentary sequences (fig 2).

426 The occurrence of extremely thinned continental crust was already recognized in the
427 Parentis basin [e.g. *Pinet et al.,* 1987; *Bois and Gariel*, 1994; *Tomassino and Marillier*, 1997]
428 and at the toe of the continental slope of the Armorican and Western Approach margins
429 ("neck area" in *Thinon et al.* [2003]). In the southern Bay of Biscay, this domain is integrated
430 into the accretionary prism of the North Iberian margin, as indicated by refraction velocities
431 [e.g. *Ruiz*, 2007; *Gallart et al.,* 2004; *Roca et al.,* 2011; *Fernández-Viejo et al.,* 2012].
432 Onshore in the Pyrenees (fig 6), this domain is characterized by numerous granulitic rocks
433 (e.g. in the Labourd, Trois Seigneurs, Agly massifs) interpreted as mid to lower crustal rocks
434 [e.g. *Vielzeuf*, 1984] exhumed during Cretaceous rifting [e.g. *Jammes et al.,* 2009; *Vauchez et*
435 *al.,* 2013].

436 *4.1.4. Exhumed mantle domain*

437 The onset of the exhumed mantle domain can be observed where complete thinning of the
438 continental crust is achieved (fig 5c/d). Local remnants of continental crust may be preserved
439 as extensional allochthons on top of the exhumed mantle basement of this domain (outcrop
440 scale observation; fig 2). The seismic reflection pattern and velocity structure described from
441 suspected and drilled exhumed mantle domains contrasts with the adjacent hyperthinned and
442 oceanic domains. Seismic reflection observations show a complex set of deep intra-basement
443 reflections (e.g. Armorican margin: [*Thinon et al.,* 2003]; Iberian margin: [*Pickup et al.,* 1996;
444 *Dean et al.,* 2001; *Reston and McDermott*, 2011; *Sutra et al.,* 2013]). Refraction studies
445 indicate a downward gradient of velocities commonly interpreted as the progressive decrease
446 in serpentinization with depth [e.g. *Minshull*, 2009; *Reston*, 2009, 2010]. Magmatic additions
447 can also be observed within this domain, as indicated by the local occurrence of syn- to post-
448 hyperextension alkaline magmatism in onshore remnants of exhumed mantle in the Pyrenees.
449 Offshore, volcanic bodies and volcanoclastic sediments are interpreted on the Armorican
450 margin [*Thinon et al.,* 2003]. This magmatic overprint may progressively become more
451 important toward the oceanic domain. Hyperextended sag basins are often observed in the
452 exhumed mantle domain, sometimes extending to the hyperthinned and necking domains in
453 the case of overfilled basins (e.g. the Angola margin; [*Unternehr et al.,* 2010]).
454 Exhumed mantle has already been proposed to floor the Armorican basin, [*Thinon et al.,*
455 2003] and suggested in the South Iberian margin [*Roca et al.,* 2011]. Gravity inversion results
456 combined with seismic interpretations enable us to map the eastern termination of the
457 exhumed mantle domain towards the hyperthinned Parentis basin (fig 6). Onshore, this
458 domain is characterized by the occurrence of mantle bodies and Mesozoic metamorphic rocks
459 included in tectonic units near the North Pyrenean fault in the Pyrenees (fig 6; e.g. [*Monchoux*
460 1970; *Fabriès et al.,* 1991, 1998; *Lagabrielle and Bodinier*, 2008; *Lagabrielle et al.,* 2010;

461 *Clerc et al.,* 2012, 2013]) or within the so-called Nappe des Marbres in the Basque–
462 Cantabrian basin (fig 6; [*Lamare* 1936; *Mendia and Gil-Ibarguchi*, 1991]).

463 *4.1.5. Oceanic domain*

464 The transition to the oceanic domain is characterized by a deepening of the Moho and the
465 ramp morphology of the basement referred to as an outer high [P*éron-Pinvidic and*
466 *Manatschal*, 2010; *Péron-Pinvidic et al.,* 2013]. Refraction data across this basement high in
467 the Bay of Biscay indicate the presence of an underplated high-velocity body originating in
468 the exhumed mantle domain [*Thinon et al.,* 2003]. This velocity structure may suggest a
469 possible overlap between the exhumed mantle and oceanic domains [see also *Roca et al.,*
470 2011]. It may be interpreted as an underplated gabbroic body similarly to the interpretation of
471 *Bronner et al.* [2011] for the Iberian–Newfoundland rifted margins. It may also represent the
472 oceanward termination of serpentinized mantle [*Thinon et al.,* 2003] that is overprinted by the
473 first oceanic crust. Both interpretations suggest a possible overlap or transition zone between
474 the exhumed mantle and oceanic domains. A specific seismic pattern is also observed,
475 characterized by diffractive and irregular reflections in the upper basement [*Thinon et al.,*
476 2003] and locally strong reflections parallel to the top basement at deeper levels [*Sutra et al.,*
477 2013]. The first onlapping and overlying sediments are of post-rift age. In the central part of
478 the Bay of Biscay, one drill-hole (DSDP site 118, leg 12; [*Laughton et al.,* 1972]) reached the
479 oceanic basement. This domain is characterized by E–W to ESE–WNW trending magnetic
480 anomalies [*Matthews and Williams*, 1968] attributed to the magnetic anomaly 34 [e.g.
481 *Srivastava et al.,* 1990]. The absence of the magnetic anomaly 33 [*Cande and Kristoffersen*,
482 1977] suggests that seafloor spreading stopped after anomaly 34 and before anomaly 33,
483 corresponding to Santonian–Early Campanian time [e.g. *Montadert et al.,* 1979a; 1979b]. No
484 remnants of oceanic domain (ophiolites) can be observed onshore in the Pyrenean or Basque
485 Cantabrian basins (*Lagabrielle and Bodinier*, 2008).

4.2. Key structures and lateral extent of domains

The definition of rift domains also relies on the identification of key structures (i.e. compressional, extensional and transfer fault systems) as they represent markers of the deformation during the different extensional and compressional events.

4.2.1. Compressional systems

The overall WNW to ESE trend of compressional structures (foreland basins, boundary between internal and external domains) results from the Iberian/European convergence. Compressional deformation is important in the Southern Bay of Biscay and controls the evolution of the North Iberian frontal thrust system [e.g. *Derégnancourt and Boillot*, 1982; *Roca et al.,* 2011; *Fernández-Viejo et al.,* 2011, 2012]. In its eastern termination it represents the boundary between continental and oceanic domains without evidence for oceanic subduction ([*Ayarza et al.,* 2004]; refraction data along the IAM 12 line; [*Fernández-Viejo et al.,* 1998]). To the West, it delimits the accretionary prism and reactivation in the exhumed mantle domain [*Roca et al.,* 2011; *Fernández-Viejo et al.,* 2012]. Locally NW–SE trending thrusts are observed in the Northern Bay of Biscay, mainly located at domain transitions [*Thinon et al.,* 2001].

Most of the compressive structures can be observed onshore. The North and South Pyrenean frontal thrusts delimit the almost E–W trending Pyrenean–Cantabrian orogen from the adjacent foreland basins. Onshore remnants of rift domains are delimited by thrusts systems. Among them, the North Pyrenean fault [e.g. *Mattauer*, 1968; *Choukroune and Mattauer*, 1978] and Basque–Cantabrian equivalent, the Leiza fault [*Boillot et al.,* 1973; *Choukroune*, 1976; *Rat*, 1988; *Combes et al.,* 1998; *Mathey et al.,* 1999] can be mapped discontinuously.

4.2.2. Extensional faults

NW–SE to E–W trending extensional structures can be mapped in the Northern Bay of Biscay [*Derégnancourt and Boillot*, 1982; *Thinon*, 1999; *Thinon et al.,* 2003] related to the rifting phase in the Bay of Biscay. Top basement detachment faults may develop to become the boundary between the proximal and necking domains (e.g. Southern boundary of the Parentis basin, [*Jammes et al.,* 2010b, 2010c]). Only few half-graben basins (i.e. low-β extensional settings; fig 2) are described from the hyperthinned domain of the Armorican margin [Thinon 1999; Thinon *et al.,* 2003]. Remnants of extensional rift structures and top basement extensional detachment faults are described locally onshore in the Mauléon basin [e.g. *Canérot et al.,* 1978; *Canérot*, 1989; *Johnson and Hall*, 1989a, 1989b; *Jammes et al.,* 2009; *Masini et al.*, 2014], in the Aulus basin [e.g. *Lagabrielle et al.,* 2010] or in the Basque–Cantabrian basin [e.g. *Tavani and Muñoz*, 2012; *Bodego and Agirrezabala*, 2013 and reference therein].

4.2.3. Transfer/transform faults

A striking observation resulting from this mapping is the importance of transfer faults. These structures strongly segment offshore and onshore rift systems. The segmentation of the Northern Biscay margin is characterized by NE–SW transfer faults [*Derégnancourt and Boillot*, 1982; *Thinon et al.,* 2003] that may be partly related to the Variscan structuration observed onshore [*Thinon*, 1999]. The offshore prolongation over the continental shelf is underlined by magnetic and gravity trends and is suggested to be partly controlled by the Armorican shear zone [e.g. *Sibuet*, 1973; *Thinon,* 1999]. The influence of the inferred structures can be observed on the segmentation of the limit between necking and exhumed mantle domains between the Goban Spur, Western Approach and Armorican margins (fig 6). Other inherited structures locally break the NW–SE straight orientation of the southern part of the Armorican margin [*Thinon*, 1999], but the control of these structures on the subsequent rift structures is complex and not directly observable. In contrast, the South Iberian margin is

segmented by NW–SE structures [*Derégnancourt and Boillot*, 1982], such as the Ventaniella fault that records a Permo-Carboniferous post-Variscan evolution [*Burg et al.,* 1994a, 1994b].

Fossil remnants of the rift system preserved in the Pyrenean-Cantabrian orogen are segmented by NNE–SSW to NE–SW trending structures. These structures may result from the partial reactivation of Permo-Carboniferous strike-slip or transfer faults [*Arthaud and Matte*, 1975, 1997; *Burg et al.,* 1994a, 1994b]. Locally they may have been reactivated as normal faults during the formation of Permo-Triassic intra-continental basins [*Curnelle et al.,* 1982]. The observed segmentation may reactivate existing faults, but these pre-existing faults (Permian or older) cannot be traced with confidence across the Pyrenees.

To the east, the Cevennes fault system delimits the Pyrenean from the Provencal domain (fig 6); to the south, it also may partly control the shape of the South Pyrenean compressional thrust system [*Vergés et al.,* 2002; *Muñoz*, 1992].

The Toulouse fault, also referred to as the Villefrance or Sillon Houiller fault, can be mapped from the Massif Central region to the northern Aquitaine basin (fig 6). The southern continuation towards the Pyrenees delimits the eastern termination of the Arzacq–Aquitaine basin from the Occitan high [*Curnelle et al.,* 1982]. This structure can be identified on gravity inversion maps as a major crustal discontinuity (fig 5). In the Axial zone, a transfer zone may be mapped discontinuously at the eastern boundary of a large Carboniferous basin and further to the south to the west of the Organya basin (fig 6) in the South Pyrenean zone (segmentation also described by *Muñoz*, [1992]; *Vergés and García-Senz*, [2001]).

The Pamplona fault delimits the Mauléon and the Basque–Cantabrian basins [*Turner*, 1996]. Although this structure is not exposed continuously, it controlled the Mesozoic sedimentation [*Larrasoaña et al.,* 2003] and represents a major crustal offset observed from gravity modelling (Bouguer anomaly map; [*Jammes et al.,* 2010c]).

559 The segmentation of the Basque–Cantabrian basin is well-defined from its sub-division
560 into an eastern "Alava" and western "Peri-Asturian" domain [e.g. *Rat*, 1988; *García-*
561 *Mondéjar et al.,* 1996]. This NE–SW structuration terminates towards the Landes High to the
562 north. The western termination of Basque–Cantabrian basin is poorly defined due the
563 Cenozoic tectonic uplift and erosion of Mesozoic sediments south of the "Le Danois basin"
564 and north of the Duero basin [*Gallastegui et al.,* 2002; *Pedreira et al.,* 2003, 2007; *Alonso et*
565 *al.,* 2007]. In this area, *Roca et al.* [2011] proposed the existence of the Santander soft transfer
566 zone that would relay the compressional front of the Pyrenees to the north into the Bay of
567 Biscay. This transfer zone may also be suggested from gravity inversion maps (fig 5)
568 facilitating the relay of the necking domain of the South Iberian margin to the South at the
569 eastern termination of the "Le Danois" basin (fig 6).

570 ***4.3. Two distinct rift systems***

571 The previous definition of rift domains, associated structures and segmentation enables us
572 to distinguish two extensional systems: (1) the Bay of Biscay–Parentis rift in the NW and (2)
573 the Pyrenean–Basque–Cantabrian rift to the SE. Both preserve a specific spatial and temporal
574 evolution.

575 *4.3.1 The Bay of Biscay–Parentis rift*

576 The V–shaped Bay of Biscay–Parentis rift system preserves different stages of the
577 lithospheric scale thinning process ranging from hyperthinned basins in the East to oceanic
578 domains in the West. The Parentis basin is interpreted to show a progressive lateral decrease
579 in extension going eastward [*Jammes et al.,* 2010c]. Onshore, a crustal discontinuity is
580 observed (fig 5) that may represent the northern continuation of the Pamplona fault (e.g. the
581 Bordeaux fault; [*Lefort et al.,* 1997]). This structure corresponds to the eastern termination of
582 the Parentis basin. We have mapped the continuation of the relatively sharp necking and

583 hyperthinned domains of the northern Parentis basin westwards into the Armorican margin.
584 To the south, the Landes High forms a weakly thinned crustal block connecting south-
585 westwards to the necking domain of the North Iberian margin (fig 6).

586 The initiation of extensional to transtensional deformation in the Bay of Biscay rift system
587 is difficult to date with precision and relies on local observations. A phase of pre-Cretaceous
588 extensional deformation may be recorded by a late Jurassic subsidence in the Parentis basin
589 [*Brunet*, 1994] and by a thickening of the pre-Cretaceous sequence towards the basin centre
590 (e.g. Ibis fault of *Bois and Gariel*, [1994]; *Jammes et al.,* [2010a, 2010b, 2010c]).
591 Hyperextensional processes may have been initiated during the Early Cretaceous (Berriasian
592 to Barremian) resulting in the formation of the necking and hyperthinned domains. During the
593 late Aptian, mantle may have been exhumed in the Bay of Biscay as suggested by *Thinon et*
594 *al.* [2002]. The onset of sea floor spreading is dated around Aptian-Albian time [*Montadert et*
595 *al.,* 1979b; *Boillot*, 1984; *Vergés and García-Senz*, 2001] but may not be synchronous
596 through the entire Bay of Biscay.

597 The major change in rift domain architecture between the Western Approach and
598 Armorican margins occurs across the Armorican shear zone corresponding to a partially
599 inherited transfer/transform fault (fig 6). A similar change in the overall domain architecture
600 can be observed between the eastern and western North Iberian margin west of the "Le
601 Danois basin" (fig 6).

602 *4.3.2. The Pyrenean–Basque–Cantabrian rift*

603 The Landes High and the Ebro block (fig 6) form weakly thinned crustal blocks delimiting
604 to the North and to the South the Pyrenean–Basque–Cantabrian rift system from the Bay of
605 Biscay–Parentis (figs 5 and 6; see also *Roca et al.,* [2011]) and Central Iberian rift systems
606 [e.g. *Salas and Casas*, 1993; *Salas et al.*, 2001]. Onshore, the overall crustal architecture of
607 the different domains is not preserved. Only remnants included in the compressional nappe

608 stack can be observed. Complete ophiolite sequences that could be considered as remnants of
609 typical oceanic lithosphere are never observed within the Pyrenean–Basque–Cantabrian rift
610 system [Lagabrielle and Bodinier, 2008]. The only Cretaceous magmatic additions observed
611 are Late Aptian to Early Santonian (~113 to 85 Ma; [*Lamolda et al.,* 1983; *Montigny et al.,*
612 1986]) alkaline sills and flows preserved into remnants of an exhumed mantle domain or the
613 overlying sediments. This observation suggests that this extensional system did not evolve
614 into a mature oceanic domain. Furthermore, mantle outcrops are usually associated with small
615 fragments of continental crust (in the Pyrenees: [*Duée et al.,* 1984; *Fortané et al.,* 1986;
616 *Lagabrielle et al.,* 2010; *Debroas et al.,* 2010]; and Basque–Cantabrian basin: [*Mendia and*
617 *Gil-Ibarguchi*, 1991]) indicating that probably only local windows of exhumed mantle
618 existed.

619 The increasing subsidence recorded in the onshore Arzacq and Tarbes basins [*Désegaulx*
620 *and Brunet*, 1990] during the Late Jurassic to Early Cretaceous may indirectly date the onset
621 of transtensional deformation [*Canérot*, 2008; *Jammes et al.,* 2009]). Hyperextension only
622 initiated in the Late Aptian to Albian time in the Pyrenean–Basque–Cantabrian rift [*Jammes*
623 *et al.,* 2009; *Lagabrielle et al.,* 2010] coinciding with the onset of sea-floor spreading in the
624 Bay of Biscay [*Montadert et al.,* 1979b]. The sedimentary record preserved in the Pyrenean–
625 Cantabrian orogen indicates a progressive deepening of the basin from Late Aptian to Mid-
626 Albian (Pyrenees: [*Debroas* 1987, 1990]; Basque–Cantabrian basin: [*García-Mondéjar et al.,*
627 1996, 2005]). Mantle exhumation processes may have lasted until Early Cenomanian as
628 suggested by the reworking of mantle rocks in Mid-Albian to Lower Cenomanian breccias
629 (fig 3; Urdach breccia: [*Jammes* et al., 2009; *Debroas et al.,* 2010; *Lagabrielle et al.,* 2010];
630 Aulus breccia: [*Clerc et al.,* 2012]).

631 In spite of the well-defined NE–SW segmentation, an overall lateral continuity of
632 hyperextended domains can be observed throughout the Pyrenean orogen (fig 6). The

633 Pamplona fault represents a major crustal discontinuity [*Turner*, 1996; *Larrasoaña et al.,*
634 2003; *Jammes et al.,* 2010c] delimiting the Basque–Cantabrian from the Arzacq–Mauléon
635 basin.

636 **5. Structural evolution: insights from geological sections**

637 The mapping of the rift domains across the Bay of Biscay–Pyrenees enables us to
638 characterize the progressive compressional overprint of the former rift systems. To the west,
639 the initiation of reactivation can be investigated to the east, a complete reactivation of rift
640 structures is observed. In order to decipher the possible interaction between the two
641 extensional rift systems during the Late Cretaceous to Oligocene compression, three segments
642 are distinguished (fig 6 and 7): (1) a western "Bay of Biscay segment"; (2) a central "Basque–
643 Parentis segment" preserving heterogeneously reactivated hyperextended domains and (3) an
644 eastern "Pyrenean segment" that is completely inverted, exemplified by the Mauléon–Arzacq
645 basin.

646 ***5.1. Western Bay of Biscay segment***

647 *5.2.1. Constraints from seismic interpretations and gravity inversion*

648 The western Bay of Biscay segment initiates at the western termination of the onshore
649 Pyrenean–Basque–Cantabrian rift system. Located at the junction with the Atlantic Ocean, it
650 preserves the ultimate stage of lithosphere thinning in the Bay of Biscay.

651 In order to characterize the architecture of this domain, two conjugate geological sections
652 are proposed, extending from the proximal to oceanic domains in the Western Approach
653 margin to the North (fig 7a and 8) and across the North Iberian margin to the South (fig 7a
654 and 9). The sediment and basement architectures of these sections are derived from the
655 interpretation of the Norgasis 11-12 seismic sections (fig 8; [*Avedik et al.,* 1993, 1996;
656 *Thinon*, 1999]) and IAM 12 line (fig 8; [*Banda et al.,* 1995; *Alvarez-Marron et al.,* 1997]),

657 extending into the Western Approach and North Iberian margins respectively. Moho depth is
658 determined from gravity inversion results (fig 5; parameters are given in table 1) combined
659 with refraction data under the proximal domain of the North Iberian margin [*Fernández-Viejo*
660 *et al.,* 1998].

661 *5.2.2. Architecture of the Western Approach margin*

662 The rift-related crustal architecture of the Western Approach margin is well preserved.
663 Detailed descriptions of seismic observations supporting the interpretation of this section are
664 proposed by *Tugend et al.,* [accepted] and summarized below. The proximal domain is
665 characterized by half graben-type basins (fig 7a and 8) and by deformation interpreted to
666 decouple at mid-crustal levels. No drill hole has reached the basement of the necking domain,
667 but based on the overlying sedimentary architecture (fig 8) and onshore analogy (fig2;
668 [*Tugend et al.,* accepted]) it is suggested to be structured by a conjugate set of top basement
669 detachment faults delimiting a crustal necking zone [*Mohn et al.,* 2012; *Sutra et al.,* 2013].
670 The hyperthinned domain is characterized by a tilted block architecture limited by short-offset
671 normal faults dipping oceanward (fig 7a and 8). These structures are rooting onto the "S"-
672 reflector (fig 8; [*De Charpal et al.,* 1978; *Montadert et al.,* 1979b; *Thinon*, 1999]) interpreted
673 as the crust-mantle boundary. The southern edge of this domain is proposed to be structured
674 by a top basement detachment fault that exhumed rocks from the lower crust and mantle to
675 the seafloor during the final stage of rifting. The occurrence of an extensional allochthon
676 overlaying the exhumed mantle is proposed. It is delimited at its base by the "S"-reflector on
677 seismic sections (fig 8; [*Thinon*, 1999]). The transition to the oceanic domain may not be a
678 sharp boundary and may result from a progressive magmatic overprint of the exhumed mantle
679 domain as suggested by refraction data [*Thinon et al.,* 2003]. The only important
680 compressional reactivation is observed close to the transition between the exhumed mantle
681 and hyperthinned domains, forming the Trevelyan structure [*Debyser et al.,* 1971;

682 *Derégnaucourt and Boillot*, 1982; *Thinon et al.,* 2001]. The associated thrust fault system is
683 interpreted to root in the serpentinized upper mantle (fig 7a and 8).

684 *5.2.2. Reactivation of the North Iberian margin*

685 The distal part of the North Iberian margin was interpreted in the past as an accretionary
686 prism related to the formation of an oceanic subduction [e.g. *Boillot* 1984; *Alvarez-Marron et*
687 *al.,* 1997]. Based on the refraction results [*Fernández-Viejo et al.,* 1998; *Ruiz*, 2007] any
688 important underthrusting of oceanic crust below the South Iberian margin is precluded.
689 Therefore, many authors suggested a complete or partial overprint of the former rift
690 architecture [*Gallastegui et al.,* 2002; *Fernández-Viejo and Gallastegui*, 2005; *Alonso et al.,*
691 2007; *Roca et al.,* 2011; *Fernández-Viejo et al.,* 2012]. The identification of the rift domains
692 (fig 6) enables us to propose a new interpretation that characterizes the deformation in each
693 rift domain clearly unraveling the role of the rift inherited architecture. No major evidence of
694 reactivation can be observed from the proximal and necking domains preserving their rift-
695 related architecture delimited oceanwards by a crustal necking zone similar to the structures
696 proposed for the Western Approach margin. The accretionary wedge characterizing the distal
697 part of the North Iberian margin (fig 9) is interpreted as the former hyperthinned domain that
698 has been reactivated (fig 7a). Refraction velocities are compatible with the hypothesis of a
699 deformed wedge made of continental crust and sediments rather than of sediments only [*Ruiz*,
700 2007; *Fernández-Viejo et al.,* 2012]. The existence of an exhumed mantle domain is proposed
701 northwards and eastwards and may have also occurred in this part of the Bay of Biscay. We
702 suggest that it may be partly underthrust below the hyperthinned domain during the
703 compressional overprint and formation of a Tertiary flexural basin on top of the oceanic
704 domain (fig 7a and 9*;* [*Alvarez-Marron et al.,* 1997]). In our interpretation the exhumed
705 serpentinized mantle represents a low friction surface between the hyperthinned domain and
706 the oceanic domain (fig 7a).

5.2. Eastern Bay of Biscay: Parentis and Basque–Cantabrian segment

5.2.1. Constraints from geological and geophysical datasets

In the Parentis and Basque–Cantabrian segment, both preserved and reactivated rift structures can be investigated. The eastern Bay of Biscay is characterized by its progressive termination into the hyperthinned Parentis basin. Eastwards this segment terminates towards the Pamplona fault delimiting the Basque–Cantabrian basin from the Western Pyrenees.

The geological section shown in fig 7b is based on the interpretation of the sedimentary and top basement architecture of the ECORS Bay of Biscay section [*Pinet et al.,* 1987; *Bois and Gariel*, 1994] located in the Parentis basin. The southward extension into the Basque–Cantabrian basin is based on published field studies supported by local sub-surface data [*IGME*, 1987]. Moho depth is based on refraction studies in the Parentis basin [*Tomassino and Marillier*, 1997]. In the Basque–Cantabrian basin, the crustal architecture is based on one of the possible solutions derived from gravity and magnetic modelling proposed by Pedreira *et al.* [2007].

5.2.2. The rift architecture preserved in the Parentis basin

The Parentis basin is only weakly reactivated in its central part and the overall rift-related sedimentary and crustal architectures are relatively well preserved (fig 7b). The architecture of the basin is strongly asymmetric unravelling a major crustal discontinuity towards the emplacement of the so-called sub-vertical Ibis fault [fig 7b; *Jammes et al.,* 2010a, 2010b, 2010c]. The northern geometry is characterized by the progressive transition from a proximal to a hyperthinned domain without any major rift structure and the complete record of the pre-, syn-, and post-hyperextension sedimentary sequences. The southern part of the basin is more complex. The necking domain is structured by a conjugate system of detachment faults. Evidence for such structures is based on drill-hole observations (the Saint Girons en Marensin and Contis boreholes; [*Jammes et al.,* 2010b]). The structural limit between the northern and

732 southern part of the hyperthinned domain of the Parentis basin is also interpreted as a top
733 basement detachment fault rooting towards the Ibis fault and associated with salt tectonics and
734 diapir formation [e.g. *Mathieu*, 1986; *Biteau and Canérot*, 2007; *Jammes et al.,* 2010b]. The
735 Landes High and the Cantabrian shelf belonging to the proximal domain represent a weakly
736 thinned crustal block and form a major boundary between the Parentis and Basque–
737 Cantabrian basin (see also Roca *et al.* [2011]).

738 *5.2.3. Rift-remnants and reactivation in the Basque–Cantabrian basin*

739 In contrast the Basque–Cantabrian basin to the South is completely inverted (fig 7b).
740 Sedimentary sequences are decoupled on upper Triassic evaporites [*Cámara*, 1997] and the
741 basement is buried under thick sedimentary sequences. Field and sub-surface observations
742 provide good constraints on the stratigraphic evolution of the Mesozoic sediments [e.g. *Soler*
743 *et al.,* 1981; *García-Mondéjar et al.,* 1985; *Rat*, 1988; *IGME*, 1987] and on locally preserved
744 rift related-structures [e.g. *García-Mondéjar et al.,* 1996; *Tavani and Muñoz*, 2012; *Bodego*
745 *and Agirrezabala*, 2013]. Similarly as for the northern Landes high, the Rioja shelf to the
746 South (buried under the Ebro basin and forming the western continuation of the Ebro block,
747 fig 6) is representative of a proximal domain, characterized by the deposition of thin Late
748 Cretaceous post-hyperextension shallow marine sediments [e.g. *Cámara*, 1997]. The
749 sedimentary sequences of the conjugate necking domains are preserved in the Zumbaya and
750 Alava synclines (respectively in the northern and southern part of the basin). These units are
751 characterized by thickening of syn- (Late Aptian to Cenomanian) to post-hyperextensional
752 sequences toward the basin axis and locally absent pre-hyperextensional sequences (Castillo
753 5; [*IGME*, 1987]). The North Biscay and Bilbao anticline are mapped as remnants of
754 hyperthinned domains and characterized by thick pre-hyperextension sediments. The Bay of
755 Biscay syncline is mapped as the western continuation of the "Nappe des Marbres" locally
756 sampling mantle rocks and associated high temperature low pressure metamorphic marbles of

757 Mesozoic age [*Mendia and Gil-Ibarguchi*, 1991] representative of a former exhumed mantle
758 domain. An important gravity anomaly is centered on the basin and interpreted to result from
759 the stacking of lower crustal rocks [*Pedreira et al.,* 2003, 2007] or mantle rocks emplaced at
760 shallow levels during compression. In analogy with the interpretation proposed for the
761 Labourd anomaly [*Jammes et al.,* 2010c], we favor the mantle body solution that would be
762 coherent with this unit being a remnant of a former exhumed, partly serpentinized, mantle
763 domain. Nevertheless the lower crustal interpretation proposed by *Pedreira et al.* [2003,
764 2007] cannot be excluded. Another important observation resulting from the gravity modeling
765 proposed by *Pedreira et al.* [2007] is the occurrence of a large northward dipping crustal root
766 reaching a 55 to 60 km depth and interpreted as the former thinner basement of the Basque–
767 Cantabrian basin [*Pedreira*, 2004; *Pedreira et al.,* 2007].

768 ***5.3. Arzacq–Mauléon basin: Pyrenean segment***

769 *5.3.1. Constraints from field and sub-surface geology*

770 The Pyrenean segment initiates at the eastern termination of the Parentis and Basque–
771 Cantabrian basins and is delimited from the two basins by the Pamplona fault. Therefore this
772 segment only preserves rift remnants derived from the former hyperextended Pyrenean–
773 Basque–Cantabrian rift system.

774 Insights on the sedimentary and basement architecture come from the reinterpretation of
775 the ECORS Arzacq–W Pyrenees seismic profile [*Daignères et al.,* 1994] extended to the
776 South based on the Anso transect proposed by *Teixell*, [1998]. Field geology, sub-surface
777 observations [*BRGM*, 1974] and local refraction data [*Daignières et al.,* 1982; *Banda et al.,*
778 1983] are combined to further constrain the interpretation proposed in fig 7c.

779 *5.3.2. Compressional architecture of a reactivated hyperextended basin*

780 Arguments for the determination of rift-related remnants in the Arzacq–Mauléon basin
781 have been previously presented and described relying on the identification of key field
782 observations (fig 3; see also *Tugend et al.,* accepted). Field observations from the "Béarnais
783 range" area, in the eastern part of the basins (fig 3) are used to further constrain the
784 compressional overprint of former rift domains (figs 7c, 10 and 11). The present-day
785 geometry of the Mauléon basin results from its inversion within a large pop-up structure along
786 north and south vergent thrusts (fig7c and 10).

787 To the south, distal parts of the basin (corresponding to the former hyperextended domain)
788 are thrust over the proximal domain preserved in the axial zone along the south-directed
789 Lakoura thrust system and lateral equivalents (figs 7c, 10 and 11; [*Muñoz*, 1992; *Teixell*,
790 1998]). The proximal domain is weakly deformed as a large-scale anticline (geological
791 sections fig 10; see also *Teixell*, [1990]) and by local thick-skin structures related to the final
792 stage of deformation (D2 phase; e.g. Guarga and Gavarnie thrusts fig 7c; Eaux-Chaudes thrust
793 fig 10). The sedimentary cover of the axial zone is characterized by thin-skin thrusts
794 decoupling in Upper Triassic evaporites (*Teixell*, [1998]; geological section BB‟ fig 10).

795 The transition from the proximal to necking domains (see structural maps; figs 3, 10 and
796 11) corresponds to a thrust fault characterized by an intense deformation of the sediments
797 close to the contact (e.g. Upper Triassic formation within the Bedous unit; fig 11; [*Canérot et*
798 *al.,* 2001; *Ternet et al.,* 2004]). Locally, this thrust fault is folded by the anticlinal deformation
799 of the axial zone as indicated by the steep northward dipping Cretaceous cover of the axial
800 zone (fig 10 and 11). Remnants of the necking domain are only locally sampled within the
801 Bedous-Mendibelza unit as syncline structures. In contrast, the rift-related sedimentary and
802 basement architecture of the conjugate remnants of the necking domain preserved in the
803 Arzacq basin is interpreted to be well preserved (fig 7c).

804 The initial contact between units preserving the necking and hyperthinned domains is only
805 locally preserved [*Masini et al.,* 2014]. In most cases it is overprinted by North-directed
806 thrusts resulting from the second phase of deformation (figs 7c, 10 and 11). The hyperthinned
807 and exhumed mantle domains are characterized by the widespread occurrence of this second
808 phase of deformation that locally invert and overprint the tectonic units where remnants of
809 these domains are preserved (e.g. the Ossau thrust; [*Canérot et al.,* 2001]; figs 7c, 10 and 11).
810 As a result, a large part of the hyperthinned and exhumed mantle domains may be underthrust
811 as suggested in the geological sections in figs 7c and 10.

812 Field observations from the Mauléon basin unravel the contrast in compressional
813 deformation between the different rift domains. The proximal domain is only weakly
814 deformed, whereas the hyperthinned and exhumed mantle domains are affected by a stronger
815 compressional overprint.

816 **6. Discussion**

817 ***6.1. Spatial and temporal evolution of hyperextended rift systems***

818 *6.1.1. Insights on the formation and architecture of hyperextended rift systems*

819 The mapping of rift domains across the Bay of Biscay and Pyrenees unravelled the
820 occurrence of two spatially disconnected hyperextended rift systems characterized by a strong
821 segmentation (fig 6 and 12). These rift systems are delimited by the "Landes High" and "Ebro
822 block" representing crustal blocks probably characterized by a rheologically stronger
823 basement inherited from the pre-rift history [Matte, 1991; Lefort, 1997] resulting in their
824 weak crustal thinning (fig 6 and 12). Their crustal structure as well as their relationship to the
825 surrounding hyperextended domains (fig 12) compares well with continental ribbons
826 described by *Péron-Pinvidic and Manatschal* [2010] from the North Atlantic (e.g. Flemish
827 Cap, Rockall Bank, Galicia Banks).

828 The relative timing of hyperextensional processes is diachronous between the Bay of
829 Biscay–Parentis and Pyrenean–Basque–Cantabrian rift systems (respectively Berriasian-
830 Barremian to late Aptian and Aptian-Albian to at least Early Cenomanian; [see also Jammes
831 et al. 2009; Roca et al. 2011]). This diachronous evolution may illustrate the eastwards
832 migration of extension in the Pyrenean–Basque–Cantabrian rift system contemporaneous with
833 ongoing seafloor spreading in the western Bay of Biscay. The complexity of rift system
834 architecture has also been examplified by *Gernigon et al.,* 2014 for the Southwestern Barents
835 Sea, emphasizing the 3D polyphased evolution of rift systems and eventually the role of
836 inheritance.

837 *6.1.2. The role of pre-rift inheritance: insights from the Bay of Biscay–Parentis system*

838 The southern edge of the hyperthinned domain of the Western Approach margin is
839 suggested to be structured by the break-away of a detachment system related to final crustal
840 thinning and mantle exhumation (fig 7a). This architecture is interpreted to characterize distal
841 lower plate margins [*Sutra et al.,* 2013], implying that the Western Approach margin may
842 correspond to a lower plate margin (fig 7a and 8). The situation is inverted at the eastern end
843 of the Bay of Biscay where the northern part of the Parentis basin can be interpreted as an
844 upper plate margin [see also *Jammes et al.,* 2010a, 2010b, 2010c]. This change between upper
845 and lower plate margins seems well-expressed from a mapping point of view (fig 6 and 12).
846 The Western Approach margin is characterized by wide necking and hyperthinned domains,
847 contrasting with sharper domains observed from the Armorican margin to northern Parentis
848 basin. This switch from an upper to a lower plate margin occurs where the Armorican Shear
849 zone intersects with the margin. The shear zone structure is described as a major lithospheric
850 structure delimiting Variscan domains [e.g. *Sibuet*, 1973; *Matte*, 2001; *Ballèvre et al.,* 2009;
851 2012 and reference therein].

852 In the North Iberian margin, the hyperthinned and exhumed mantle domains are
853 reactivated within north directed thrust systems, precluding the identification of the rift-
854 vergence of the detachment system in seismic sections. However, along the North Iberian
855 margin (exemplified by the IAM 12 section; fig 7a and 9) and the "Le Danois basin", a
856 change in the size of the necking and hyperthinned domain can be observed in the map view
857 (fig 6). The transition is relatively abrupt and not progressive, probably not resulting from a
858 difference of shortening along strike. This change could be inherited from the former rift
859 architecture, as proposed for the northern Bay of Biscay margin. It may illustrate a former
860 switch between an upper plate margin (to the west) and a lower plate margin (to the east).
861 Furthermore, this variation of architecture seems to coincide with the intersection of the rift
862 system with major inherited Variscan structures separating the Central Iberian Zone to the
863 West from the West Asturien Leonese Zone to the East [fig 6 and 12; e.g. *Matte*, 2001;
864 *Martínez-Catalán,* 2011; and references therein].

865 Based on observations from the conjugate margins of the Bay of Biscay, it seems that
866 switches between upper and lower plate architecture impact the architecture of the necking,
867 hyperthinned and exhumed mantle domains. It is therefore likely that the evolution of these
868 domains was controlled by the pre-rift history and inherited rheology of the crust as they
869 bound distinct Variscan domains (also discussed by *Pérez-Gussinyé et al.* [2003] or *Sutra and*
870 *Manatschal* [2012] for the West Iberia margin). It is interesting to note that these inherited
871 structures do not seem to offset the contact to the first oceanic crust. This observation may
872 suggest that while rift systems may be controlled by crustal and lithospheric inheritance,
873 oceanic systems are mainly controlled by deep-seated asthenospheric processes and are
874 therefore insensitive to continental lithospheric inheritance.

875 *6.1.3. Importance of segmentation: insights from the Pyrenean–Basque–Cantabrian*
876 *hyperextended rift system*

877 The Pyrenean–Basque–Cantabrian rift system is characterized by its strong segmentation
878 corresponding to a set of NE–SW to NNE–SSW trending transfer/transform faults regularly
879 spaced across the studied area (e.g. the Santander, Pamplona, Toulouse and Cevennes faults,
880 fig 6 and 12; see also [*Jammes et al.,* 2009; *Roca et al.,* 2011]). These transfer faults control
881 the large-scale lateral evolution of the Late Aptian–Early Albian hyperextended rift system
882 (see the restoration prior to the onset of compression; fig 12). They can either juxtapose rift
883 domains that experienced different amounts of extension (e.g. the Santander transfer zone in
884 the Basque-Cantabrian basin) or transfer the overall extension to another basin as observed
885 along the Pamplona fault (fig 12). The segmentation pattern of the Pyrenean–Basque–
886 Cantabrian rift system is presumably controlled by lithospheric-scale structures inherited from
887 the late to post-Variscan evolution [e.g. *Arthaud and Matte*, 1975, 1997; *Burg et al.,* 1994a,
888 1994b].
889 The Toulouse fault may have played an additional role. A switch in exhumation vergence
890 is proposed to have occurred along the Toulouse fault (*Jammes* [2009]). This change may
891 have controlled variations of the rift architecture between the western and eastern Pyrenees, as
892 described in the Western Bay of Biscay between the Western Approach and Armorican
893 margins. In the western Pyrenees, top basement detachment fault systems that exhumed mid-
894 crustal granulites and mantle rocks are described to be north-dipping [e.g. in the Arzacq–
895 Mauléon basin; *Jammes et al.,* 2009; *Lagabrielle et al.,* 2010; *Masini et al.*, 2014]. In the
896 eastern Pyrenees, the situation seems to be inverted. *Vauchez et al.* [2013] showed the
897 occurrence of south-dipping detachment fault systems that exhumed the Agly massif. A
898 similar exhumation of the North Pyrenean massif in the eastern Pyrenees is possible as most
899 of them are also characterized by a tectonic contact between mid to lower crustal rocks and
900 Cretaceous sediments [as suggested by *Vauchez et al.* 2013].

The suggested change in the rift-related pre-compressional architecture may partly explain the change in the orogen architecture described between the western and eastern Pyrenees [e.g. *Muñoz*, 2002 and reference therein]. Also, this interpretation emphasizes the necessity to evaluate the former rift-related architecture to understand the present-day structuration of orogenic systems (see also [Roca et al., 2001; Jammes et al. 2014; Mohn et al. 2014]).

6.2. Role of rift inheritance for reactivation initiation and mountain building processes

6.2.1. Role of hyperextension for the heterogeneous reactivation

The Late Cretaceous to Late Oligocene convergence shows a heterogeneous distribution of compressional deformation. Based on the mapping of rift domains (fig 5) and on the restoration of the stage prior to compression (figs 12), we aim to discuss the role of the complex 3D rift architecture in the subsequent reactivation. In the previously described Bay of Biscay and Pyrenean segments, deformation is only accommodated in one of the rift systems (respectively the Bay of Biscay–Parentis and Pyrenean–Basque–Cantabrian rift systems). In the Western Bay of Biscay deformation is localized in between the exhumed mantle and hyperthinned domains (figs 7 and 12) while the oceanic domain is characterized by a diffuse deformation [*Thinon et al.,* 2002]. In the Pyrenean segment former hyperextended rift basins are completely inverted and integrated in the orogen (fig 6; e.g. [*Roca et al.,* 2011] and reference therein). One of the major differences between the two settings is related to the initial size, structure and nature of basement in the different rift basins. In the Basque–Parentis segment, the occurrence of the two rift systems will lead to a "competition" during convergence. The Parentis basin is well preserved and only minor reactivation can be observed in the central part of the basin where the crust is extremely thinned [*Jammes et al.,* 2010a, 2010b, 2010c; *Tugend et al.,* accepted]. In contrast the Basque–Cantabrian basin is completely inverted (fig 7). It is difficult to understand why the Parentis basin was preserved while the Basque–Cantabrian basin was reactivated. One

926 possible interpretation could be that the Basque–Cantabrian basin was locally floored by
927 exhumed serpentinized mantle (as proposed by *Roca et al.* [2011]) and was consequently
928 easier to reactivate. Westwards where mantle may be exhumed, compressional deformation is
929 partitioned between the Bay of Biscay–Parentis and Pyrenean–Basque–Cantabrian rift
930 systems, as indicated by the occurrence of the North Iberian Frontal thrust system [e.g.
931 *Derégnancourt and Boillot*, 1982; *Roca et al.,* 2011; *Fernández-Viejo et al.,* 2012] and by the
932 tectonic uplift of the western termination of the Basque–Cantabrian basin [*Gallastegui et al.,*
933 2002; *Pedreira et al.,* 2003, 2007; *Alonso et al.,* 2007].

934 *6.2.2. Conceptual model to explain the evolution from inversion initiation to orogen*
935 *formation*

936 Thanks to the heterogeneous reactivation of the rift systems, we have access to the
937 different stages of the compressional deformation. This enables us to propose a conceptual
938 model that explains the progressive integration of the rift-related domains into the orogen
939 architecture.

940 *6.2.2.1. Initiation of reactivation: the role of exhumed serpentinized mantle*

941 Only a weak reactivation is described on the Western Approach and Armorican margins
942 mainly at the boundary between the exhumed mantle and hyperthinned domains [*Thinon et*
943 *al.,* 2001]. The serpentinisation of exhumed mantle rocks may be responsible for the creation
944 of a weak horizon where compressional deformation may initiate (as previously described for
945 the West Iberian margin by *Péron-Pinvidic et al.* [2008]; also discussed by *Lundin and Doré*,
946 [2011]). At this stage the former top basement detachment fault may be used as a decoupling
947 layer, potentially resulting in the sampling of mantle rocks. The former vergence of the
948 detachment system may not play an important role for the onset of reactivation. In the Bay of
949 Biscay, compressional deformation in the exhumed mantle domain can be observed on
950 conjugate margins as exemplified by the Western Approach and North Iberian margin

examples (figs 7a, 8, 9 and 12; [*Thinon et al.,* 2001; *Fernández-Viejo et al.,* 2012] and reference therein).

6.2.2.2. Accretionary prism and "subduction" stage: the role of hyperthinned domains

The progressive underthrusting of the former exhumed mantle domain will lead to the propagation of compressional deformation into the hyperthinned domain. This domain is characterized by a strongly hydrated, brittle crust containing low-friction minerals such as clays [*Pérez-Gussinyé and Reston*, 2001; *Reston and Pérez-Gussinyé*, 2007]. At this stage the former hyperthinned domain can be progressively deformed, resulting in structures similar to those observed in accretionary prisms, however, with a larger component of crustal material. Such structures have been observed along the North Iberian margin [e.g. *Fernández-Viejo et al.,* 2012]. In the former hyperextended basins, the initially smaller size of the system will lead to the progressive closure of exhumed mantle domain. Subsequently, the convergence of the two conjugate margins may trigger the initiation of a proto-subduction of the former hyperthinned domain as exemplified by the Arzacq–Mauléon and Basque–Cantabrian examples (fig 13). Shortcuts or incisions from new thrust faults may occur into the footwall of the former top basement detachment fault while it is progressively reactivated. They can result in the emplacement of hyperthinned and exhumed mantle rocks within the overlying compressional stack system formed predominantly by rocks originally located in the former detachment faults [e.g. *Lagabrielle et al.,* 2010]. An example of a former hyperthinned domain incorporated into an accretionary prism has been described from the SW termination of the Taiwan Island [*McIntosh et al.,* 2013].

6.2.2.3. Continental collision and orogen formation: the role of the necking domain

In a later stage of convergence, after the early deformation and progressive subduction/underthrusting of the hyperthinned and exhumed mantle domains, the arrival of

975 the necking and proximal domains result in a major change in the compressional history. This
976 stage is related to a new phase of deformation as observed and described for the Arzacq–
977 Mauléon example. We interpret this second phase of deformation as related to the progressive
978 collision between the former conjugate necking and proximal domains. The former set of
979 conjugate top basement detachment faults interpreted to structure the necking domain [*Mohn*
980 *et al.,* 2012; *Sutra et al.,* 2013] may be reactivated during the onset of collision. At this stage,
981 the former necking domains can act as buttresses [*Mohn et al., 2014*]. The collision between
982 these two "buttresses" leads to a change in the mode of deformation. The subduction stage is
983 mainly controlled by asymmetric deformation. In contrast the collision stage may induce
984 symmetric processes including pro and retro thrusting (e.g. Pyrenean segment; figs 7c and
985 10). In the Pyrenean segment, a new phase of deformation can initiate the pop-up inversion of
986 the Arzacq-Mauléon basin along north vergent thrusts (e.g. the Saint Palais, Sainte Suzannne
987 and Ossau thrusts) and south-directed back-thrusting in the Axial zone (e.g. Gavarnie, Guarga
988 thrust systems; [*Teixell*, 1998]).
989 In this new interpretation of the orogen architecture (fig 14) the crustal roots imaged from
990 geophysical methods [e.g. *Daignières et al.,* 1994; *Roure and Choukroune*, 1998; *Pedreira et*
991 *al.,* 2003, 2007] represent the subducted hyperthinned and exhumed mantle domain. In the
992 case of the North Iberian margin the necking domain may play a similar role, representing the
993 buttress for the accreted hyperthinned domain. *Neves et al.* [2009] proposed a similar model
994 to explain the distribution of compressional deformation observed in the Tagus Abyssal plain
995 (West Iberian margin) and interpreted the former necking zone as a crustal indentor.
996 This evolutionary model underlines two major points: (1) most of the deformation is
997 located at the limits of rift domains implying that the former extensional structures separating
998 rift domains were preferentially reactivated during compressional processes [*Jammes et al.,*
999 2009; *Roca et al.,* 2011] and (2) the hyperthinned and exhumed mantle domains accommodate

1000 most of the deformation while the necking and proximal domains act as buttresses and
1001 consequently accommodate a relatively weak crustal shortening.

1002 **6.3 General implications**

1003 *6.3.1 Partitioning of the deformation and shortening rate estimations*

1004 The reinterpretation of the orogen architecture proposed in this study (fig 14) emphasises
1005 the role of the former rift domains (and not only of rift-inherited structures) for reactivation
1006 and collisional orogen formation (figs 12, 13 and 14). It has additional implications for the
1007 restoration of the area and hyperextended rift systems in general. In order to propose a
1008 complete restoration of the former rift architecture, it is necessary to quantify the horizontal
1009 movement accommodated during the reactivation of rift structures (in particular top basement
1010 detachment faults) and to estimate the underthrust/subducted part of the hyperthinned and
1011 exhumed mantle domains (figs 13 and 14).

1012 Many restorations are focused on the thick skin deformation observed in external parts of
1013 the orogens (e.g. in the Western Pyrenees; [*Teixell*, 1996, 1998]). In the previous discussion,
1014 we showed that at least in the Western Pyrenees, this deformation may be minor and only
1015 corresponds to the final stage of compression (figs 13 and 14). Therefore only considering the
1016 restoration of structures in the external domains leads to underestimations of the initial
1017 shortening related to the underthrusting/subduction of the hyperthinned and mantle domains
1018 preserved in the internal parts of the orogen (fig 14).

1019 Restorations of the crustal roots inferred from geophysical methods (e.g. refraction, gravity
1020 modelling) are also proposed [e.g. *Muñoz*, 1992; *Daignières et al.,* 1994; *Pedreira*, 2004].
1021 Although some of these restorations unravelled previously thinned domains, they cannot
1022 restore quantitatively the underthrust/subducted portions of the former exhumed mantle
1023 domain based on crustal scale geophysical imaging alone.

1024 Finally, in order to estimate the shortening accommodated at the scale of the overall Bay of
1025 Biscay and Pyrenees it is necessary to apprehend the partitioning of compressional
1026 deformation between two former rift systems as well as their complex 3D rift architecture
1027 (Bay of Biscay–Parentis and Pyrenees–Basque–Cantabrian rift systems). Therefore, the
1028 increasing deformation observed eastwards from the Bay of Biscay to the Pyrenees may not
1029 be related to an increasing shortening but related to the heterogeneous reactivation of a
1030 complex pattern of rift systems.

1031 *6.3.2. Nature of the North Pyrenean fault and plate kinematic implications*

1032 The NNE–SSW to NE–SW segmentation characterising the Pyrenean–Basque–Cantabrian
1033 rift system (see also *Jammes et al.* [2009]; *Roca et al.* [2011]) controls the spatial evolution of
1034 the rift domains mapped in this study at least from Late Aptian to Early Albian. The relative
1035 continuity of these structures across the former rift system preclude any strike-slip or major
1036 left lateral movements after Late Aptian time (as previously discussed by *Jammes et al.*
1037 [2009, 2010a]).

1038 The North Pyrenean fault was interpreted as a major crustal discontinuity defining the plate
1039 boundary between the European and the Iberian plates [*Mattauer*, 1968; *Choukroune and*
1040 *Mattauer*, 1978; *Choukroune and ECORS Team*, 1989]. This structure was supposed to
1041 accommodate a left lateral displacement of the Iberian plate during mid-Cretaceous time [e.g.
1042 *Le Pichon et al.,* 1971; *Mattauer and Séguret*, 1971; *Olivet*, 1996]. However, the nature and
1043 lateral continuity of this fault was questioned by several authors [e.g. *Mattauer and Seguret*,
1044 1971; *Canérot et al.,* 2001; *Canérot*, 2008 and reference therein].

1045 In the light of our mapping results, the North Pyrenean fault system coincides with the
1046 occurrence of the exhumed mantle domain. In the east this domain corresponds to a narrow,
1047 sub-vertical zone that can be mapped as a highly deformed zone (see geological sections in
1048 *Lagabrielle et al.* [2010]) indirectly also characterized by a HT–LP metamorphism attributed

1049 to the extreme rift-related thinning [e.g. *Goldberg and Leyreloup*, 1990]. Controversies on the
1050 western continuation of this structure [*Canérot et al.,* 2001] correspond with the progressive
1051 widening of the exhumed mantle domain characterized by a weaker compressional overprint.
1052 Therefore, we suggest that the North Pyrenean Fault represents a "suture" zone related to the
1053 inversion of the former hyperextended and exhumed mantle domains.

1054 **Conclusions**

1055 The aim of this study was to characterize the spatial and temporal evolution of
1056 hyperextended rift systems and their progressive reactivation. We used gravity inversion,
1057 seismic interpretation and field mapping to propose a map of the rift domains from the
1058 offshore Bay of Biscay to their onshore fossil remnants preserved in the Pyrenees. The key
1059 observations and learnings of this work on the formation and deformation of hyperextended
1060 systems can be summarized as follow:
1061 (1) Two spatially distinct rift systems can be described: the Bay of Biscay–Parentis and the
1062 Pyrenean–Basque–Cantabrian rift systems characterized by the diachronous initiation of
1063 hyperextensional processes.
1064 (2) These rift systems are characterized by a strong segmentation that may be partially
1065 inherited from the complex structuration of the Variscan orogen and/or from the Permo-
1066 Carboniferous post-Variscan history. This segmentation may control lateral variations in the
1067 architecture of the rift systems but does not control the formation of the oceanic domain. This
1068 last observation may indicate that rift systems are sensitive to inherited structures and
1069 rheology while oceanic domains are more likely to be controlled by asthenospheric processes.
1070 (3) The NE–SW to NNE–SSW segmentation observed across the Pyrenean–Basque–
1071 Cantabrian rift system preclude the accommodation of an important left lateral movement
1072 after Late Aptian to Early Albian time in this rift system as proposed from previous studies.

(4) Different steps in compressional deformation are related to the rift domain inheritance. At first reactivation is initiated in the serpentinized layers of the exhumed mantle domain. The progressive closure of this domain may lead to the propagation of compressional deformation to the hyperthinned domain resulting in the formation of an accretionary prism. In the former rift system preserved onshore, the proximity of the conjugate system enables the underthrusting/subduction of the former hyperthinned domains. The final architecture of the orogen is acquired during the collision of the former necking domains representing conjugate buttresses.

Finally, we believe that the complex evolution and architecture of the Bay of Biscay and Pyrenees may be used as an analogue to understand the partitioning of extensional deformation in other rift systems. Additionally, the role of rift inheritance for reactivation and orogen formation may provide new insights for the formation of collisional orogens.

Acknowledgments

The authors thank Per Terje Osmundsen and Yves Lagabrielle for thoughtful and encouraging reviews. We acknowledge the Geophysical data repository of the Research group on the Structure and Dynamics of the Earth (http:/geodb.ictja.csic.es) for providing us the IAM 12 seismic line and Ifremer for the Norgasis 11 and 12 seismic sections. This research was supported by the Margin Modelling Phase 3 partners (BP, Conoco Phillips, Statoil, Petrobras, Total, Shell, Hess, BHP-Billiton and BG).

References

Alonso, J. L., J. A. Pulgar, and D. Pedreira (2007), El relieve de la cordillera cantábrica, *Enseñanza de las Ciencias de la Tierra*, 15, 151–163.

Alvarez-Marron, J., E. Rubio, and M. Torne (1997), Subduction-related structures in the North Iberian Margin, *Journal of Geophysical Research*, 102, 22497–22511, doi:10.1029/97JB01425.

Alvey, A., C. Gaina, N. J. Kusznir, and T. H Torsvik, (2008), Integrated crustal thickness mapping and plate reconstructions for the high Arctic, *Earth and Planetary Science Letters*, 274, 310–321.

1099 Andersen, T.B., F. Corfu, L. Labrousse, and P. T. Osmundsen (2012), Evidence for hyperextension in
1100 the Pre-Caledonian continental margin of Baltica, *Journal of the Geological Society*, London,
1101 169, 601–612, doi: 10.1144/0016-76492012-011.
1102 Arthaud, F., and P. Matte (1975), Les décrochements tardi-hercynien du sud–ouest de l'Europe.
1103 Géométrie et essai de reconstitution des conditions de déformation, *Tectonophysics*, 25, 139–
1104 171, doi:10.1016/0040-1951(75)90014-1.
1105 Arthaud, F. and P. Matte (1977), Late Paleozoic strike-slip faulting in southern Europe and northern
1106 Africa: Result of a right-lateral shear zone between the Appalachians and the Urals,*Geological*
1107 *Society of America Bulletin*, 88, 1305–1320, doi: 10.1130/0016-
1108 7606(1977)88<1305:LPSFIS>2.0.CO;2.
1109 Aslanian, D., M. Moulin, J. L. Olivet, P. Unternehr, L. Matias, F. Bache, M. Rabineau, H. Nouzé, F.
1110 Klingelheofer, I. Contrucci, and C. Labails (2009), Brazilian and African passive margins of the
1111 Central Segment of the South Atlantic Ocean: Kinematic constraints, *Tectonophysics*, 468, 98–
1112 112, doi:10.1016/j.tecto.2008.12.016.
1113 Avedik, F., A. L. Camus, A. Ginzburg, L. Montadert, D. G. Roberts, and R. B. Whitmarsh (1982), A
1114 seismic refraction and reflection study of the continent–ocean transition beneath the north
1115 Biscay margin, *Philosophical Transactions of the Royal Society of London*, 305, 5–25.
1116 Avedik, F., V. Renard, J. P. Allenou, B. and Morvan (1993), Single-bubble airgun array for deep
1117 exploration, *Geophysics*, 38, 366–382.
1118 Avedik, F., A., Hirn, V., Renard, R., Nicolich, J. L. Olivet, and M. Sachpazi (1996), „Single-bubble"
1119 marine source offers new perspectives for lithospheric exploration, *Tectonophysics*, 267, 57–71.
1120 Ayarza, P., J. R. Martínez-Catalán, J. Alvarez-Marrón, H. Zeyen, and C. Juhlin (2004), Geophysical
1121 constraints on the deep structure of a limited ocean-continent subduction zone at the North
1122 Iberian Margin, *Tectonics,* 23, TC1010, doi:10.1029/2002TC001487.
1123 Ballèvre, M., Bosse, V., Ducassou, C., & Pitra, P. (2009), Palaeozoic history of the Armorican Massif:
1124 models for the tectonic evolution of the suture zones, *Comptes Rendus Geoscience*, 341, 174-
1125 201.
1126 Ballèvre, M., Fourcade, S., Capdevila, R., Peucat, J. J., Cocherie, A., & Fanning, C. M. (2012),
1127 Geochronology and geochemistry of Ordovician felsic volcanism in the Southern Armorican
1128 Massif (Variscan belt, France): Implications for the breakup of Gondwana, *Gondwana*
1129 *Research*, 21, 1019-1036.
1130 Banda, E., A. Udias, S. Mucher, J. Mczcua, M. Boloix, J. Gallart, and A. Aparicio (1983), Crustal
1131 structure beneath Spain from deep sounding experiments, *Physics of the Earth and Planetary*
1132 *Interiors*, 31, 277–280.
1133 Banda, E., M. Torné, and The Iberian Atlantic Margins Group (1995), Iberian Atlantic Margins Group
1134 investigates Deep Structure of Ocean Margins, *Eos Trans. American Geophysical Union*, 76,
1135 25–29, doi:10.1029/EO076i003p00025.

1136 Biteau, J. J. and J. Canérot (2007), La chaîne des Pyrénées et ses avants-pays d'Aquitaine et de l'Ebre:
1137 caractéristiques structurales, évolution géodynamique et tectono sédimentaire, *Géologues,* 155,
1138 16-28.
1139 Biteau, J. J., A. Le Marrec, M. Le Vot, and J. M. Masset (2006), The Aquitaine Basin, *Petroleum*
1140 *Geoscience*. 12, 247–273*,* doi: 10.1144/1354-079305-674.
1141 Bodego, A. and L. M. Agirrezabala (2013), Syn-depositional thin- and thick-skinned extensional
1142 tectonics in the mid-Cretaceous Lasarte sub-basin, western Pyrenees, *Basin Research*, 25, 594–
1143 612, doi: 10.1111/bre.12017.
1144 Boillot, G. (1984), Le Golfe de Gascogne et les Pyrénées, in *Les marges continentales actuelles et*
1145 *fossiles autour de la France*, edited by G. Boillot, M. Montadert, M. Lemoine, and B. Biju-
1146 Duval, 5–81, Masson, Paris.
1147 Boillot, G., R. Capdevilla, I. Hennequin-Marchand, M. Lamboy, and J. P. Lepretre, (1973), La zone
1148 nord-pyrénéenne, ses prolongements sur la marge continentale nord-espagnole et sa
1149 signification structurale, *Comptes-Rendus de l'Académie des Sciences*, *Paris*, 277, 2629–2632.
1150 Boillot, G., M. Recq, E. L. Winterer, A. W. Meyer, J. Applegate, M. Baltuck, J. A. Bergen, M. C.
1151 Comas, T. A. Davies, K. Dunham, C. A. Evans, J. Girardeau, G. Goldberg, J. Haggerty, L. F.
1152 Jansa, J. A. Johnson, J. Kasahara, J. P. Loreau, E. Luna-Sierra, M. Moullade, J. Ogg, M. Sarti, J.
1153 Thurow, and M. Williamson (1987), Tectonic denudation of the upper mantle along passive
1154 margins: a model based on drilling results (ODP leg 103, western Galicia margin, Spain),
1155 *Tectonophysics*, 132, 335–342, doi:10.1016/0040-1951(87)90352-0.
1156 Bois, C. and O. Gariel (1994), Deep Seismic Investigation in the Parentis Basin (Southwestern
1157 France), in *Hydrocarbon and Petroleum Geology of France*, edited by A. Mascle, Special
1158 Publication of the European Association of Petroleum Geoscientists*,* 4, 173–186.
1159 Boissonnas, J., J. P. Destombes, C. Heddebaut, G. Le Pochat, S. Lorsignol, P. Roger and Y. Ternet,
1160 (1974), Feuille de Iholdy (1027), Carte géologique de la France, scale 1/50,000, *Bureau de*
1161 *Recherche Géologique et Minières,* Orléans, France.
1162 Boltenhagen, C., G. Le Pochat, and C.Thibault (1976), Feuille de Mauléon-Licharre (1028), Carte
1163 géologique de la France, scale 1/50,000, *Bureau de Recherche Géologique et Minières*, Orléans,
1164 France.
1165 Bronner, A., D., Sauter, G.,Manatschal, G.Péron-Pinvidic, and M. Munschy (2011), Magmatic
1166 breakup as an explanation for magnetic anomalies at magma-poor rifted margins, *Nature*
1167 *Geoscience,* 4, 549–553, doi:10.1038/ngeo1201.
1168 Bronner, A., D. Sauter, G. Manatschal, G. Péron-Pinvidic, and M. Munschy (2012), Reply to
1169 "Problematic plate reconstruction", *Nature Geoscience*, 5, 677–677, doi:10.1038/ngeo1597.
1170 Brunet, M. F. (1994), Subsidence in the Parentis Basin (Aquitaine, France): Implications of the
1171 Thermal Evolution, in *Hydrocarbon and Petroleum Geology of France*, edited by A. Mascle,
1172 Special Publication of the European Association of Petroleum Geoscientists, 4, 187–198.

1173 Bureau De Recherches Géologiques Et Minières (1963), Feuille de Pau (1029), Carte géologique de la
1174 France, scale 1/50,000, *Service de la Carte Géologique de la France,* Orléans*,* France.
1175 Bureau De Recherches Géologiques Et Minières (1974), *Géologie du bassin d'Aquitaine*, 26 pp.,
1176 Paris.
1177 Burg, J. P., J. Van-Den-Driessche, and J. P. Brun (1994a), Syn to post-thickening extension: Modes
1178 and structural consequences, *Comptes Rendus de l'Académie des Sciences*, 319, 1019–1032.
1179 Burg, J. P., J. Van-Den-Driessche, and J. P. Brun (1994b), Syn to post-thickening extension in the
1180 Variscan Belt of western Europe: Modes and structural consequences, *Géologie de la France*, 3,
1181 33–51.
1182 Burger, J. J., Kieken, Maurice and R. Bocherens (1972), Feuille de Hasparren (1002), Carte
1183 géologique de la France, scale 1/50,000, *Bureau de Recherche Géologique et Minières,* Orléans,
1184 France.
1185 Cámara, P. (1997), The Basque–Cantabrian basin‟s Mesozoic tectono-sedimentary evolution,
1186 *Mémoires de la Société Géologique de France*, 171, 187–191.
1187 Cande, S. C. and Y. Kristoffersen (1977), Late Cretaceous magnetic anomalies in the north Atlantic,
1188 *Earth and Planetary Science Letters*, 35, 215–224.
1189 Canérot, J. (1989), Early Cretaceous rifting and salt tectonics on the Iberian margin of the Western
1190 Pyrenees (France). Structural consequences, *Bulletin Des Centres de Recherches Exploration-*
1191 *Production Elf-Aquitaine*, 13, 87–99.
1192 Canérot, J. (2008), *Les Pyrénées: histoire géologique et itinéraires de découvertes*, Atlantica-BRGM.
1193 Canérot, J., B.Peybernès, and R.Ciszak (1978), Présence d'une marge méridionale à l'emplacement de
1194 la zone des Chaînons béarnais (Pyrénées basco-béarnaises), *Bulletin de la Société Géologique*
1195 *de France*, 5, 673–676.
1196 Canérot, J., C. Majesté-Menjoulas, and Y.Ternet (2001), La faille Nord Pyrénéenne: mythe ou
1197 réalité ?, *Strata*, 37, pp. 36.
1198 Casteras, M., J. Canérot, J. P. Paris, D. Tisin, B. Azambre, and H. Alimen (1970a), Feuille de Oloron
1199 Sainte Marie (1051), Carte géologique de la France, scale 1/50,000, *Bureau de Recherche*
1200 *Géologique et Minières*, Orléans, France.
1201 Casteras, M., Y. Godechot, M. Villanova (1970b), Feuille de Lourdes (1052), Carte géologique de la
1202 France 1/50,000, *Bureau de Recherche Géologique et Minières,* Orléans, France.
1203 Casteras, M., M. Gottis, M. Clin, J. D. Guignard, J. P. Paris, J. Galharague, and M. Frey (1971),
1204 Feuille de Tardets Sorholus (1050), Carte Géologique de la France, scale 1/50,000, *Bureau de*
1205 *Recherche Géologique et Minières*, Orléans, France.
1206 Casteras, M., P. Souquet, G. Culot, J. Galharague, M. Frey, R. Ribis, and J. P. Paris (1970c), Feuille
1207 de Larrau (1068), Carte géologique de la France, scale 1/50,000. *Bureau de Recherche*
1208 *Géologique et Minières*, Orléans, France.

1209 Chappell, A.R. and N.J. Kusznir (2008a), Three-dimensional gravity inversion for Moho depth at
1210 rifted continental margins incorporating a lithosphere thermal gravity anomaly correction,
1211 *Geophysical Journal International,* 174, 1–13, doi: 10.1111/j.1365-246X.2008.03803.x.
1212 Chappell, A.R. and N.J., Kusznir (2008b), Three-dimensional gravity inversion for Moho depth at
1213 rifted continental margins incorporating a lithosphere thermal gravity anomaly correction,
1214 *Geophysical Journal International*, 174, 1-13.
1215 Choukroune, P. (1976), Structure et évolution de la zone nord-pyrénéenne (analyse de la déformation
1216 dans une portion de chaîne à schistosité subverticale), *Mémoires de la Société Géologique de*
1217 *France*, 127, 1–116.
1218 Choukroune, P. (1992), Tectonic Evolution of the Pyrenees, *Annual Review of Earth and Planetary*
1219 *Sciences*, 20, pp. 143.
1220 Choukroune, P. and Ecors Team (1989), The ECORS Pyrenean deep seismic profile reflection data
1221 and the overall structure of an orogenic belt, *Tectonics*, 8, 23–39,
1222 doi*:*10.1029/TC008i001p00023.
1223 Choukroune, P. and M. Mattauer (1978), Tectonique des plaques et Pyrénées: Sur le fonctionnement
1224 de la faille transformante nord-pyrénéenne; comparaisons avec des modèles actuels, *Bulletin de*
1225 *la Société Géologique de France*, 7, 689–700.
1226 Choukroune, P. and M. Séguret (1973), *Carte structurale des Pyrénées*, Laboratoire de Géologie
1227 Structurale, Montpellier.
1228 Claude, D. (1990), Etude stratigraphique, sédimentologique et structurale des dépôts mésozoïques au
1229 nord du massif du Labourd. Rôle de la faille de Pamplona (Pays Basque), *PhD thesis*, 436 pp.,
1230 University of Bordeaux II, Bordeaux, France.
1231 Clerc, C., Y. Lagabrielle, M. Neumaier, J. Y. Reynaud, and M.De Saint Blanquat (2012), Exhumation
1232 of subcontinental mantle rocks: evidence from ultramafic-bearing clastic deposits nearby the
1233 Lherz peridotite body, French Pyrenees, *Bulletin de la Société Géologique de France*, 183, 443–
1234 459.
1235 Clerc, C., P. Boulvais, Y. Lagabrielle, and M. De Saint Blanquat (2013), Ophicalcites from the
1236 northern Pyrenean belt: a field, petrographic and stable isotope study, *International Journal of*
1237 *Earth Sciences.* DOI 10.1007/s00531-013-0927-z
1238 Combes, P. J., B. Peybernès, and F. Leyreloup (1998), Altérites et bauxites, témoins des marges
1239 européenne et ibérique des Pyrénées occidentales au Jurassique supérieur-Crétacé inférieur, à
1240 l"ouest de la vallée d"Ossau (Pyrénées-Atlantiques, France), *Comptes-Rendus de l'Académie des*
1241 *Sciences*, Paris, 327, 271–278.
1242 Contrucci, I., L. Matias, M. Moulin, L. Géli, F. Klingelhofer, H. Nouzé, D. Aslanian, J. L. Olivet, J. P.
1243 Réhault, J. C. and Sibuet (2004), Deep structure of the West African continental margin (Congo,
1244 Zaïre, Angola), between 5°S and 8°S, from reflection/refraction seismics and gravity data,
1245 *Geophysical Journal International*, 158, 529–553.

1246 Cowie, L. & Kusznir, N. J. (2013), Mapping crustal thickness and oceanic lithosphere distribution in
1247 the Eastern Mediterranean using gravity inversion, Petroleum Geoscience, 10, 373-380.
1248 doi:10.1144/petgeo2011-071.
1249 Curnelle, R. (1983), Evolution structuro-sedimentaire du Trias et de l'Infra-Lias d'Aquitaine, *Bulletin*
1250 *des Centres de Recherches Exploration-Production Elf- Aquitaine,* 7, 69–99.
1251 Curnelle, R., P. Dubois, and J. C. Seguin (1982), The Mesozoic-Tertiary evolution of the Aquitaine
1252 Basin, *Philosophical Transactions of the Royal Society of London*, 305, 63–84.
1253 Daignières, M., J., Gallart, E. Banda, and A. Hirn, (1982), Implications of the seismic structure for the
1254 orogenic evolution of the Pyrenees range, *Earth and Planetary Science Letters,* 57, 88–110.
1255 Daignières, M., M. Séguret, M. Specht, and Ecors Team (1994), The Arzacq-Western Pyrenees
1256 ECORS deep seismic profile, in *Hydrocarbon and Petroleum Geology of France,* Special
1257 Publication of the European Association of Petroleum Geoscientists, 4, 199–208.
1258 De Charpal, O., P. Guennoc, L. Montadert, and D. G. Roberts (1978), Rifting, crustal attenuation and
1259 subsidence in the Bay of Biscay, *Nature*, 275, 706–711, doi:10.1038/275706a0.
1260 Dean, S. M., T. A. Minshull, R. B. Whitmarsh, and K. E. Louden (2001), Deep structure of the ocean-
1261 continent transition in the southern Iberia Abyssal Plain from seismic refraction profiles: The
1262 IAM-9 transect at 40°20′N, *Journal of Geophysical Research B: Solid Earth,* 105, 5859–5885.
1263 Debroas, E. J. (1987), Modèle de bassin triangulaire à l'intersection de décrochements divergents pour
1264 le fossé albo-cénomanien de la Ballongue (zone nord-Pyrénéenne, France), *Bulletin de la*
1265 *Société Géologique de France*, 8, 887–898.
1266 Debroas, E. J. (1990), Le flysch noir albo-cénomanien témoin de la structuration albienne à
1267 sénonienne de la Zone nord-pyrénéenne en Bigorre (Hautes-Pyrénées, France), *Bulletin de la*
1268 *société Géologique de France*, 8, 273–285
1269 Debroas, E. J., J. Canérot and M. Bilotte (2010), Les Brèches d'Urdach, témoins de l'exhumation du
1270 manteau pyrénéen dans un escarpement de faille vraconnien-cénomanien inférieur (zone nord-
1271 pyrénéenne, Pyrénées-Atlantiques, France), *Géologie de la France,* **2**, 53–64.
1272 Debyser, J., X. Le Pichon, and L. Montadert (1971), *Histoire structurale du Golfe de Gascogne*,
1273 Institut Français du Pétrole, Paris.
1274 Delfaud, J., P. Pailhe, and G. Thomas, (1982), Feuille de Morlàas (1030), Carte géologique de la
1275 France, scale 1/50,000, *Bureau de Recherche Géologique et Minières*, Orléans, France.
1276 Derégnaucourt, D. and G. Boillot (1982), Structure géologique du golfe de Gascogne, *Bulletin du*
1277 *Bureau de Recherche Géologique et Minière*, 2, 149–178.
1278 Désegaulx, P. and M. F. Brunet (1990), Tectonic subsidence of the Aquitaine basin since Cretaceous
1279 times, *Bulletin de la Société géologique de France,* 6, 295–305.
1280 Driscoll, N.W. and G. D. Karner (1998), Lower crustal extension across the Northern Carnarvon
1281 basin, Australia: Evidence for an eastward dipping detachment, *Journal of Geophysical*
1282 *Research B: Solid Earth,* 103, 4975–4991.

1283 Dubreuilh, J. and G. Karnay (1997), Feuille Arthez-de-Béarn (1004), Carte géologique de la France,
1284 scale 1/50,000, *Bureau de Recherche Géologique et Minières,* Orléans, France.
1285 Ducasse, L. and P. C. Velasque (1988), Geotraverse dans la partie Occidentale des Pyrénées de
1286 l‟avant–pays Aquitain au bassin de l‟Ebre, effet d‟une inversion structurale sur l‟édification
1287 d‟une chaîne intracontinentale, *Thèse de Doctorat,* Université d‟Aix-Marseille III, Marseille,
1288 France*,* pp. 248.
1289 Espurt, N., Callot, J.-P., Roure, F., Totterdell, J. M., Struckmeyer, H. I. M. and Vially, R. (2012),
1290 Transition from symmetry to asymmetry during continental rifting: an example from the Bight
1291 Basin–Terre Adélie (Australian and Antarctic conjugate margins), *Terra Nova*, 24: 167–180.
1292 doi: 10.1111/j.1365-3121.2011.01055.x
1293 Fabriès, J., J. P. Lorand, J. L. Bodinier, and C. Dupuy (1991), Evolution of the upper mantle beneath
1294 the Pyrenees: Evidence from orogenic spinel lherzolite massifs, *Journal of Petrology*, 2, 55–76.
1295 Fabriès, J., J. P. Lorand, and J. L. Bodinier (1998), Petrogenetic evolution of orogenic lherzolite
1296 massifs in the central and western Pyrenees, *Tectonophysics*, 292, 145–167.
1297 Fernández-Viejo, G., J. Gallart, J. A. Pulgar, J. Gallastegui, J. J. Dañobeitia, and D. Córdoba (1998),
1298 Crustal transition between continental and oceanic domains along the north Iberian Margin from
1299 wide-angle seismic and gravity data, *Geophysical Research Letters*, 25, 4249–4252.
1300 Fernández-Viejo, G. and J. Gallastegui (2005), The ESCI-N project after a decade: a synthesis of the
1301 results and open questions, *Trabajos de Geología, Universidad de Oviedo*, 25, 9–25.
1302 Fernández-Viejo, G., J. Gallastegui, J. A. Pulgar, and J. Gallart (2011), The MARCONI reflection
1303 seismic data: A view into the eastern part of the Bay of Biscay, *Tectonophysics,* 508, 34–41.
1304 Fernández-Viejo, G., J. A. Pulgar, J. Gallastegui, and L. Quintana (2012), The Fossil Accretionary
1305 Wedge of the Bay of Biscay: Critical Wedge Analysis on Depth-Migrated Seismic Sections and
1306 Geodynamical Implications, *The Journal of Geology*. 120, 315–331.
1307 Fixari, G. (1984), Strastigraphie, faciès et dynamique tecto-sédimentaire du flysh albien (flysh noir et
1308 poudingue de Mendibelza) dans la région de Mauléon-Tardets (Pyrénées Atlantiques), *PhD*
1309 *thesis*, Université de Toulouse, Toulouse, France.
1310 Fréchengues, M. (1993), Stratigraphie séquentielle et micropaléontologie du Trias moyen supérieur
1311 des Pyrénées franco-espagnoles, *PhD thesis*, Université de Toulouse 3, Toulouse, France.
1312 Gallart, J., J. A. Pulgar, J. A. Muñoz, and The Marconi Team (2004), Integrated studies on the
1313 lithospheric structure and Geodynamics of the North Iberian Continental Margin: The Marconi
1314 Project, *Geophysical Research Abstract,* 6, 04196.
1315 Gallastegui, J.*,* J. A. Pulgar, J. Gallart (2002), Initiation of an active margin at the North Iberian
1316 continent-ocean transition, *Tectonics,* 21*,* doi:10.1029/2001TC901046.
1317 García-Mondéjar, J., F. M. Hines, V. Pujalte, H. G. Reading (1985), Sedimentation and tectonics in
1318 the western Basque-Cantabrian area (northern Spain) during Cretaceous and Tertiary times, in:

1319 *6th European Regional Meeting,* Excursion guide book, edited by M. D. Mila, and J. Rosell,
1320 (eds), 307–392.
1321 García-Mondéjar, J., L. M. Agirrezabala, A. Aranburu, P. A. Fernández-Mendiola, I. Gómez-Pérez,
1322 M. López-Horgue, and I. Rosales (1996), Aptian–Albian tectonic pattern of the Basque–
1323 Cantabrian Basin (Northern Spain), *Geological Journal*, 31, 13–45.
1324 García-Mondéjar, J., M. A. López-Horgue, A. Aranburu, and P. A. Fernández-Mendiola (2005),
1325 Pulsating subsidence during a rift episode: stratigraphic and tectonic consequences (Aptian–
1326 Albian, northern Spain), *Terra Nova*, 17, 517–525, doi: 10.1111/j.1365-3121.2005.00644.x
1327 Garrido- Megías, A. and L. M. Ríos (1972), Síntesis geologica del Secundario y Terciario entre los
1328 ríos Cinca y Segre (Pirineo Central de la vertiente surpirenaica, provincias de Huesca y Lerida),
1329 *Boletín Geológico y Minero,* 83, 1–47.
1330 Gernigon, L., M. Brönner, D. Roberts, O. Olesen, A. Nasuti, and T. Yamasaki (2014), Crustal and
1331 basin evolution of the southwestern Barents Sea: From Caledonian orogeny to continental
1332 breakup, Tectonics, 33, doi:10.1002/2013TC003439.
1333 Greenhalgh, E. E. and N. J. Kusznir (2007), Evidence for thin oceanic crust on the extinct Aegir
1334 Ridge, Norwegian Basin, NE atlantic derived from satellite gravity inversion, *Geophysical*
1335 *Research Letters,* 34**,** L06305, doi:10.1029/2007GL029440.
1336 Golberg, J. M. and A. F. Leyreloup (1990), High temperature–low pressure Cretaceous metamorphism
1337 related to crustal thinning (eastern north Pyrenean zone, France), *Contributions to Mineralogy*
1338 *and Petrology*, 104, 194–207.
1339 Gong, Z., C. G. Langereis, and A. T. Mullender (2008), The rotation of Iberia during the Aptian and
1340 the opening of the Bay of Biscay, *Earth and Planetary Science Letters,* 273, 80–93
1341 Henry, J., G. Zolnaï, G. Le Pochat, and C. Mondeilh (1989), Feuille de Orthez (1003), Carte
1342 géologique de France, scale 1/50,000, *Bureau de Recherche Géologique et Minières*, Orléans,
1343 France.
1344 Instituto Geologico Y Minero De Espana (1987), Contribution de la exploracion petrolifera al
1345 conocimients de la geologia e Espana, Madrid: IGME 465 p.
1346 Jammes. S., (2009), Processus d"amincissement crustal en contexte transtensif : l"exemple du Golfe de
1347 Gascogne et des Pyrénées Basques. *PhD Thesis*, Université de Strasbourg, France.
1348 Jammes, S., R. S. Huismans, and J. A. Muñoz (2014), Lateral variation in structural style of mountain
1349 building: controls of rheological and rift inheritance, *Terra Nova*, 26, 201–207,
1350 doi: 10.1111/ter.12087.
1351 Jammes, S., G. Manatschal, L. Lavier, and E. Masini (2009), Tectonosedimentary evolution related to
1352 extreme crustal thinning ahead of a propagating ocean: Example of the western Pyrenees,
1353 *Tectonics*, 28, TC4012, doi:10.1029/2008TC002406.

1354 Jammes, S., L. Lavier, and G. Manatschal (2010a), Extreme crustal thinning in the Bay of Biscay and
1355 the Western Pyrenees: From observations to modeling, *Geochemistry, Geophysics, Geosystems,*
1356 11, Q10016, doi:10.1029/2010GC003218.
1357 Jammes, S., G. Manatschal, and L. Lavier (2010b), Interaction between prerift salt and detachment
1358 faulting in hyperextended rift systems: The example of the Parentis and Mauléon basins (Bay of
1359 Biscay and western Pyrenees), *American Association of Petroleum Geologists Bulletin,* 94,
1360 957–975.
1361 Jammes, S., C. Tiberi, and G. Manatschal (2010c), 3D architecture of a complex transcurrent rift
1362 system: The example of the Bay of Biscay-Western Pyrenees, *Tectonophysics,* 489, 210–226.
1363 Johnson, J. A and C. A. Hall (1989a) The structural and sedimentary evolution of the Cretaceous
1364 North Pyrenean Basin, southern France, *Bulletin of the Geological Society of America,* 101**,**
1365 231–247.
1366 Johnson, J. A and C. A. Hall (1989b), Tectono-stratigraphic model for the massif d'Igountze-
1367 Mendibelza, western Pyrenees, *Journal of the Geological Society, London,* 146, 925–932.
1368 Lagabrielle, Y. and J. L. Bodinier (2008), Submarine reworking of exhumed subcontinental mantle
1369 rocks: field evidence from the Lherz peridotites, French Pyrenees, *Terra Nova*, 20, 11–21,
1370 doi: 10.1111/j.1365-3121.2007.00781.x
1371 Lagabrielle, Y., P. Labaume, and M. De Saint Blanquat (2010), Mantle exhumation, crustal
1372 denudation, and gravity tectonics during Cretaceous rifting in the Pyrenean realm (SW Europe):
1373 Insights from the geological setting of the lherzolite bodies, *Tectonics*, 29, TC4012,
1374 doi:10.1029/2009TC002588.
1375 Lamare, P. (1936), Recherches géologiques dans les Pyrénées basques d'Espagne, *Mémoires de la*
1376 *Société Géologique de France*, 27, pp. 465.
1377 Lamolda, M. A., B. Mathey, M. Rossy, and J. Sigal (1983), La edad del volcanisme cretacico de
1378 Vizcaya y Guipuzcoa, *Estudios Geológicos*, 39, 151–155.
1379 Larrasoaña, J. C., J. M. Parès, J. Del Valle, and H. Millán (2003), Triassic paleomagnetism from the
1380 Western Pyrenees revisited: implications for the Iberian–Eurasian Mesozoic plate boundary,
1381 *Tectonophysics*, 362, 161–182.
1382 Laughton, A. S., W. A. Berggren, R. N. Benson, T. A. Davies, U. Franz, L. F. Musich, K. Perch-
1383 Nielsen, A. S. Ruffman, J. E. Van Hinte, R. B. Whitmarsh, F. Aumento, B. D. Clarke, J. R.
1384 Cann, W. B. Bryan, P. J. C. Ryall, and D. Bukry (1972), Site 118, in: *Initial reports of the Deep*
1385 *Sea Drilling Project covering Leg 12 of the cruises of the drilling vessel Glomar Challenger,*
1386 *Boston, Massachusetts to Lisbon, Portugal*, edited by A. S. Laughton, W. A. Berggren, R. N.
1387 Benson, U. Franz, L. F. Musich, K. Perch-Nielsen, A. S. Ruffman, J. E. Van Hinte, R. B.
1388 Whitmarsh, and T. A. Davies, College Station, TX (Ocean Drilling Program), 12, 673–751.

1389 Le Pichon, X. and F. Barbier (1987), Passive margin formation by low-angle faulting within the upper
1390 crust: the northern Bay of Biscay margin, *Tectonics*, 6, 133–150,
1391 doi:10.1029/TC006i002p00133.
1392 Le Pichon, X., J. Bonnin, J. Francheteau, and J. C. Sibuet (1971), Une hypothèse d"évolution
1393 tectonique du Golfe de Gascogne,in *Histoire Structurale du Golfe de Gascogne*, J., Debyser, Le
1394 X. Pichon, and L. Montadert, Institut Français du Pétrole, Paris, VI.11.1–VI.11.44.
1395 Lefort, J. P., C. Bois, N. Liewig, J. J. Peucat, B. Agarwal, and O. Gariel (1997), Contribution of the
1396 ECORS–Bay of Biscay deep seismic profile to the location of the southern variscan front
1397 beneath the Aquitaine Basin (France), *Mémoires de la Société Géologique de France*, 171, 1–
1398 212.
1399 Le Pochat, G., C. Heddebaut, M. Lenguin, S. Lorsignol, P. Souquet, J. Muller, and P. Roger (1978),
1400 Feuille de St Jean Pied de Port (1049), Carte Géologique de la France, scale 1/50,000, *Bureau*
1401 *de Recherche Géologique et Minières*, Orléans, France.
1402 Lemoine, M., G., Boillot, P., Tricart, 1987. Ultramafic and gabbroic ocean floor of the Ligurian
1403 Tethys (Alps, Corsica, Apennines): In search of a genetic model, Geology 15, 622–625.
1404 Lundin, E. R. and Doré, A. G. (2011), Hyperextension, serpentinization, and weakening: A new
1405 paradigm for rifted margin compressional deformation, *Geology*, 39, 347–350.
1406 Majesté-Menjoulàs, C. and F. Debon (1999), Feuille de Gavarnie (1082), Carte géologique de la
1407 France, scale 1/50,000. *Bureau de Recherche Géologique et Minières,* Orléans, France.
1408 Manatschal, G. (2004), New models for evolution of magma-poor rifted margins based on a review of
1409 data and concepts from West Iberia and the Alps, *International Journal of Earth Sciences*, 93,
1410 432–466.
1411 Martínez-Catalán, J. R. M. (2012),The Central Iberian arc, an orocline centered in the Iberian Massif
1412 and some implications for the Variscan belt, *International Journal of Earth Sciences*, 101, 1299-
1413 1314.
1414 Mas, R., A. Alonso, and J. Guimerá (1993), Evolución tectonosedimentaria de una cuenca extentional
1415 intraplaca : la cuenca finijurásica-eocretácica de Los Cameros (La Rioja-Soria), *Revista de la*
1416 *Sociedad Geológica de España*, 6, 129–144.
1417 Masini, E., G. Manatschal, G. Mohn, and P. Unternehr (2012), Anatomy and tectono-sedimentary
1418 evolution of a rift-related detachment system: The example of the Err detachment (central Alps,
1419 SE Switzerland), *Bulletin of the Geological Society of America*, 124, 1535–1551.
1420 Masini, E., G. Manatschal, J. Tugend, G. Mohn (2014), The tectono-sedimentary evolution of a hyper-
1421 extended rift basin: the example of the Arzacq-Mauléon rift system (Western Pyrenees, SW
1422 France), *International Journal of Earth Sciences*, 1-28, 10.1007/s00531-014-1023-8.
1423 Mathieu, C. (1986), Histoire géologique du sous-bassin de Parentis. *Bulletin des Centres de*
1424 *Recherches Exploration-Production Elf-Aquitaine*, 10, 33–47.

1425 Mathey, B., M. Floquet, and L. M. Martínez-Torres (1999), The Leiza palaeo-fault: role and
1426 importance in the Upper Cretaceous sedimentation and palaeogeography of the Basque
1427 Pyrenees (Spain), *Comptes-Rendus de l'Académie des Sciences, Paris,* 328, 393–399.
1428 Mattauer, M. (1968), Les traits structuraux essentiels de la chaîne pyrénéenne, *Revue de Géologie*
1429 *Dynamique et de Géographie physique*, 10, 3–11.
1430 Mattauer, M. and J. Henry (1974), The Pyrenees, in *Mesozoic-Cenozoic Orogenic Belts. Data for*
1431 *orogenic Studies: Alpine–Himalayan Orogens*, edited by A. M. Spencer, (ed) Geological
1432 Society, Special Publications, London, 4, 3–21.
1433 Mattauer, M. and M. Séguret (1971), Les relations entre la chaîne des Pyrénées et le Golfe de
1434 Gascogne, in *Histoire Structurale du Golfe de Gascogne*, edited by J., Debyser, X. Le Pichon,
1435 and L. Montadert, Institut Français du Pétrole, Paris, IV.4.1–IV.4.13.
1436 Matte, P. (1991), Accretionary history and crustal evolution of the Variscan belt in Western Europe, in
1437 *Accretionary Tectonics and Composite Continents*, edited by Hatcher, R. D. JR. and
1438 Zonenshain, L. Tectonophysics, 196, 309–337.
1439 Matte, P. (2001), The Variscan collage and orogeny (480–290 Ma) and the tectonic definition of the
1440 Armorica microplate: a review, *Terra Nova*, 13, 122–128.
1441 Matthews, D. H. and C. A. Williams (1968), Linear magnetic anomalies in the Bay of Biscay: A
1442 qualitative interpretation, *Earth and Planetary Science Letters,* 4, 315–320.
1443 Mcclay, K., J. A. Munoz, and J. García-Senz (2004), Extensional salt tectonics in a contractional
1444 orogen: A newly identified tectonic event in the Spanish Pyrenees, *Geology,* 32, 737–740.
1445 Mcintosh, K., H. Van Avendonk, L. Lavier, W. R. Lester, D. Eakin, F. Wu, C. S. Liu, and C. S. Lee
1446 (2013), Inversion of a hyper-extended rifted margin in the southern Central Range of Taiwan,
1447 *Geology,* 41, 871–874.
1448 Mendia, M. S. and J. I. Gil-Ibarguchi (1991), High-grade metamorphic rocks and peridotites along the
1449 Leiza Fault (Western Pyrenees, Spain), *Geologische Rundschau*, 80, 93–107.
1450 Minshull, T. A. (2009), Geophysical characterisation of the ocean-continent transition at magma-poor
1451 rifted margins, *Comptes Rendus-Geoscience,* 341, 382–393.
1452 Miranda-Aviles, R., R. Bourrouilh, E. H. Nava-Sanchez, M. J. Puy-Alquiza, and F. Bourrouilh-Le Jan,
1453 (2005), Analyse comparée de bassins sédimentaires transtensionnels: le bassin de Santa Rosalia
1454 (Basse Californie du Sud, Mexique) et de Mendibelza (Pyrénées, France), *Estudios Geológicos,*
1455 61, 161–176.
1456 Mohn, G., G. Manatschal, O. Müntener, M. Beltrando, and E. Masini (2010), Unravelling the
1457 interaction between tectonic and sedimentary processes during lithospheric thinning in the
1458 Alpine Tethys margins, *International Journal of Earth Sciences,* 99, 75–101.
1459 Mohn, G., G. Manatschal, M. Beltrando, E. Masini, N. J. and Kusznir (2012), Necking of continental
1460 crust in magma-poor rifted margins: Evidence from the fossil Alpine Tethys margins, *Tectonics,*
1461 31, TC1012, doi:10.1029/2011TC002961.

1462 Mohn, G., G. Manatschal, M. Beltrando, and I. Haupert, The role of rift-inherited hyper-extension in
1463 Alpine-type orogens, Terra Nova, doi: 10.1111/ter.12104.
1464 Monchoux, P. (1970), Les lherzolites Pyrénéennes: Contribution à l"étude de leur minéralogie, de leur
1465 genèse et de leurs transformations, *Ph.D. thesis*, Université de Toulouse, pp. 180.
1466 Montadert, L. and D. G. Roberts (1979a), *Initial Reports of the Deep Sea Drilling Project*, 48,
1467 Washington, US Government Printing Office.
1468 Montadert L. and E. Winnock (1971), Histoire structurale du Golfe de Gascogne, in *Histoire*
1469 *Structurale du Golfe de Gascogne*, edited by Debyser, J., X. Le Pichon, and L. Montadert,
1470 Institut Français du Pétrole, Paris, VI.16.1–VI.16.18.
1471 Montadert, L., D.G. Roberts, O. De Charpal, and P. Guennoc (1979b), Rifting and subsidence of the
1472 northern continental margin of the Bay of Biscay, in *Initial Reports of the Deep Sea Drilling*
1473 *Project,* edited by Montadert, L. and D.G. Roberts, *et al.,* 48*,* US Government Printing Office,
1474 Washington, DC, 1025–1060.
1475 Montigny, R., B. Azambre, M. Rossy, and R. Thuizat, 1986. K–Ar study of cretaceous magmatism
1476 and metamorphism in the Pyrenees: age and length of rotation of the Iberian Peninsula.
1477 *Tectonophysics*, 129, 257–273
1478 Müller, R. D., W. R. Roest, J. Y. Royer, L. M. Gahagan, and J. G. Sclater (1997), Digital isochrons of
1479 the world's ocean floor, *Journal of Geophysical Research B: Solid Earth,* 102**,** 3211–3214.
1480 Muñoz J. A. (1992), Evolution of a continental collision belt: ECORS-Pyrenees crustal balanced
1481 section, in *Thrust tectonics*, edited by K. R. Mcclay, Chapman and Hall, London, 235–246.
1482 Muñoz, J. A. (2002), The Pyrenees, in *The geology of Spain*, Geological Society, edited by W.
1483 Gibbons, and M. T. Moreno, London, 370–385.
1484 Neves, M. C., P. Terrinha, A. Afilhado, M. Moulin, L. Matias, and F. Rosas (2009), Response of a
1485 multi-domain continental margin to compression: Study from seismic reflection-refraction and
1486 numerical modelling in the Tagus Abyssal Plain, *Tectonophysics*, 468, 113–130.
1487 Olivet, J. L. (1996), La cinématique de la plaque Ibérique, *Bulletin des Centres de Recherches*
1488 *Exploration-Production Elf Aquitaine*, 20, 131–195.
1489 Osmundsen, P.T. and J. Ebbing (2008), Styles of extension offshore mid-Norway and implications for
1490 mechanisms of crustal thinning at passive margins, *Tectonics,* 27, TC6016,
1491 doi:10.1029/2007TC002242.
1492 Osmundsen, P. T. and T. F. Redfield (2011), Crustal taper and topography at passive continental
1493 margins, *Terra Nova*, 23, 349–361.
1494 Pedreira, D. (2004), Estructura cortical de la zona de transición entre los Pirineos y la Cordillera
1495 Cantábrica, *PhD thesis*, Universidad de Oviedo, Spain
1496 Pedreira, D., J. A. Pulgar, J. Gallart, and J.Diaz (2003), Seismic evidence of Alpine crustal thickening
1497 and wedging from the western Pyrenees to the Cantabrian Mountains (north Iberia), *Journal of*
1498 *Geophysical Research*, 108, B42204, doi:10.1029/2001JB001667.

1499 Pedreira, D., J. A. Pulgar, J. Gallart, and M. Torné (2007), Three-dimensional gravity and magnetic
1500 modeling of crustal indentation and wedging in the western Pyrenees–Cantabrian Mountains,
1501 *Journal of Geophysical Research,* 112, B12405, doi:10.1029/2007JB005021.
1502 Pérez-Gussinyé, M. and T. J. Reston (2001), Rheological evolution during extension at passive non-
1503 volcanic margins: onset of serpentinization and development of detachments leading to
1504 continental break-up, *Journal of Geophysical Research*, 106, 3961–3975.
1505 Pérez-Gussinyé, M., C. R. Ranero, T. J. Reston, and D. Sawyer (2003), Mechanisms of extension at
1506 nonvolcanic margins: Evidence from the Galicia interior basin, west of Iberia, *Journal of*
1507 *Geophysical Research B: Solid Earth,* 108, 6–19.
1508 Péron-Pinvidic, G. and G. Manatschal (2009), The final rifting evolution at deep magma-poor passive
1509 margins from Iberia-Newfoundland: A new point of view, *International Journal of Earth*
1510 *Sciences,* 98, 1581–1597.
1511 Péron-Pinvidic, G. and Manatschal, G. (2010) From microcontinents to extensional allochthons:
1512 Witnesses of how continents rift and break apart, *Petroleum Geoscience,* 16, 189–197.
1513 Péron-Pinvidic, G., G. Manatschal, T. A. Minshull, and D. S. Sawyer (2007) Tectonosedimentary
1514 evolution of the deep Iberia-Newfoundland margins: Evidence for a complex breakup history,
1515 *Tectonics,* 26, TC2011, doi:10.1029/2006TC001970.
1516 Péron-Pinvidic, G., G. Manatschal, S. M. Dean and T. A. Minshull (2008), Compressional structures
1517 on the West Iberia rifted margin: controls on their distribution, in *The Nature and Origin of*
1518 *Compression in Passive Margins*, edited by Johnson, H., T. G. Doré, R. W. Gatliff, R. W.
1519 Holdsworth, E. R. Lundin, and J.D. Ritchie, Geological Society, Special Publications, London,
1520 306, 169–183.
1521 Péron-Pinvidic, G., Manatschal, G. and Osmundsen, P. T. (2013), Structural comparison of archetypal
1522 Atlantic rifted margins: A review of observations and concepts, *Marine and Petroleum Geology,*
1523 43, 21–47.
1524 Pickup, S. L. B., Whitmarsh, R. B., Fowler, C. M. R. and Reston, T. J. (1996), Insight into the nature
1525 of the ocean-continent transition off West Iberia from a deep multichanel seismic reflection
1526 profile, *Geology*, 24, 1079–1082.
1527 Pinet, B., Montadert, R. *ET AL.,* (1987), Crustal thinning on the Aquitaine shelf Bay of Biscay, from
1528 deep seismic data, *Letters to nature, Nature*, 325, 513–516.
1529 Pulgar, J. A., Gallart, J., Fernández-Viejo, G., Pérez-Estaun, A., Alvarrez-Marron, J. and Escin Group
1530 (1996), Seismic image of the Cantabrian Mountains in the western extension of the Pyrenees
1531 from integrated ESCIN reflection and refraction data. *Tectonophysics,* 264, 1–19.
1532 Rat, P. (1988), The Basque–Cantabrian basin between the Iberian and European plates some facts but
1533 still many problems, *Revista de la Sociedad Geológica de España*, 1, 327–348.

1534 Razin, P. (1989). Évolution tecto-sédimentaire alpine des Pyrénées basques à l'ouest de la
1535 transformante de Pamplona (Province du Labourd), *Thèse de doctorat,* Université de Bordeaux
1536 III, pp. 464.
1537 Reston, T. J. (2009), The structure, evolution and symmetry of the magma-poor rifted margins of the
1538 North and Central Atlantic: A synthesis, *Tectonophysics,* 468, 6–27.
1539 Reston, T. J. (2010), The opening of the central segment of the South Atlantic: symmetry and the
1540 extension discrepancy, *Petroleum Geoscience*, 16, 199–206.
1541 Reston, T. J. and K. G. McDermott (2011), Successive detachment faults and mantle unroofing at
1542 magma-poor rifted margins, *Geology*, 39, 1071–1074.
1543 Reston, T. J. and M. Pérez-Gussinyé (2007), Lithospheric extension from rifting to continental break-
1544 up at magma-poor margins: rheology, serpentinisation and symmetry, *International Journal of*
1545 *Earth Sciences*, 96, 1033–1046.
1546 Roca, E., J. A. Muñoz, O. Ferrer, and N. Ellouz (2011), The role of the Bay of Biscay Mesozoic
1547 extensional structure in the configuration of the Pyrenean orogen: Constraints from the
1548 MARCONI deep seismic reflection survey, *Tectonics,* 30, TC2001,
1549 doi:10.1029/2010TC002735.
1550 Roest, W. R. and W. P.Srivastava (1991), Kinematics of the plate boundaries between Eurasia, Iberia
1551 and Africa in the North Atlantic from Late Cretaceous to present, *Geology*, 19, 613–616.
1552 Rosenbaum, G., G.S. Lister, and C. Duboz (2002), Relative motions of Africa, Iberia and Europe
1553 during Alpine orogeny, *Tectonophysics,* 359, 117–129.
1554 Rossi, P., A. Cocherie, C. M. Fanning, and Y. Ternet (2003), Datation U–Pb sur zircons des dolérites
1555 tholéiitiques pyrénéennes (ophites) à la limite Trias–Jurassique et relations avec les tufs
1556 volcaniques dits "infra-liasiques" nord-pyrénéens, *Comptes Rendus Géoscience*, 335, 1071–
1557 1080.
1558 Roure, F. and P. Choukroune (1998), Contribution of the ECORS seismic data to the Pyrenean
1559 geology: crustal architecture and geodynamic evolution of the Pyrenees, in *The ECORS*
1560 *Pyrenean deep seismic surveys, 1985-1994*, edited by Damotte, B., Mémoires de la Société
1561 Géologique de France, 37–52
1562 Roux, J. C. (1983), Recherches stratigraphiques et sédimentologiques sur les flyshs crétacés pyrénéens
1563 au sud d'Oloron (Pyrénées-Atlantiques), *PhD thesis*, Université de Toulouse, Toulouse, France.
1564 Ruiz, M. (2007), Caracterització estructural i sismotectònica de la litosfera en el Domini Pirenaico-
1565 Cantàbric a partir de mètodes de sísmica activa i passiva, *PhD thesis*, Universidad de Barcelona,
1566 Spain.
1567 Salas, R. and A. Casas (1993), Mesozoic extensional tectonics, stratigraphy and crustal evolution
1568 during the Alpine cycle of the eastern Iberian basin, *Tectonophysics*, 228, 33–35.
1569 Salas, R., J., Guimerá, R., Mas, C., Martín-Closas, A., Meléndez, and A., Alonso (2001), Evolution of
1570 the Mesozoic Central Iberian Rift System and its Cenozoic inversion (Iberian chain), in *Peri-*

Tethys Memoir 6: Pery-Tethyan Rift/Wrench Basins and Passive Margins, edited by P. A. Ziegler, W. Cavazza, A. H. F.Robertson and S., Crasquin-Solea. *Mémoires du Muséum National d'Histoire Naturelle*, Paris, 186, 145–185.

Sandwell, D. T. and W. H. F. Smith (2009), Global marine gravity from retracked Geosat and ERS-1 altimetry: Ridge segmentation versus spreading rate, *Journal of Geophysical Research*, 114, B01411, doi:10.1029/2008JB006008.

Schettino, A. and C. R. Scotese (2002), Global kinematic constraints to the tectonic history of the Mediterranean region and surrounding areas during the Jurassic and Cretaceous, in *Reconstruction of the Evolution of the Alpine-Himalayan Orogen*, edited by G. Rosenbaum, and G. Lister, Journal of the Virtual Explorer, 8, 149–168.

Serrano, O., J. Delmas, F. Hanot, R. Vially, J. P. Herbin, P. Houel, and B. Tourlière (2006), Le bassin d"Aquitaine: Valorisation des données sismiques, cartographie structurale et potentiel pétrolier, *Rapport Régional d'Evaluation Pétrolière, BRGM, Orléans,* pp. 245.

Sibuet, J. C. (1973), South Armorican shear zone and continental fit before the opening of the Bay of Biscay, *Earth and Planetary Science Letters*, 18, 153-157.

Sibuet, J.C., S. P. Srivastava, and W. Spakman (2004), Pyrenean orogeny and plate kinematics, *Journal of Geophysical Research*, 109, B08104, doi: 10.1029/2003JB002514.

Sibuet, J. C., S. Srivastava, and G. Manatschal (2007), Exhumed mantle-forming transitional crust in the Newfoundland–Iberia rift and associated magnetic anomalies, *Journal of Geophysical Research,* 112*,* B06105, doi:10.1029/2005JB003856.

Smith, W. H. F. and D. T. Sandwell (1997), Global sea floor topography from satellite altimetry and ship depth soundings, *Science,* 277, 1956–1962.

Soler, R., . L pez-Vilchez, and C. Riaza (1981), Petroleum geology of the Bay of Biscay, in *Petroleum geology of the continental shelf of north-west Europe*, edited by L. V. Illing, and G. D. Hobson, Institute of Petroleum, London, 474–482.

Souquet, P., E. J. Debroas, J. M. Boirie, P. Pons, G. Fixari, J. C. Roux, J. Dol, J. P. Thieuloy, M. Bonnemaison, H. Manivit, and B. Peybernès (1985), The black flysh group (Albian-Cenomanian) of the Pyrenees, *Bulletin des Centres de Recherches Exploration-Production Elf Aquitaine*, 9, 183–252.

Srivastava, S. P., W. R. Roest, L. C. Kovacs, G. Oakey, S. Lévesque, J. Verhoef, and R. Macnab, (1990), Motion of Iberia since the Late Jurassic: Results from detailed aeromagnetic measurements in the Newfoundland Basin, *Tectonophysics*, 184, 229–260.

Srivastava, S. P., Sibuet, J. C., Cande, S., Roest, W. R. & Reid I. D. (2000), Magnetic evidence for slow seafloor spreading during the formation of the Newfoundland and Iberian margins, *Earth and Planetary Science Letters*, 182, 61–76.

Sutra, E. and G. Manatschal (2012), How does the continental crust thin in a hyperextended rifted margin? Insights from the iberia margin, *Geology,* 40, 139–142.

1608 Sutra, E., G. Manatschal, G. Mohn, and P. Unternehr (2013), Quantification and restoration of
1609 extensional deformation along the Western Iberia and Newfoundland rifted margins,
1610 *Geochemistry, Geophysics, Geosystems,* 14, 2575–2597.
1611 Tavani, S. (2012), Plate kinematics in the Cantabrian domain of the Pyrenean orogen, *Solid Earth*, 3,
1612 265-292.
1613 Tavani, S. and J. A. Muñoz (2012), Mesozoic rifting in the Basque–Cantabrian Basin (Spain):
1614 Inherited faults, transversal structures and stress perturbation, *Terra Nova*, 24, 70–76.
1615 Teixell, A. (1990), Alpine thrusts at the western termination of the Pyrenean Axial Zone, *Bulletin de la*
1616 *Société Géologique de France*, 6, 241–249.
1617 Teixell, A. (1996), The Ansó transect of the southern Pyrenees: Basement and cover thrust geometries,
1618 *Journal of the Geological Society,* 153, 301–310.
1619 Teixell, A. (1998), Crustal structure and orogenic material budget in the west central Pyrenees,
1620 *Tectonics,* 17**,** 395–406.
1621 Ternet, Y. (1980), Feuille de Argelès-Gazost (1070), Carte géologique de la France, scale 1/50,000,
1622 *Bureau de Recherche Géologique et Minières,* Orléans, France
1623 Ternet Y., P. Barrère, J. Canérot and C. Majesté-Menjoulàs (2004a), Feuille de Laruns-Somport
1624 (1069), Carte géologique de la France, scale 1/50,000, *Bureau de Recherche Géologique et*
1625 *Minières,* Orléans, France.
1626 Ternet, T., C. Majeste-Menjoulas, J. Canerot, T. Baudin, A. Cocherie, C. Guerrot, and P. Rossi,
1627 (2004b), Notice explicative, Feuille de Laruns-Somport (1069), Carte géologique de la France,
1628 scale 1/50,000, 192 pp., *Bureau de Recherche Géologique et Minières,* Orléans, France.
1629 Thinon, I. (1999), Structure profonde de la Marge Nord Gascogne et du Bassin Armoricain, *PhD*
1630 *thesis*, *Ifremer-IUEM*, Brest, France.
1631 Thinon, I., L. Fidalgo-González, J.-P. Réhault, and J.-L. Olivet (2001), Pyrenean deformations in the
1632 Bay of Biscay, *Comptes Rendus de l'Academie de Sciences - Serie IIa: Sciences de la Terre et*
1633 *des Planètes,* 332, 561–568.
1634 Thinon, I., J. P. Réhault, and L. Fidalgo-González (2002), The syn-rift sedimentary cover of the North
1635 Biscay Margin (bay of Biscay): From new reflection seismic data, *Bulletin de la Société*
1636 *Géologique de France,* 173, 515–522.
1637 Thinon, I., L. Matias, J. P. Réhault, A. Hirn, L. Fidalgo-González, and F. Avedik (2003), Deep
1638 structure of the Armorican Basin (Bay of Biscay): A review of Norgasis seismic reflection and
1639 refraction data, *Journal of the Geological Society,* 160, 99–116.
1640 Tomassino, A. and F. Marillier (1997), Processing and interpretation in the tau-p domain of the
1641 ECORS Bay of Biscay expanding spread profiles, *Mémoires de la Société Géologique de*
1642 *France*, 171, 31–43.
1643 Tucholke, B. E. and J. C. Sibuet (2012), Problematic plate reconstruction, *Nature Geoscience*, 5, 676–
1644 677, doi:10.1038/ngeo1596.

1645 Tugend, J., G. Manatschal, N. J. Kusznir, and E. Masini, (Accepted for publication), Characterizing
1646 and identifying structural domains at rifted continental margins and its western pyrenean fossil
1647 remnants, In *Sedimentary Basins and Crustal Processes at Continental Margins: From Modern*
1648 *Hyper-extended Margins to Deformed Ancient Analogues,* edited by G. Gibson, F. Roure and G.
1649 Manatschal, Geological Society of London, Special Publications.
1650 Unternehr, P., G. Péron-Pinvidic, G. Manatschal, and E. Sutra (2010), Hyper-extended crust in the
1651 south Atlantic: in search of a model, *Petroleum Geoscience,* 16, 207–215.
1652 Turner, J. P. (1996), Switches in subduction direction and the lateral termination of mountain belts:
1653 Pyrenees-Cantabrian transition, Spain, *Journal of the Geological Society*, 153, 563–571.
1654 Vauchez, A., C. Clerc, L. Bestani, Y. Lagabrielle, A. Chauvet, A. Lahfid, and D. Mainprice (2013),
1655 Preorogenic exhumation of the North Pyrenean Agly massif (Eastern Pyrenees-France),
1656 *Tectonics,* 32, 95–106.
1657 Vergés, J. and J. García-Senz (2001), Mesozoic evolution and Cenozoic inversion of the Pyrenean
1658 Rift, in *Peri-Tethys Memoir 6*: *Pery-Tethyan Rift/Wrench Basins and Passive Margins,* edited
1659 by P. A., Ziegler, W., Cavazza, A. H. F. Robertson, and S. Crasquin-Soleau, *Mémoires du*
1660 *Muséum National d'Histoire Naturelle*, Paris, 186, 187–212.
1661 Vergés, J., M. Fernàndez, and A. Martínez (2002), The Pyrenean orogen: Pre-, syn-, and post-
1662 collisional evolution, in *Reconstruction of the Evolution of the Alpine-Himalayan Orogen*,
1663 edited by G. Rosenbaum, and G. Lister, Journal of the Virtual Explorer, 8, 57–76.
1664 Vielzeuf, P. (1984), Relations de phases dans le facies granulite et implications géodynamiques:
1665 l'exemple des granulites des Pyrénées, *Thesis*, Université Blaise Pascal Clermont-Ferrand II,
1666 Clermont-Ferrand, France.
1667 Vissers, R. L. M. and P. Meijer (2012), Mesozoic rotation of Iberia: Subduction in the Pyrenees?
1668 *Earth-Science Reviews,* 110, 93-110.
1669 White, R. S., D. Mckenzie, and R. K. O'nions (1992), Oceanic crustal thickness from seismic
1670 measurements and rare earth element inversions, *Journal of Geophysical Research*, 97, 19683–
1671 19715.
1672 Wilson, J. T. (1966), Did the Atlantic close and then re-open? *Nature,* 211, 676–681,
1673 doi:10.1038/211676a0
1674 Wilson, R. C. L, G. Manatschal, and S. Wise (2001), Rifting along non-volcanic passive margins:
1675 Stratigraphic and seismic evidence from the Mesozoic successions of the Alps and Western
1676 Iberia, *Geological Society Special Publications*, *London*, 187, 429–452.
1677 Winnock, E. (1971), Géologie succinte du Bassin d'Aquitaine (contribution à l'histoire du Golfe de
1678 Gascogne), in *Histoire Structurale du Golfe de Gascogne*, edited by Debyser, J., X. Le Pichon,
1679 and L. Montadert, Institut Français du Pétrole, Paris, IV.1.1–IV.1.30.
1680 Wortmann, U. G., H. Weissert, H. Funk, and J. Hauck (2001), Alpine plate kinematics revisited: The
1681 Adria problem, *Tectonics*, 20, 134–147.

Figure Captions:

Figure 1: Bathymetric map of the Bay of Biscay and Pyrenees showing the major tectonic structures and the main Mesozoic basins. Magnetic anomalies are based on *Sibuet et al.* [2004].

Figure 2: Philosophy of the onshore/offshore approach applied in this study. Left side: synthetic diagram combining geophysical (upper part) and geological (lower part) diagnostic elements of structural/genetic rift domains at continental rifted margins (after *Tugend et al.,* 2014). The terminology used in this study is indicated in the central part. Right side: this approach is used to map rifted domains offshore (gravity inversion results and seismic interpretations) and onshore (structural map of the Mauléon basin and of the southern part of the Arzacq basin and field observations).

Figure 3: (a) Geological map of the Mauléon basin and the Southern part of the Arzacq basin. Lithologies and age of sequences are synthetized in a log. (b) Field photographs of the main observations. Ka: Kalkuetta canyon, contact between the "Calcaires des Cañons" platform and underlying eroded Palaeozoic basement (0°50‟59,72"W/42°59‟17,31"N). Me: Mendibelza massif, tectono-sedimentary breccia at the contact with the top basement detachment fault (1°6‟55,78"W/43°5‟40,16"N). Ar: Abarratia quarry, deformation of the granulitic basement (gouges, cataclastic overprint) charactering the top basement detachment fault described by *Jammes et al*. [2009] (1°14‟17,69"W/43°20‟55,64"N). Ur: Urdach quarry, syn-rift breccia reworking mantle and basement rocks (0°40‟39,62W/43°7‟10,91"N). (c) Simplified cartoons of the key observations from remnants of the former rift system preserved in the Pyrenean nappe stack. Axial zone unit: remnant of the proximal domain. Bedous-Mendibelza unit: remnant of the Necking domain. Layens-Labourd unit: remnant of the

hyperthinned domain. Sarrance-Mail arrouy unit: remnant of the exhumed mantle domain. Grand Rieu High: remnant of the hyperthinned domain. Arzacq basin: transition from proximal to necking domain. The map is simplified after the BRGM (1/50000) geological map of: Arthez de Béarn, Argelès-Gazost, Gavarnie, Hasparren, Iholdy, Laruns-Somport, Larrau, Lourdes, Oloron-Sainte-Marie, Orthez, Mauléon-Licharre, Morlaàs, Pau, Saint-Jean-Pied-de-Port, Tardets (see references in the bibliography)

Figure 4: Raw data used for the gravity inversion (a) Bathymetry and topography [*Smith and Sandwell*, 1997] (b) Free-air gravity [*Sandwell and Smith*, 2009] (c) Oceanic age isochrones [*Müller* et al., 1997] (d) Sediment thickness is derived from offshore seismic interpretations (Raw seismic lines from the Norgasis survey: [*Thinon*, 1999; *Avedik et al.,* 1993; 1996]; ECORS Bay of Biscay: [*Pinet et al.,* 1987; *Bois and Gariel*, 1994]; IAM 12 and ESCIN 4 seismic lines: [*Gallart* et al., 2004; *Gallastegui et al*., 2002; *Banda* et al., 1995]) and the depth to basement map of the Aquitaine basin from *Serrano* et al. [2006]).

Figure 5: (a) Moho depth, (b) crustal thickness, (c) residual continental crust and (d) continental lithosphere thinning factor maps resulting from gravity inversion. The limits of rifted domains determined from seismic interpretations are also indicated.

Figure 6: Map of the rift domains preserved in the Bay of Biscay and their fossil analogues from the Pyrenean domain. Extensional rift structures and thrust faults from the Armorican and Western Approach margins are based on the work of *Thinon* [1999] and own observations. CIZ: Central Iberian zone. WALZ: West Asturian-Leonese zone. NPF: North Pyrenean fault. The location of the geological sections from fig 7 is indicated in dashed line.

Figure 7: Geological sections, location fig 6 (a) Bay of Biscay segment: the architecture is based on the Norgasis 11-12 (after *Tugend et al.,* 2014) and IAM 12 seismic profiles (see also fig 8). (b) Basque-Parentis segment: the section is a composite between the depth

1730 interpretation of the ECORS Bay of Biscay seismic profile and the gravity modelling
1731 proposed by *Pedreira* [2003] for the Basque-Cantabrian basin. (c) Pyrenean segment: the
1732 section is based on the interpretation of the ECORS Arzacq-W Pyrenees and the southern
1733 extension is modified after *Teixell* [1998]

1734 **Figure 8**: Norgasis 11 and 12 seismic section along the Western Approach margin (a)
1735 Seismic reflection (b) Line drawing and (c) Interpretation proposed in this study. The location
1736 of the seismic lines is the same as for fig 7a.

1737 **Figure 9:** IAM 12 seismic section along the North Iberian margin (a) Seismic reflection
1738 (b) Line drawing and (c) Interpretation proposed in this study. The location of the seismic
1739 lines is the same as for fig 7a.

1740 **Figure 10**: Zoom over the "Béarnais Range" area (location fig 3). To the left: geological
1741 map and two geological sections (AA" and BB"). To the right: the same map indicating the
1742 remnants of rift domains. The associated cross sections illustrate the reactivation of the former
1743 rifted domains. EB: Eaux-Bonnes thrust; EC: Eaux-Chaudes thrust; GR: Grand Rieu High; St
1744 P: Saint Palais thrust system; Ste S: Sainte Suzanne thrust system.

1745 **Figure 11:** (a) Panoramic view showing the contact between the proximal (axial zone) and
1746 necking domains (Bedous-Mendibelza unit). Note that the contact is steepening eastwards
1747 (0°31"45,07"W/42°57"08,21"N). (b) Panoramic view showing the relashionships between the
1748 different phases of deformation observed in the hyperthinned (Layens unit) and exhumed
1749 mantle domains (Mail Arrouy unit). The initial south directed stacking of units (D1) is
1750 overprinted by north directed deformation (D2), exemplified here by the Ossau thrust
1751 (0°27"16,21"W/43°03"30,98"). The location of the photographs is indicated on fig 9. The
1752 coordinates indicate the location from which the photographs were taken.

Figure 12: Restoration of the Bay of Biscay and Pyrenean rift systems prior to the onset of compression (before the Santonian). Restored sections are proposed in the (a) Bay of Biscay segment (b) Basque-Parentis segment and (c) Pyrenean segment. WA margin: Western Approach margin.

Figure 13: Accretionary prism and "subduction" stage (Santonian-Campanian to Eocene) of the Bay of Biscay and Pyrenean rift systems. Sections are proposed in the (a) Bay of Biscay segment (b) Basque-Parentis segment and (c) Pyrenean segment. WA margin: Western Approach margin.

Figure 14: Collision stage of the Bay of Biscay and Pyrenean rift systems. Sections are proposed in the (a) Bay of Biscay segment (b) Basque-Parentis segment and (c) Pyrenean segment to illustrate the buttress role of necking domains. WA margin: Western Approach margin.

Table Caption:

Table 1: Parameters used for gravity inversion

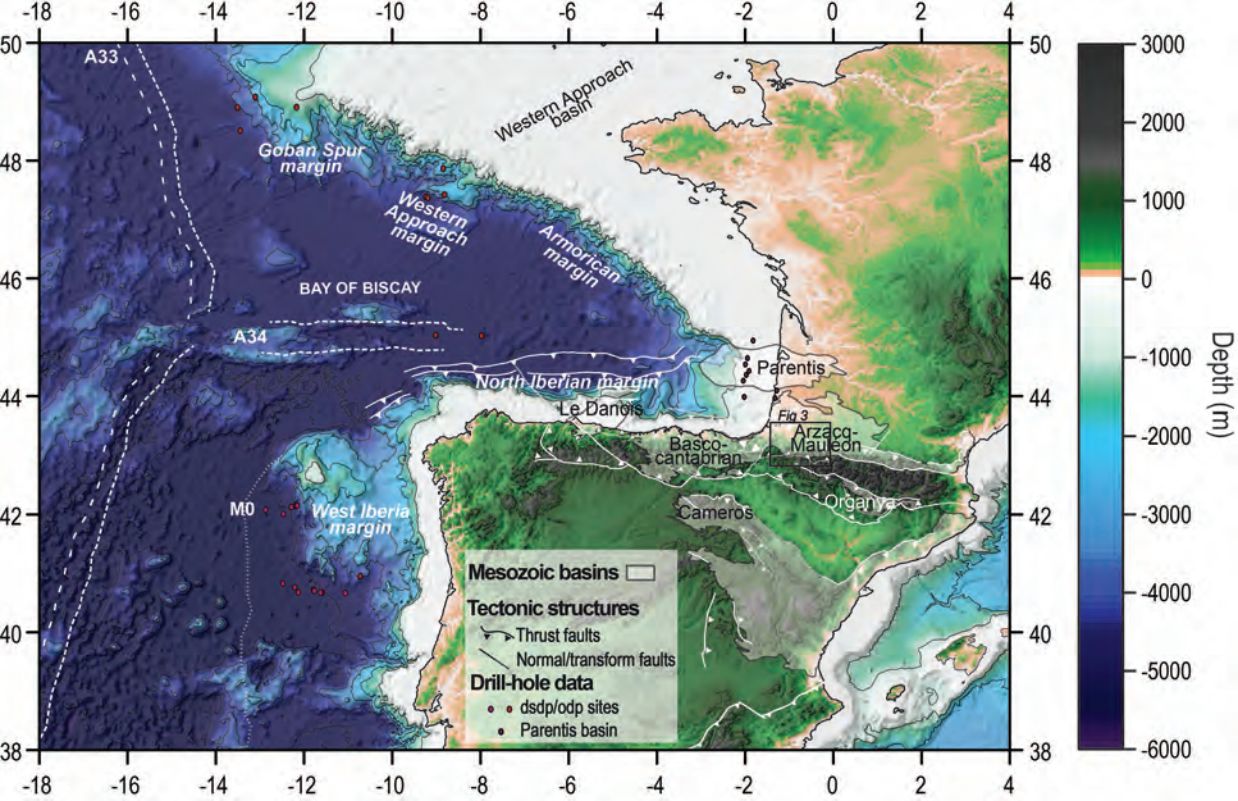
A33
Goban Spur margin
Western Approach basin
Western Approach margin
Armorican margin
BAY OF BISCAY
A34
North Iberian margin
Parentis
Le Danois
Fig 3
Arzacq-Mauléon
Basco-cantabrian
Organyà
Cameros
M0
West Iberia margin
Mesozoic basins
Tectonic structures
Thrust faults
Normal/transform faults
Drill-hole data
dsdp/odp sites
Parentis basin
-18
-16
-14
-12
-10
-8
-6
-4
-2
0
2
4
50
48
46
44
42
40
38
3000
2000
1000
0
-1000
-2000
-3000
-4000
-5000
-6000
Depth (m)

INTERPRETATIONS OF 2D SECTIONS

Geological & geophysical approaches combined

ONSHORE/OFFSHORE MAPPING: 2,5 D

Accommodation space evolution

A.S. at break up

Potential A.S.

Total A.S.

Post rift A.S.

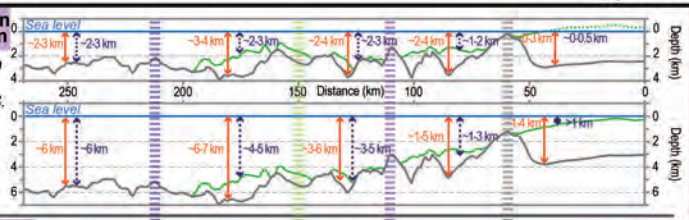

Extensional setting

Low-β

High-β

Lithosphere thinning

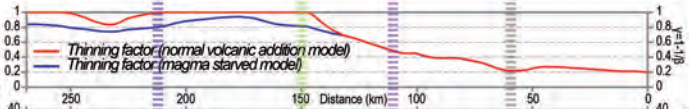

Gravity inversion results

Crustal thickness

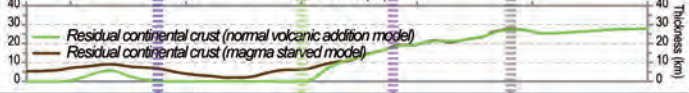

Structural domains

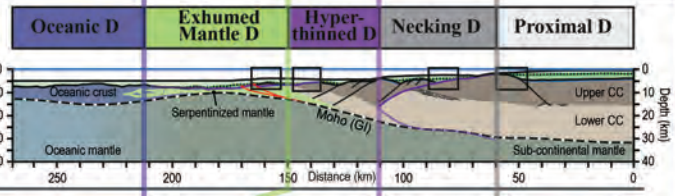

Outcrop-scale observations

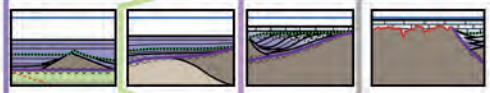

Nature of post rift sediments/aggradation

Shallow water/ poor aggration

Deep water/ large aggration

Nature of interface (basement/sediments)

Erosion

Tectonic

Magmatic

Nature of top basement

Upper continental crust

Lower continental crust

Mantle

Geophysical/Quantitative approaches (Offshore)

Geological observations (Onshore)

OFFSHORE: *SEISMIC INTERPRETATIONS & GRAVITY INVERSION*

Crustal thickness map from gravity inversion

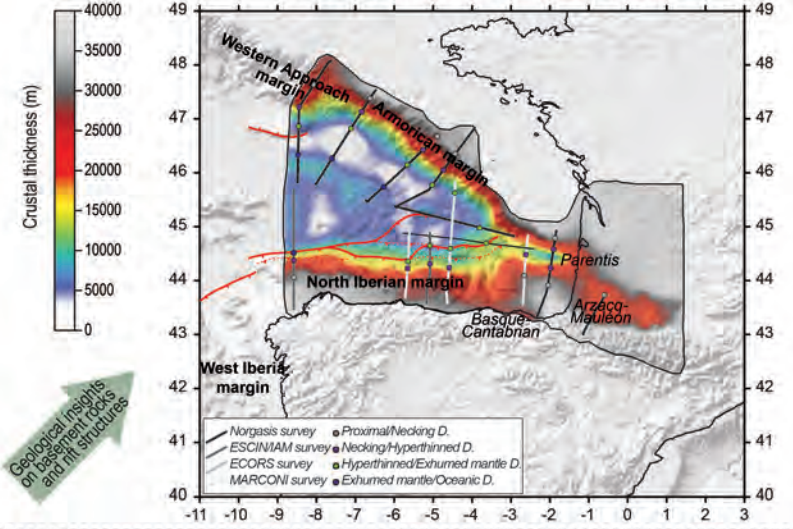

Geological insights on basement rocks and rift structures

ONSHORE: *FIELD MAPPING*

Semi-quantitative estimates of AS & crustal thickness

Structural map of the Arzacq-Mauléon basin

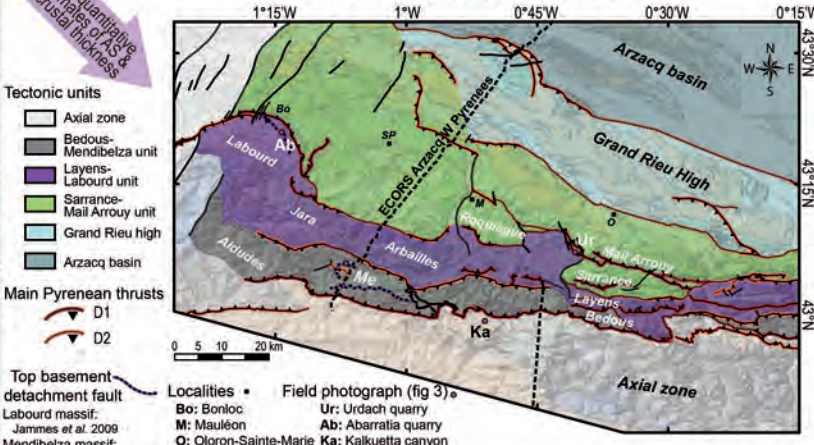

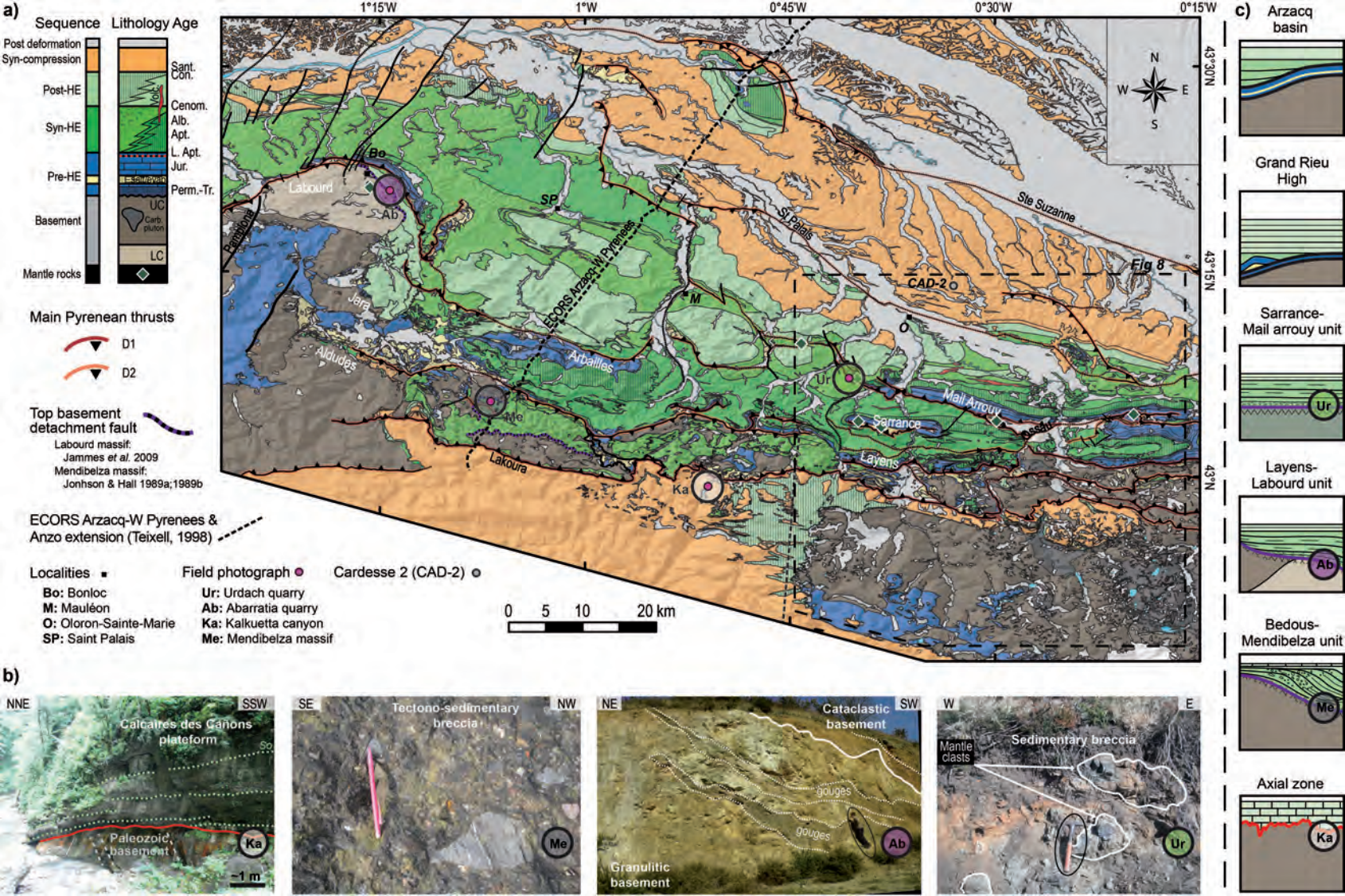
a)
Sequence
Lithology Age
Post deformation
Syn-compression
Post-HE
Syn-HE
Pre-HE
Basement
Mantle rocks
Sant.
Con.
Cenom.
Alb.
Apt.
L. Apt.
Jur.
Perm.-Tr.
UC
Carb. pluton
LC
Main Pyrenean thrusts
D1
D2
Top basement detachment fault
Labourd massif:
Jammes et al. 2009
Mendibelza massif:
Jonhson & Hall 1989a;1989b
ECORS Arzacq-W Pyrenees & Anzo extension (Teixell, 1998)
Localities
Bo: Bonloc
M: Mauléon
O: Oloron-Sainte-Marie
SP: Saint Palais
Field photograph
Ur: Urdach quarry
Ab: Abarratia quarry
Ka: Kalkuetta canyon
Me: Mendibelza massif
Cardesse 2 (CAD-2)
1°15'W
1°W
0°45'W
0°30'W
0°15'W
43°30'N
43°15'N
43°N
N
W
E
S
Labourd
Bo
Ab
SP
Pamplona
St Palais
Ste Suzanne
Fig 8
CAD-2
ECORS Arzacq-W Pyrenees
M
O
Jara
Aldudes
Arbailles
Ur
Mail Arrouy
Sarrance
Layens
Me
Lakoura
Ka
0 5 10 20 km
c)
Arzacq basin
Grand Rieu High
Sarrance-Mail arrouy unit
Layens-Labourd unit
Bedous-Mendibelza unit
Axial zone
b)
NNE
SSW
Calcaires des Canons plateform
Paleozoic basement
Ka
~1 m
SE
NW
Tectono-sedimentary breccia
Me
NE
SW
Cataclastic basement
gouges
Granulitic basement
Ab
W
E
Mantle clasts
Sedimentary breccia
Ur

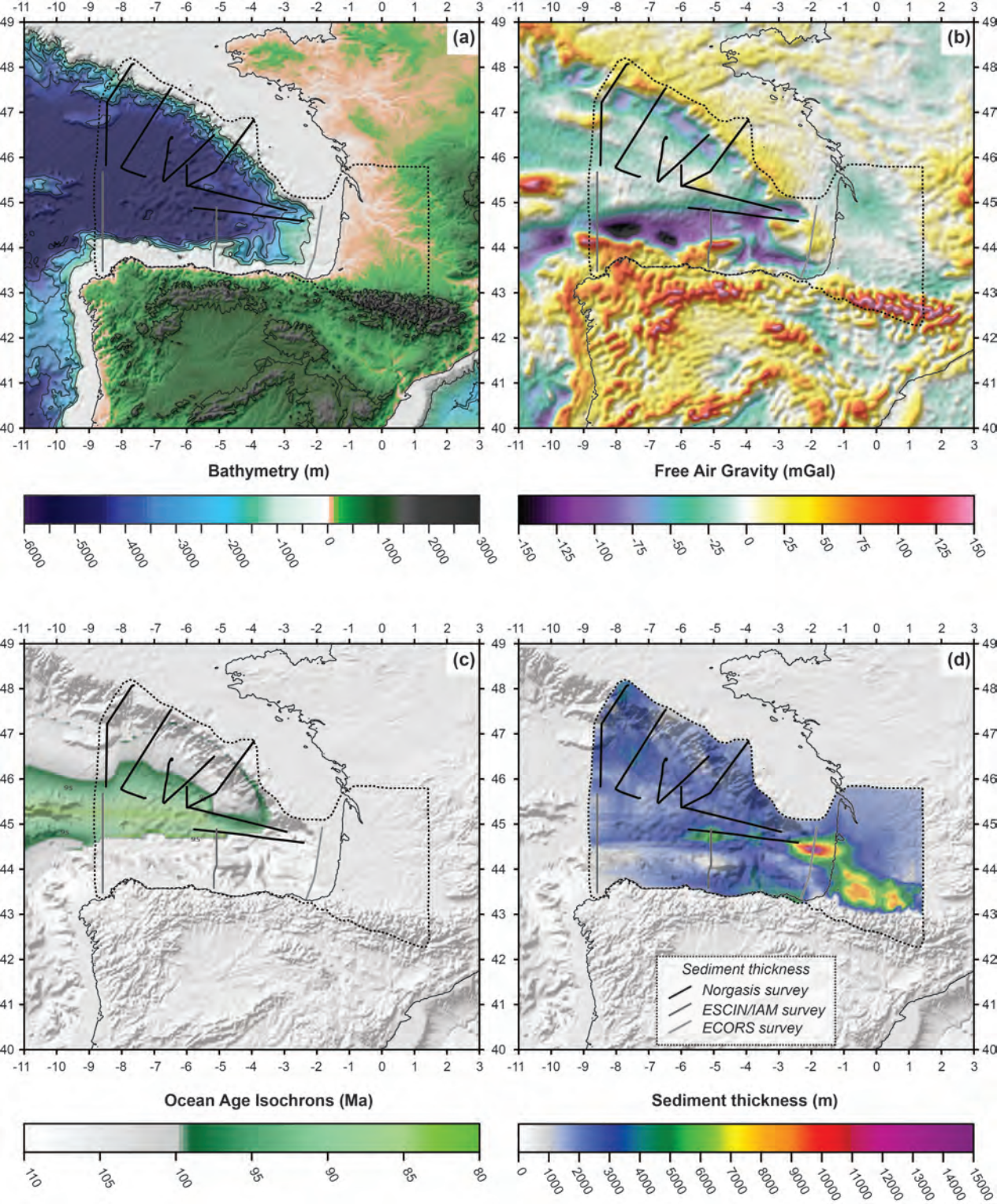
(a)
(b)
(c)
(d)
Bathymetry (m)
-6000 -5000 -4000 -3000 -2000 -1000 0 1000 2000 3000
Free Air Gravity (mGal)
-150 -125 -100 -75 -50 -25 0 25 50 75 100 125 150
Ocean Age Isochrons (Ma)
110 105 100 95 90 85 80
Sediment thickness (m)
0 1000 2000 3000 4000 5000 6000 7000 8000 9000 10000 11000 12000 13000 14000 15000
Sediment thickness
Norgasis survey
ESCIN/IAM survey
ECORS survey

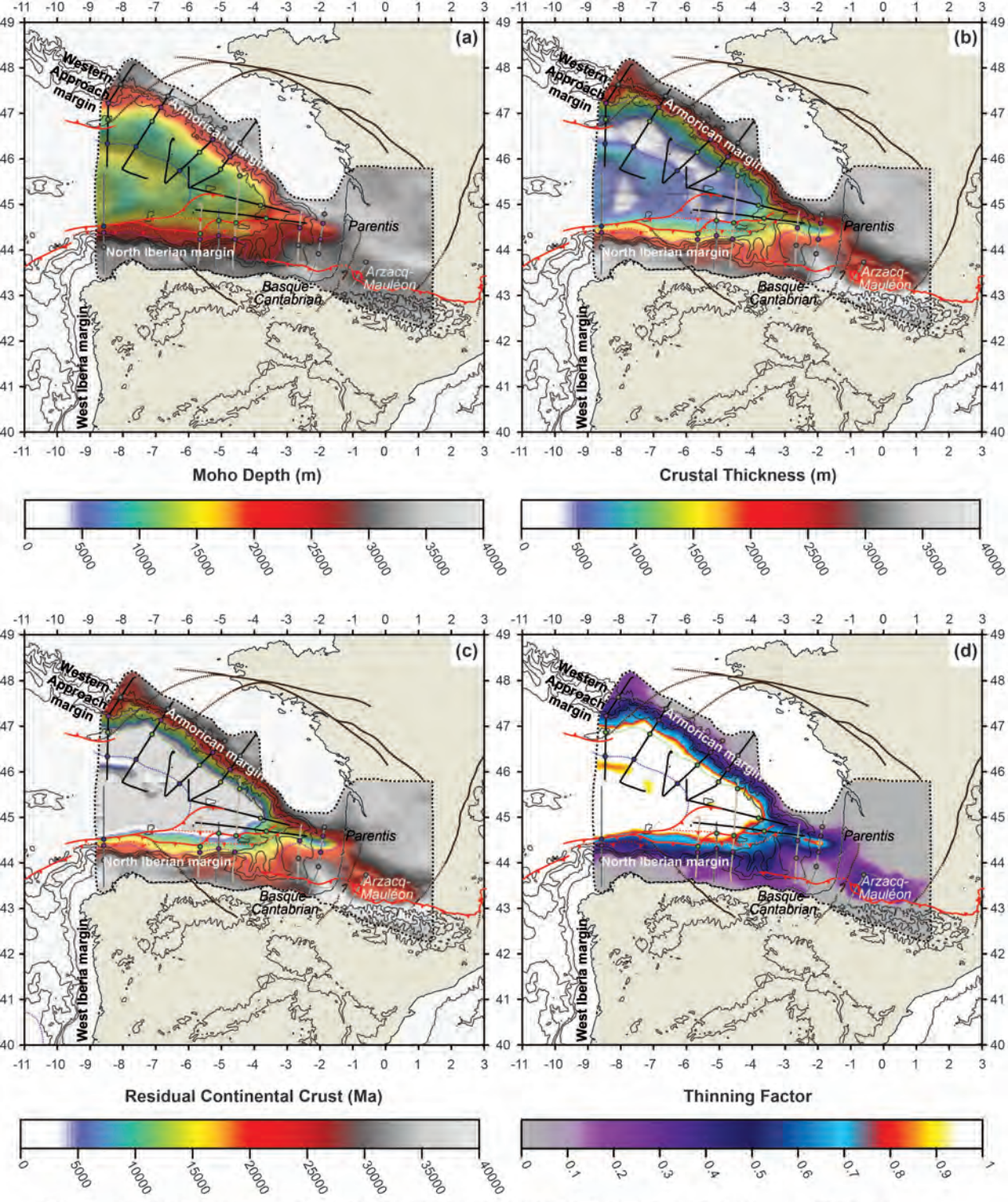
(a)
(b)
(c)
(d)
Western Approach margin
Armorican margin
Parentis
North Iberian margin
Arzacq-Mauléon
Basque-Cantabrian
West Iberia margin
Moho Depth (m)
Crustal Thickness (m)
Residual Continental Crust (Ma)
Thinning Factor
0
5000
10000
15000
20000
25000
30000
35000
40000
0.1
0.2
0.3
0.4
0.5
0.6
0.7
0.8
0.9
1
Seismic reflection survey
Norgasis survey
ESCIN/IAM survey
ECORS survey
MARCONI survey
Limits of rifted domains based on seismic interpretations
Proximal/Necking D.
Necking/Hyperthinned D.
Hyperthinned/Exhumed mantle D.
Exhumed mantle/Oceanic D.
Structures
Thrusts
Shear zone/ Transfer fault

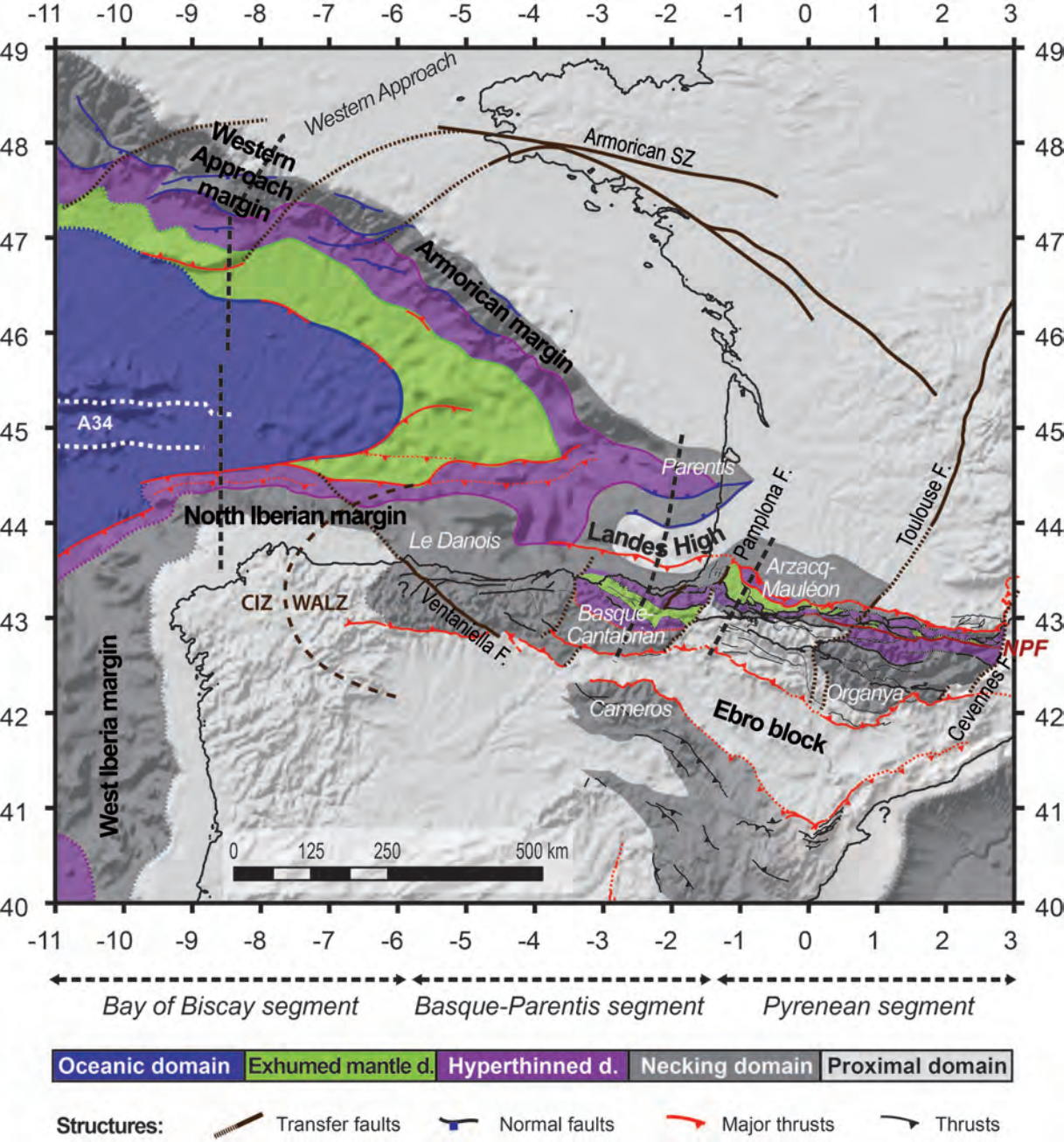
Western Approach
Western Approach margin
Armorican SZ
Armorican margin
A34
North Iberian margin
Parentis
Le Danois
Landes High
Pamplona F.
Toulouse F.
Arzacq-Mauléon
Basque-Cantabrian
Ventaniella F.
CIZ
WALZ
West Iberia margin
Organya
Cameros
Ebro block
Cevennes F.
NPF
0 125 250 500 km
Bay of Biscay segment
Basque-Parentis segment
Pyrenean segment
Oceanic domain
Exhumed mantle d.
Hyperthinned d.
Necking domain
Proximal domain
Structures:
Transfer faults
Normal faults
Major thrusts
Thrusts

(a) Bay of Biscay segment

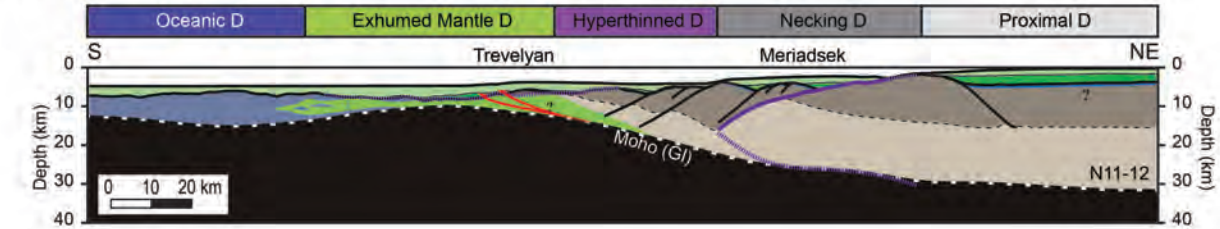

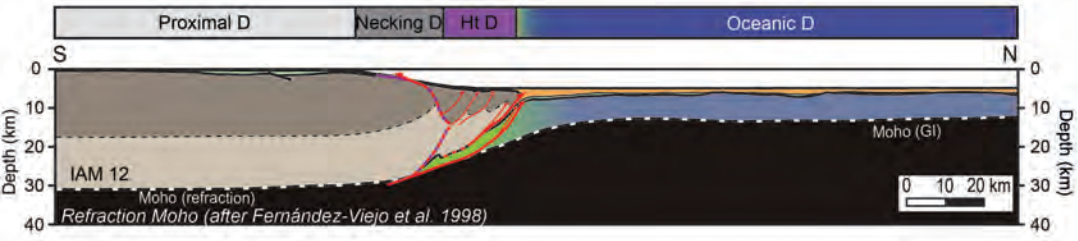

(b) Basque-Parentis segment

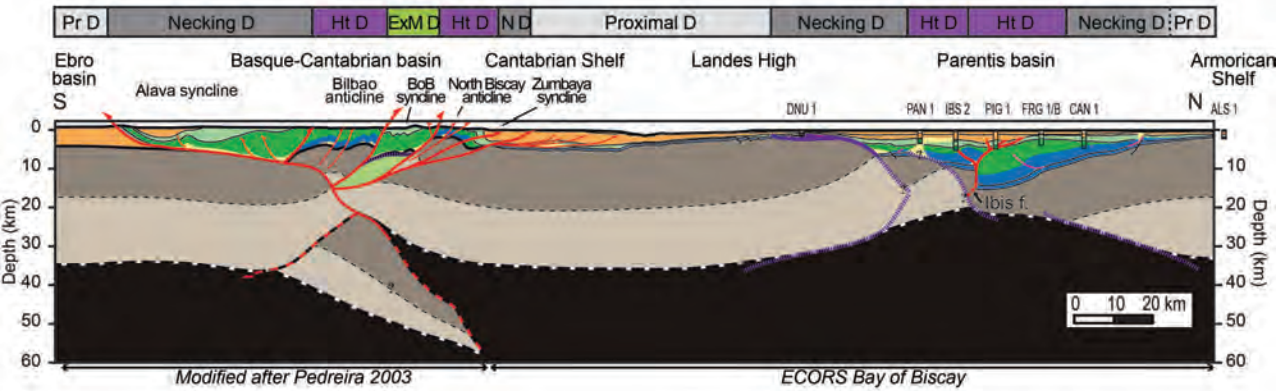

(c) Pyrenean segment

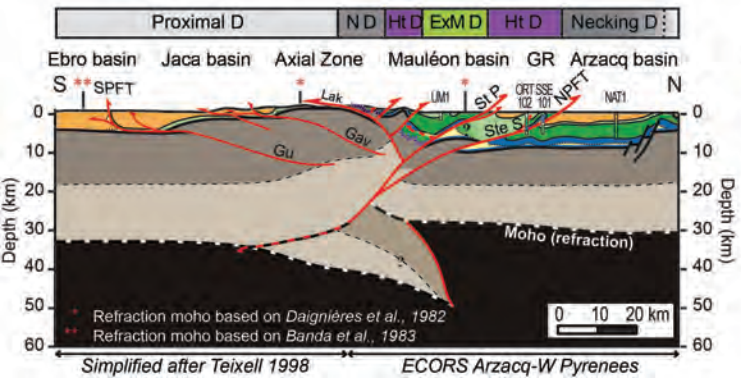

Legend of the sections

Sedimentary sequences

- Syn-compression
- Post-hyperextension
- Syn-hyperextension
- Pre-hyperextension

Nature of basement

- Upper Crust
- Lower Crust
- Oceanic Crust
- Serpentinized mantle
- Mantle (undifferenciated)

Structures

- High angle normal fault (Low-β structures)
- Top basement detachment fault (High-β structures)
- Thrust faults
- Gravitational faults

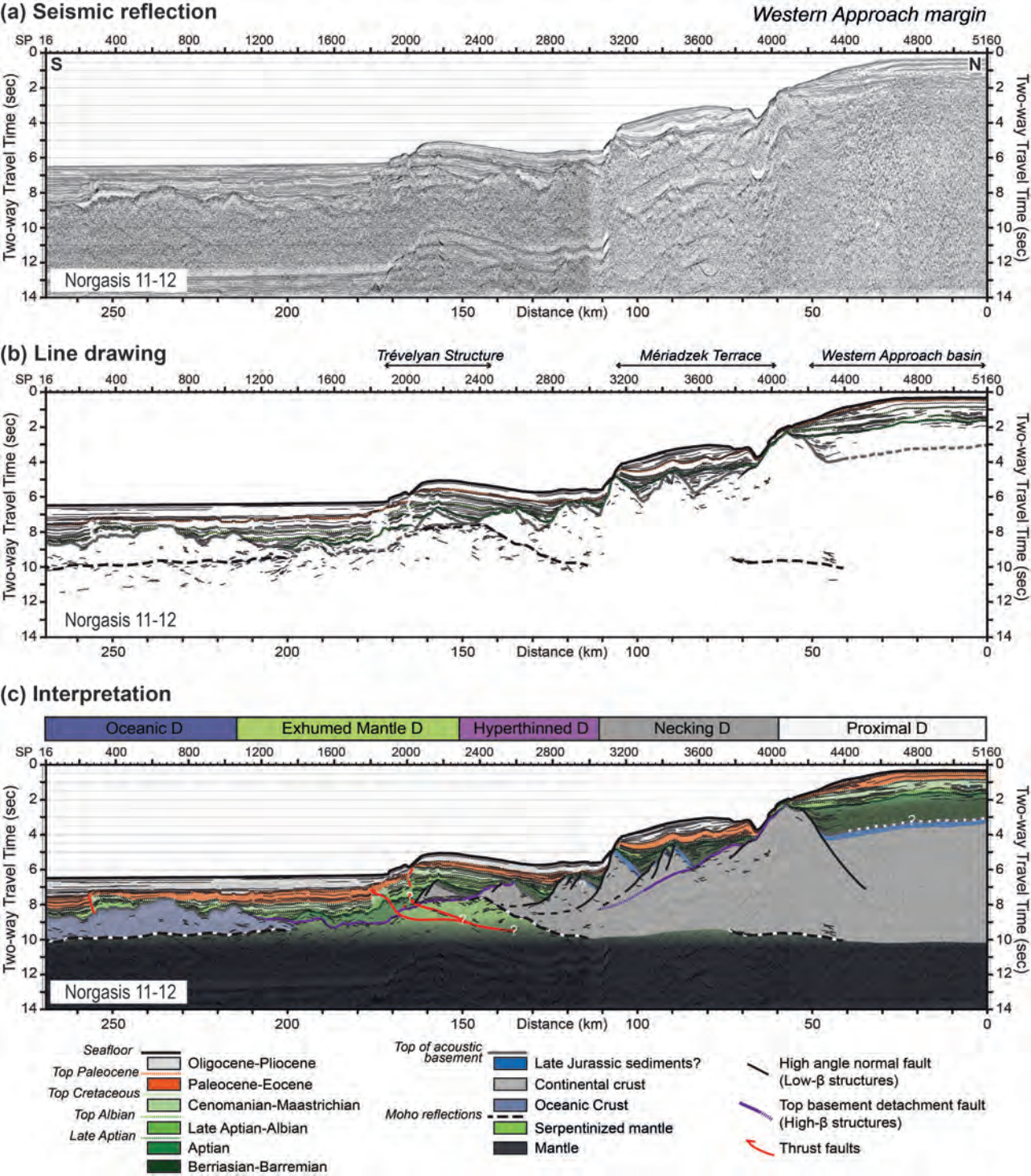
(a) Seismic reflection
Western Approach margin
SP 16 400 800 1200 1600 2000 2400 2800 3200 3600 4000 4400 4800 5160
S
N
Two-way Travel Time (sec)
Norgasis 11-12
250 200 150 Distance (km) 100 50 0
(b) Line drawing
Trévelyan Structure
Mériadzek Terrace
Western Approach basin
(c) Interpretation
Oceanic D
Exhumed Mantle D
Hyperthinned D
Necking D
Proximal D
Seafloor
Top Paleocene
Top Cretaceous
Top Albian
Late Aptian
Oligocene-Pliocene
Paleocene-Eocene
Cenomanian-Maastrichian
Late Aptian-Albian
Aptian
Berriasian-Barremian
Top of acoustic basement
Moho reflections
Late Jurassic sediments?
Continental crust
Oceanic Crust
Serpentinized mantle
Mantle
High angle normal fault (Low-β structures)
Top basement detachment fault (High-β structures)
Thrust faults

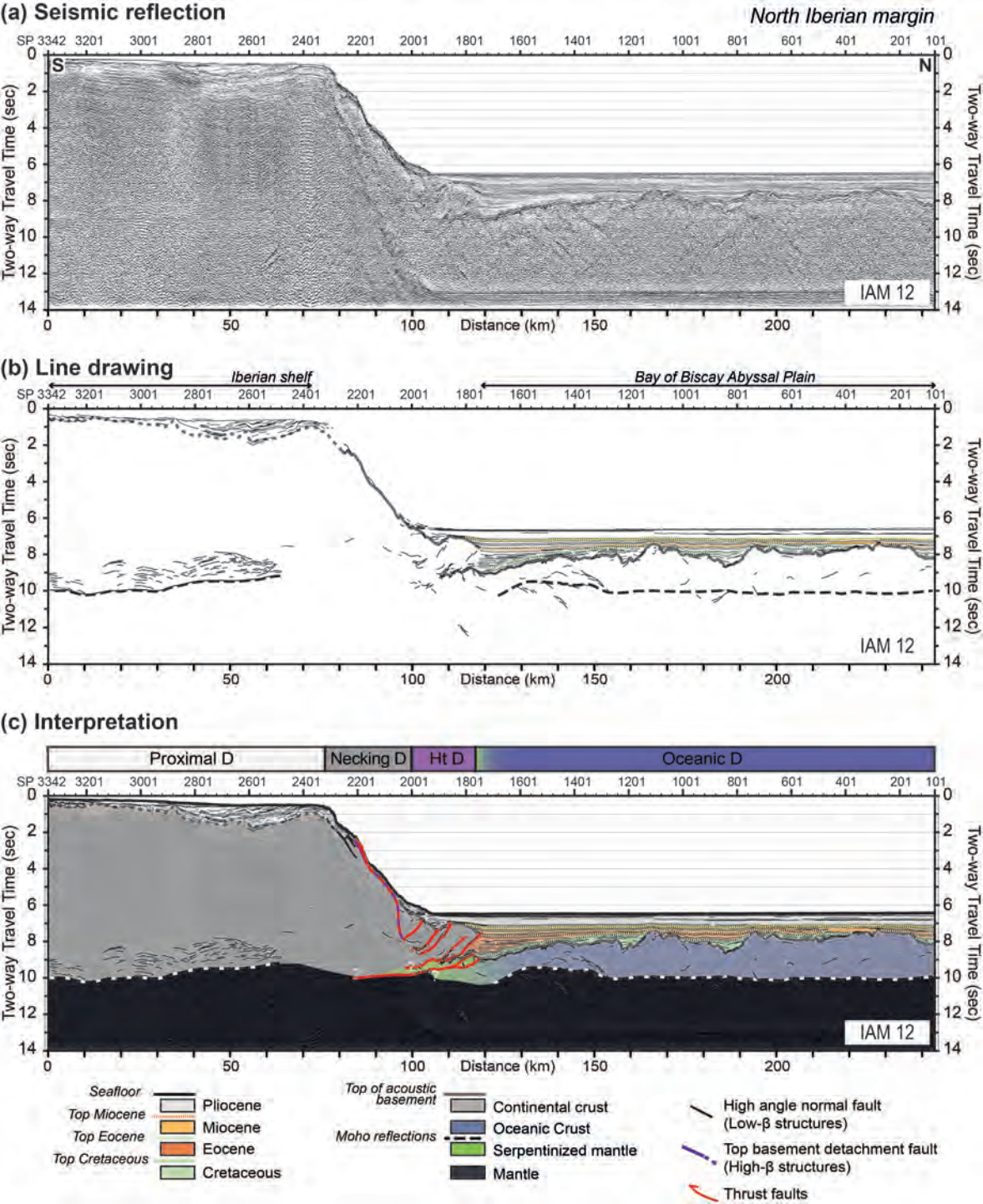
(a) Seismic reflection
North Iberian margin
SP 3342 3201 3001 2801 2601 2401 2201 2001 1801 1601 1401 1201 1001 801 601 401 201 101
S
N
IAM 12
Two-way Travel Time (sec)
Distance (km)
(b) Line drawing
Iberian shelf
Bay of Biscay Abyssal Plain
(c) Interpretation
Proximal D
Necking D
Ht D
Oceanic D
Seafloor
Top Miocene
Top Eocene
Top Cretaceous
Pliocene
Miocene
Eocene
Cretaceous
Top of acoustic basement
Moho reflections
Continental crust
Oceanic Crust
Serpentinized mantle
Mantle
High angle normal fault (Low-β structures)
Top basement detachment fault (High-β structures)
Thrust faults

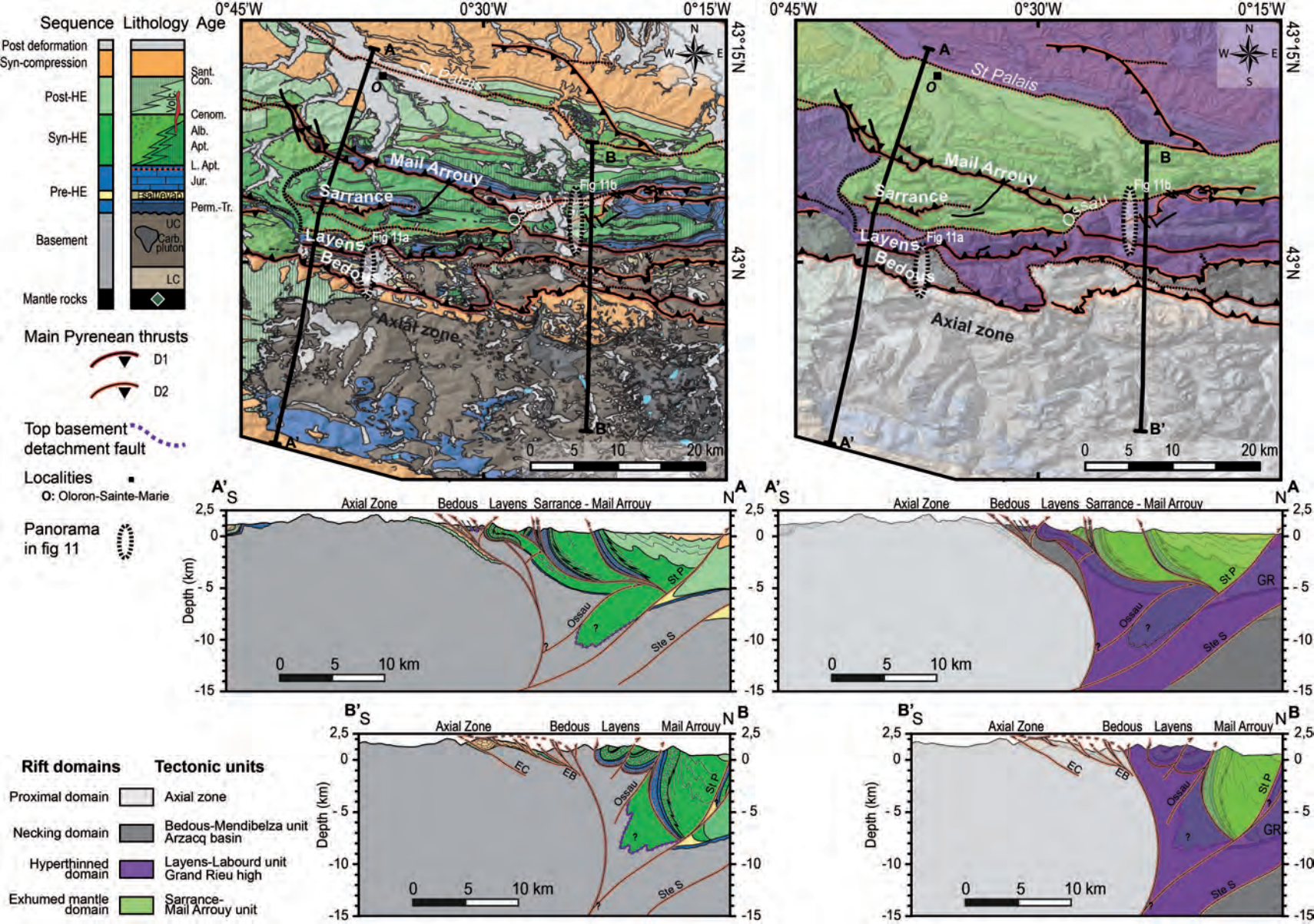
Sequence
Lithology
Age
Post deformation
Syn-compression
Post-HE
Syn-HE
Pre-HE
Basement
Mantle rocks
Sant.
Con.
Cenom.
Alb.
Apt.
L. Apt.
Jur.
Perm.-Tr.
Volc.
UC
Carb. pluton
LC
Main Pyrenean thrusts
D1
D2
Top basement detachment fault
Localities
O: Oloron-Sainte-Marie
Panorama in fig 11
0°45'W
0°30'W
0°15'W
43°15'N
43°N
St Palais
Mail Arrouy
Sarrance
Ossau
Layens
Bedous
Axial zone
Fig 11a
Fig 11b
A
A'
B
B'
0 5 10 20 km
N
W
E
S
A'S
A
Axial Zone
Bedous
Layens
Sarrance - Mail Arrouy
Depth (km)
2,5
0
-5
-10
-15
St P
GR
Ste S
0 5 10 km
B'S
B
Mail Arrouy
EC
EB
Rift domains
Tectonic units
Proximal domain
Axial zone
Necking domain
Bedous-Mendibelza unit
Arzacq basin
Hyperthinned domain
Layens-Labourd unit
Grand Rieu high
Exhumed mantle domain
Sarrance-
Mail Arrouy unit

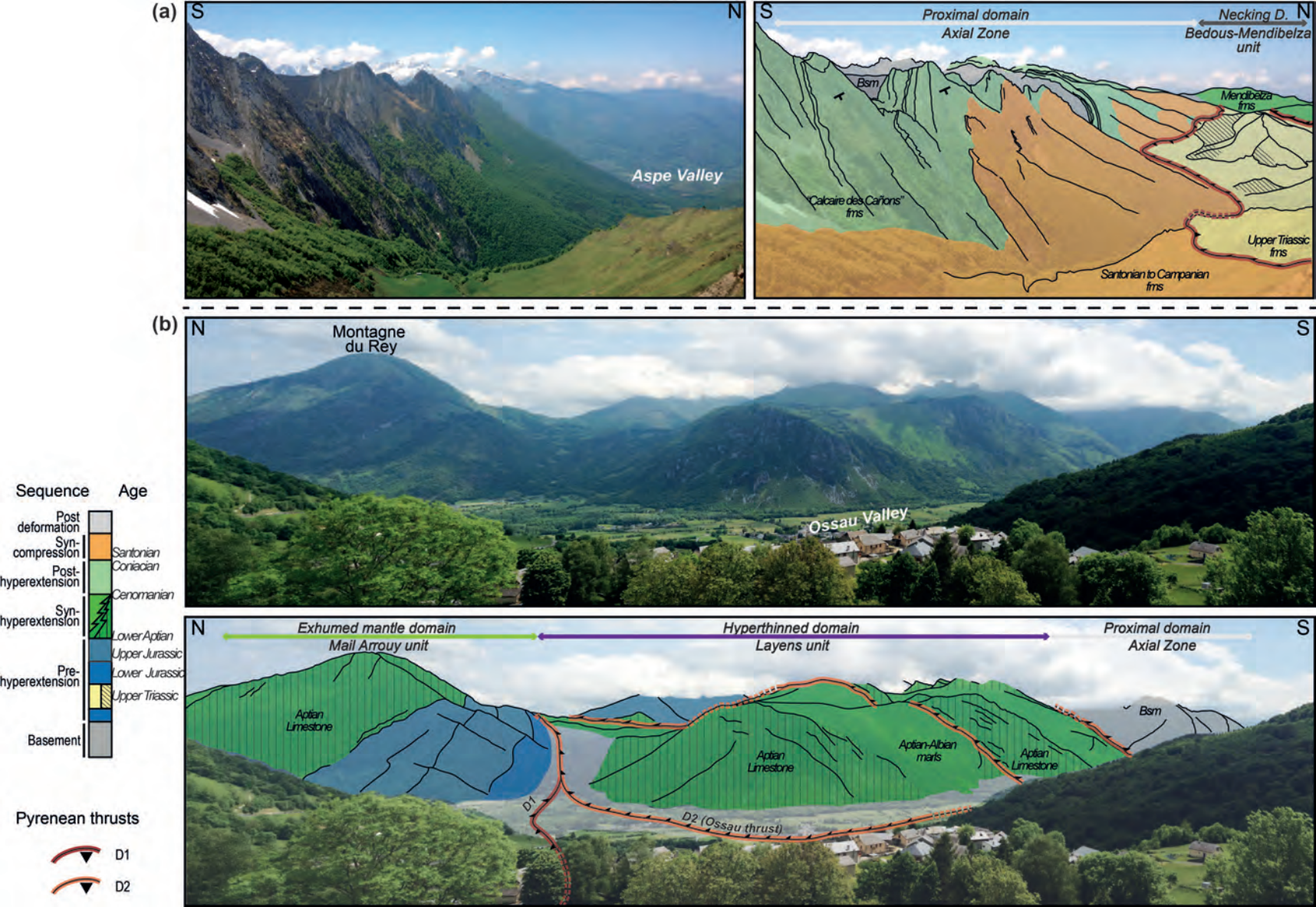
(a)
S
N
Aspe Valley
S
Proximal domain
Axial Zone
Necking D.
N
Bedous-Mendibelza
unit
Bsm
Mendibelza
fms
"Calcaire des Cañons"
fms
Upper Triassic
fms
Santonian to Campanian
fms
(b)
N
Montagne
du Rey
S
Ossau Valley
Sequence
Age
Post
deformation
Syn-
compression
Santonian
Coniacian
Post-
hyperextension
Cenomanian
Syn-
hyperextension
Lower Aptian
Upper Jurassic
Pre-
hyperextension
Lower Jurassic
Upper Triassic
Basement
Pyrenean thrusts
D1
D2
N
Exhumed mantle domain
Mail Arrouy unit
Hyperthinned domain
Layens unit
Proximal domain
Axial Zone
S
Aptian
Limestone
Aptian
Limestone
Aptian-Albian
marls
Aptian
Limestone
Bsm
D1
D2 (Ossau thrust)

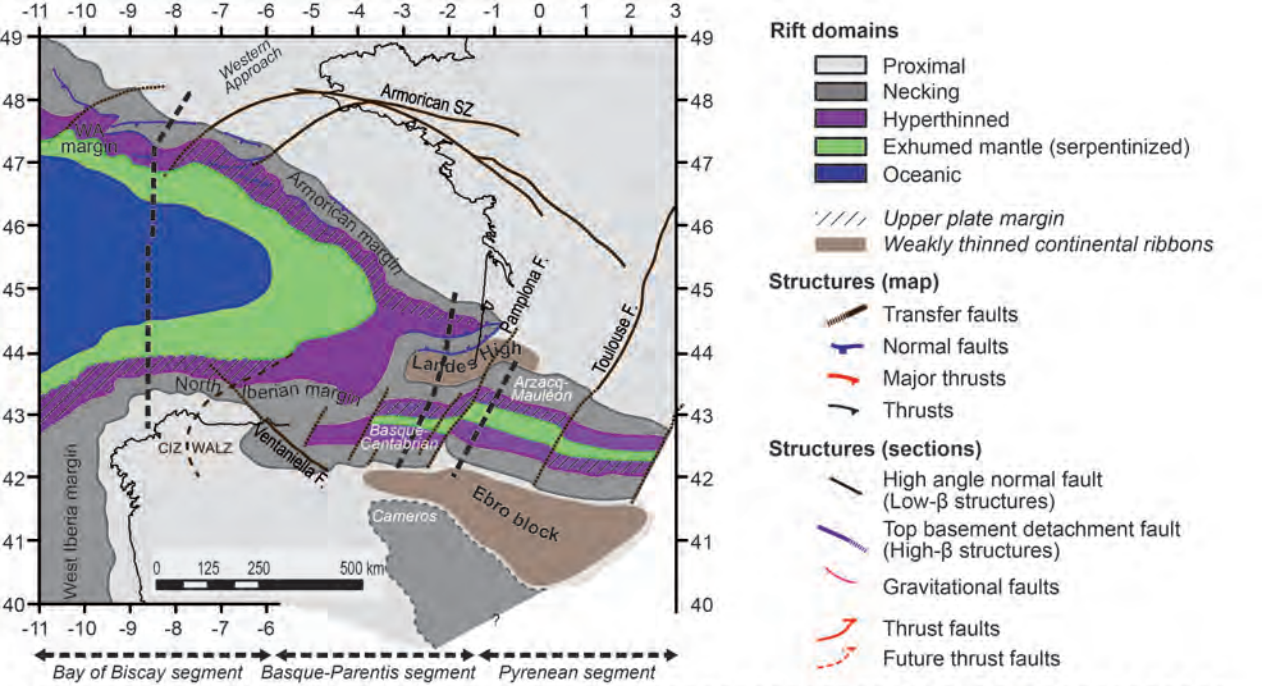
Western Approach
Armorican SZ
WA margin
Armorican margin
Pamplona F.
Toulouse F.
Landes High
Arzacq-Mauléon
North Iberian margin
Basque-Cantabrian
CIZ
WALZ
Ventaniella F.
West Iberia margin
Cameros
Ebro block
0 125 250 500 km
Bay of Biscay segment
Basque-Parentis segment
Pyrenean segment
Rift domains
Proximal
Necking
Hyperthinned
Exhumed mantle (serpentinized)
Oceanic
Upper plate margin
Weakly thinned continental ribbons
Structures (map)
Transfer faults
Normal faults
Major thrusts
Thrusts
Structures (sections)
High angle normal fault (Low-β structures)
Top basement detachment fault (High-β structures)
Gravitational faults
Thrust faults
Future thrust faults

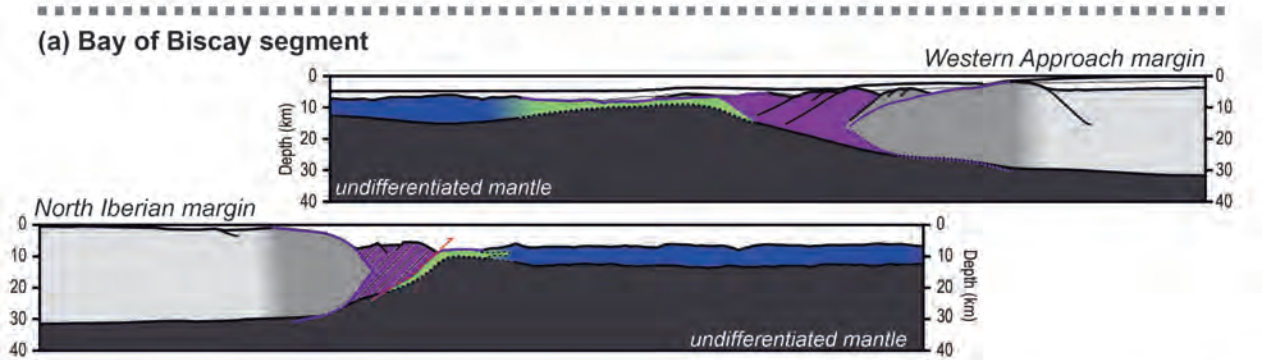
(a) Bay of Biscay segment
Western Approach margin
Depth (km)
undifferentiated mantle
North Iberian margin
undifferentiated mantle

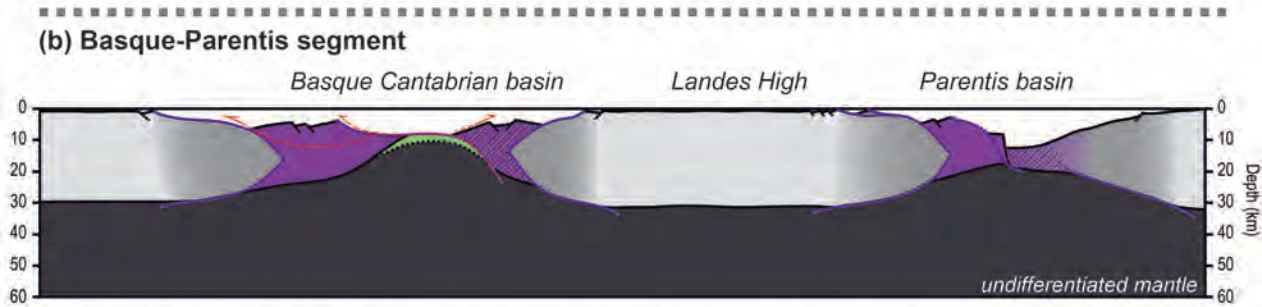
(b) Basque-Parentis segment
Basque Cantabrian basin
Landes High
Parentis basin
Depth (km)
undifferentiated mantle

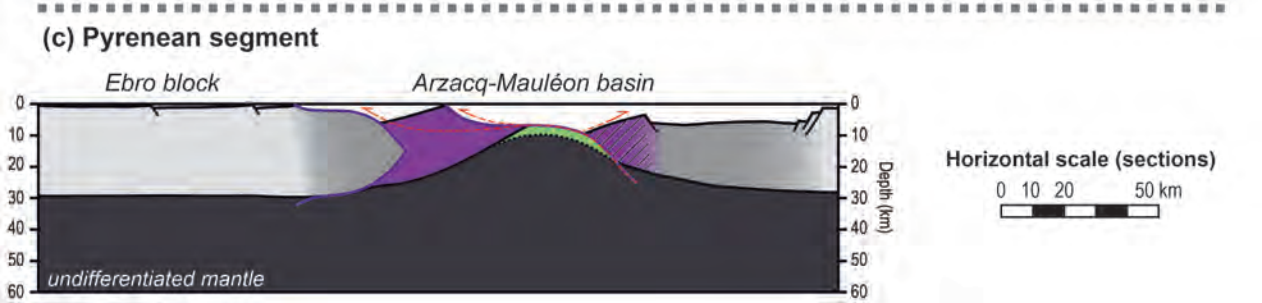
(c) Pyrenean segment
Ebro block
Arzacq-Mauléon basin
Depth (km)
undifferentiated mantle
Horizontal scale (sections)
0 10 20 50 km

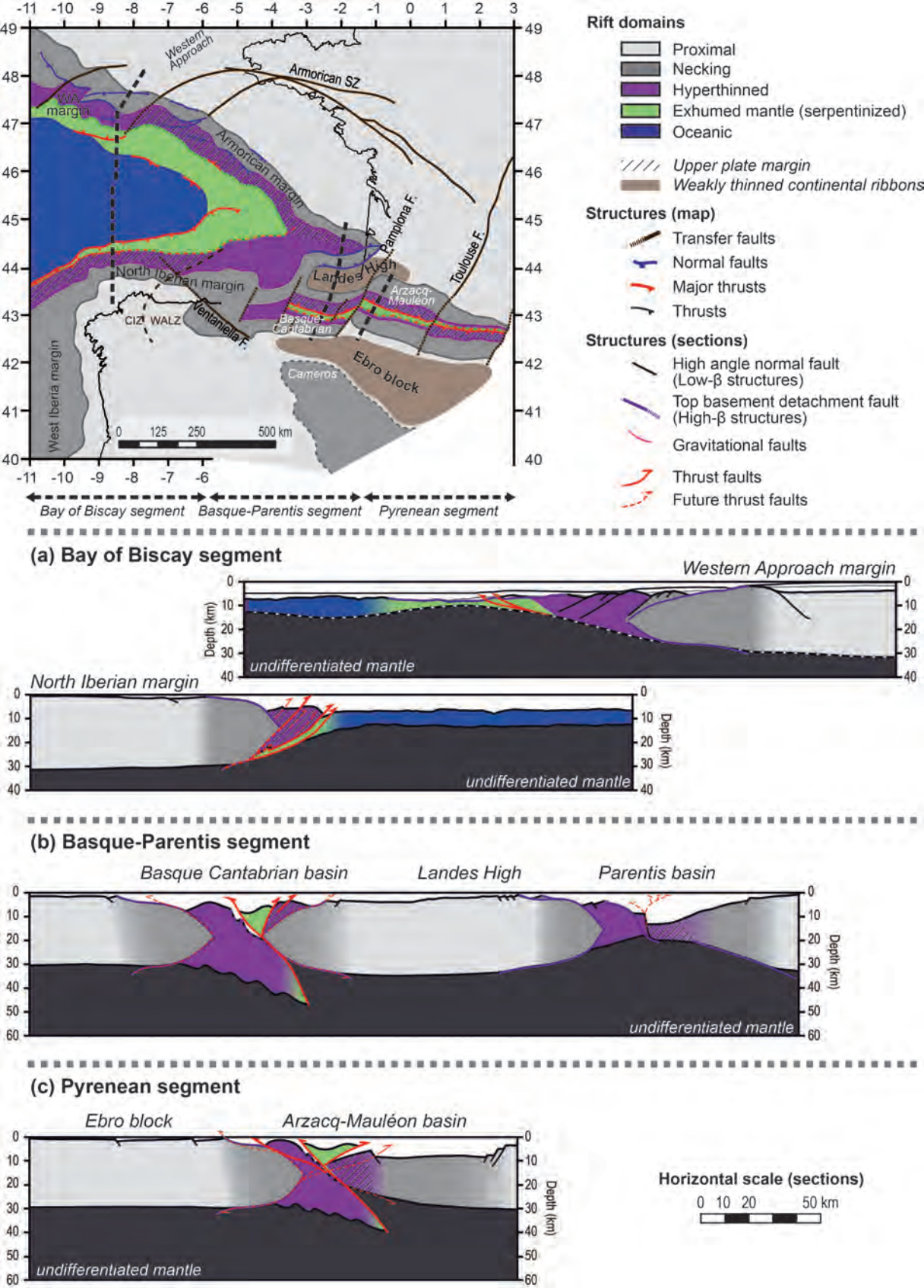
Western Approach
Armorican SZ
WA margin
Armorican margin
Pamplona F.
Toulouse F.
North Iberian margin
Landes High
Arzacq-Mauléon
CIZ
WALZ
Ventaniella F.
Basque-Cantabrian
Ebro block
Cameros
West Iberia margin
0 125 250 500 km
Bay of Biscay segment
Basque-Parentis segment
Pyrenean segment
Rift domains
Proximal
Necking
Hyperthinned
Exhumed mantle (serpentinized)
Oceanic
Upper plate margin
Weakly thinned continental ribbons
Structures (map)
Transfer faults
Normal faults
Major thrusts
Thrusts
Structures (sections)
High angle normal fault (Low-β structures)
Top basement detachment fault (High-β structures)
Gravitational faults
Thrust faults
Future thrust faults
(a) Bay of Biscay segment
Western Approach margin
Depth (km)
undifferentiated mantle
North Iberian margin
undifferentiated mantle
(b) Basque-Parentis segment
Basque Cantabrian basin
Landes High
Parentis basin
Depth (km)
undifferentiated mantle
(c) Pyrenean segment
Ebro block
Arzacq-Mauléon basin
Depth (km)
undifferentiated mantle
Horizontal scale (sections)
0 10 20 50 km

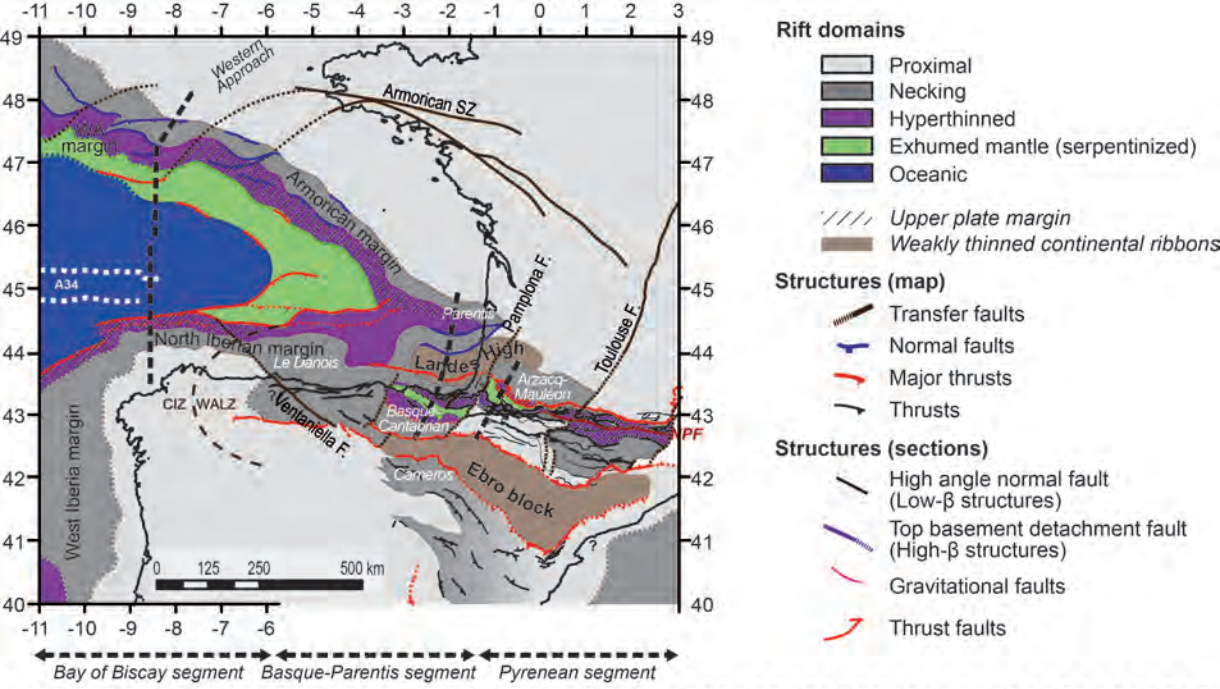

(a) Bay of Biscay segment

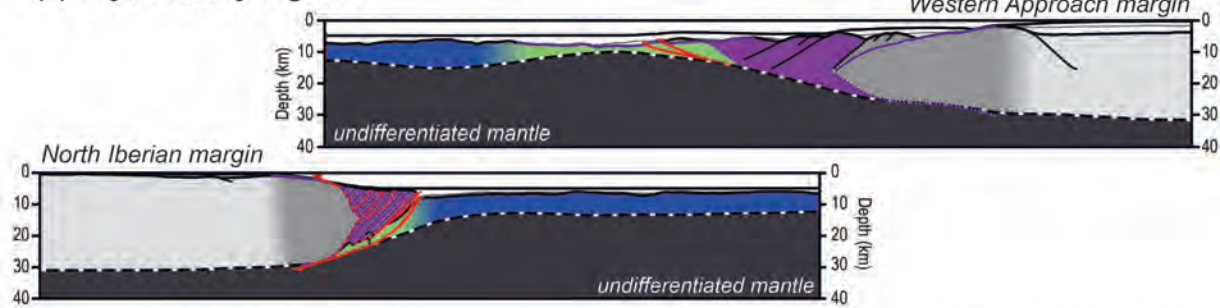

(b) Basque-Parentis segment

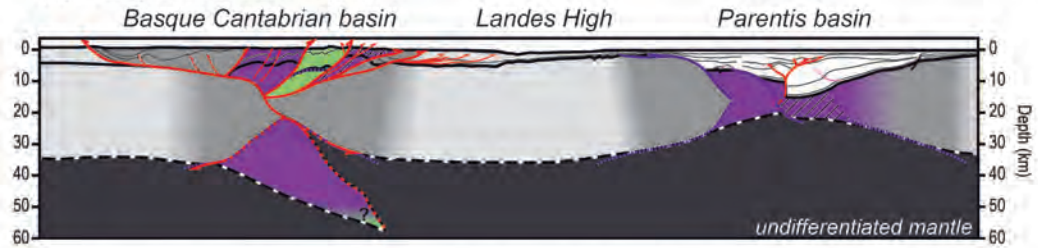

(c) Pyrenean segment

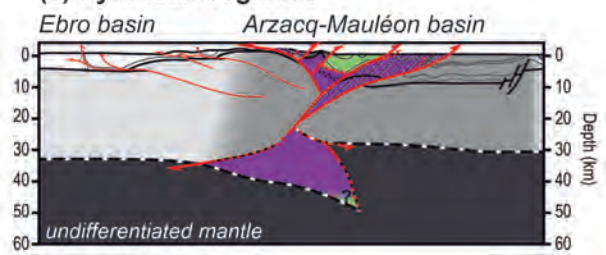

Horizontal scale (sections)

0 10 20 50 km

Table 1: Parameters used for gravity inversion

Parameters	Value and reference dataset
Critical thinning factor (γ)	0.7
Reference crustal thickness	40 km
Break up age	110 Ma
Volcanic additions	7 km